# SURFACE EROSION CHARACTERISTICS OF THREE MANAWATU SOILS

A THESIS

PRESENTED IN PARTIAL FULFILMENT OF THE REQUIREMENTS

FOR THE DEGREE

OF

MASTER OF AGRICULTURAL SCIENCE

IN SOIL SCIENCE

AT

MASSEY UNIVERSITY

LACHLAN GRANT

1992

# Abstract

Sheet erosion is the most extensively mapped erosion type in New Zealand. With the current financial returns from pastoral framing, land which was previously unaffected by sheet erosion is being cultivated and therefore becoming more susceptible to sheet erosion.

The main objective of this study was to assess quantitatively, under the same conditions of slope, cover, and rainfall, the erodibility of three soils which are suitable for either arable farming or market gardening. Whether the eroded sediment consisted of sand, silt or clay particles, or more predominantly aggregates of these primary particles was also determined.

The three soils examined were from the Manawatu region and included the Kiwitea silt loam (Dystrochrept), Levin silt loam (Dystrochrept) and the Tokomaru silt loam (Fragiaqualf). A portable rainfall simulator was used to generate runoff and sediment from soil packed in 0.2 $m^2$ trays. All "storms" were for 60 minutes in which 65 mm of rain was applied. Particle selectively was determined using pipette analysis methods and a settling tube.

Quantitatively comparing the erodibility of the three soils, it was found that the Levin soil was the most erodible and the Kiwitea was the least erodible. If the same storm intensity and soil conditions were to occur over a large area, one hectare could produce 6.4, 17.6 and 10.3 tonnes of sediment from the Kiwitea, Levin and Tokomaru soils respectively. Soil particles and aggregates were selectively removed by rainsplash and overland flow. The proportion of sand particles present in the eroded sediment was always lower than the original soil due to the inability of sand particles to be entrained by overland flow. Silt particles were easily detached and were most commonly eroded as individual particles. Clay particles were eroded and transported in the form of aggregates, a result of their binding properties. The size distribution of eroded sediment became progressively coarser over the rainfall period. This was because initially there was insufficient runoff energy available to transport the larger particles. A vegetative cover severely reduces the volume of runoff and the amount of sediment eroded by cushioning the raindrop impact.

# Acknowledgements

I express my sincere thanks to my supervisor Mr. M.P. Tuohy for his guidance and assistance during all the stages of my work.

I am also grateful for the assistance given to me by the following:

-Doug Grant for his time and effort during the preparation of this manuscript

-The Technical Staff from the Department of Soil Science

-Kevin Harris, Senior Technical Officer for the Faculty of Agricultural and Horticultural Sciences, for the use of his office and computer resources.

Finally, I would like to Acknowledge the never-ending tolerance, encouragement and support from my family and friends, especially my parents.

# Table of Contents

# List of Figures

# List of Plates

# List of Tables

# Chapter One

# Introduction

Sheet and rill erosion are just two erosion types found in New Zealand. Sheet erosion (a surface type of erosion) and rill erosion (a fluvial type of erosion), have similar characteristics in terms of their "erodibility action," but their intensities are far from congruent. The more susceptible conditions for sheet and rill erosion are those areas which are sloping and have either been cultivated, and or lack a vegetative cover. A slope allows the development of overland flow and consequently enhances particle or aggregate entrainment. A lack of a vegetative cover encourages soil detachment by rainsplash due to the inability of the vegetative cover to intercept or cushion raindrop impact. It also favours sheet wash by not restricting the runoff velocity. Water storage and water infiltration are also reduced when a vegetative cover is lacking.

*Sheet Erosion*

Sheet erosion is the removal of thin layers of surface material evenly from an area of sloping land by broad continuous sheets of running water, rather than by streams flowing in well defined channels (Bates and Johnson, 1980). It is caused by a combination of raindrop impact which dislodges fine particles and moves them only short distances, and overland flow which transports them greater distances.

Surface flow can concentrate into channel flow with resulting increases in velocity and capacity to detach and transport soil particles. The result is rill erosion. Sheet and rill erosion often occur in association. These rill channels, may if allowed, develop further into gullies.

*Rill Erosion*

Rills are many closely spaced channels resulting from the uneven removal of surface soil by concentrating running water into streamlets of sufficient discharge

and velocity to generate cutting power (Bates and Jackson, 1980). Rill channels as defined in the "New Zealand Land Resource Inventory" (NZLRI) (Eyles, 1985), are fewer than 60 cm deep and 30 cm wide. They could be smoothed out by cultivation using normal farm equipment.

Rills occur most commonly on cultivated slopes where they usually incise to the base of the cultivated layer. Generally the potential for rilling increases with increasing slope angle. Rills are only occasionally observed on slopes with pasture cover. Such occurrences are usually the result of erosion during cultivation for re-grassing.

**The extent of sheet and rill erosion in New Zealand**

Table 1 (from Eyles, 1985) shows the areas of map units from the NZLRI in which the different erosion types occur. The extent of sheet and rill erosion are high-lighted.

Table 1 also shows that sheet erosion is the most extensively mapped erosion type in New Zealand. In contrast, rill erosion hardly seems significant in terms of land area affected. However, the real extent of this erosion type was thought to have been under mapped in the NZLRI (Eyles, 1985), because most rills occurred on steeper, concave slopes (within individual cultivated paddocks) which usually comprised of only a small proportion of a map unit. Therefore, it was rarely considered to be of significance to record in the erosion inventory. In addition, rill erosion was usually masked by crop or pasture cover. Both sheet and rill erosion are more common in the South Island when compared with the North Island. This maybe because a high percentage of the South Island is mountainous composed of schist and greywacke parent material which supports a very limited vegetative cover due to the harsh climatic conditions.

Table 1. The area of NZLRI map units affected by erosion from Eyles (1985)

| Erosion type | North Island | | South Island | | New Zealand | |
|---|---|---|---|---|---|---|
| | Area (ha) | % | Area (ha) | % | Area (ha) | % |
| Wind | 526900 | 4.6 | 2865800 | 19.0 | 3392700 | 12.0 |
| **Sheet** | **2117400** | **18.6** | **8318400** | **55.0** | **10435800** | **39.0** |
| Scree | 417200 | 3.7 | 3259900 | 21.6 | 3677100 | 13.0 |
| Total Surfical Erosion* | 2662600 | 23.3 | 11150000 | 74.0 | 13812600 | 52.0 |
| Soil Slip | 3397000 | 30.0 | 3615800 | 24.0 | 7012800 | 26.0 |
| Earth Slip | 280300 | 2.5 | 58500 | 0.4 | 338800 | 1.0 |
| Debris Avalanche | 1218900 | 10.7 | 1603000 | 10.6 | 2821900 | 11.0 |
| Earthflow | 1011500 | 8.9 | 33300 | 0.2 | 1044800 | 4.0 |
| Slump | 65800 | 0.6 | 44100 | 0.3 | 109900 | - |
| Total Mass Movement* | 5038200 | 44.1 | 4602000 | 30.5 | 9640200 | 36.0 |
| **Rill** | **13700** | **0.1** | **56400** | **0.4** | **70100** | - |
| Gully | 1157400 | 10.1 | 803500 | 5.3 | 1960900 | 7.0 |
| Tunnel Gully | 327600 | 2.9 | 98700 | 0.7 | 426300 | 2.0 |
| Streambank | 240400 | 2.1 | 491100 | 3.3 | 731500 | 3.0 |
| Total Fluvial Erosion* | 1621900 | 14.2 | 1440100 | 9.6 | 3062000 | 12.0 |
| Deposition | 55100 | 0.5 | 157900 | 1.0 | 213000 | - |

* The total area of map units is less than the sum of areas affected by individual erosion types because of up to three types can be recorded in a map unit.

In the North Island, according to Eyles (1985), the most extensive sheet erosion occurs on the tephra-covered slopes of the volcanic plateau, with the most severely affected areas being the younger Ngauruhoe ash and ashes older than the Taupo ash found in the Tongariro National Park and the Kaweka Range. Sheet erosion was recorded the dominant erosion type in the North Island for 2117400 ha. Of this, only 15 % (313500 ha) was ranked more severe than a slight problem (that is, greater than 11 % of bare ground was exposed), and only 0.5 % (10800 ha) was considered severe (that is, greater than 60 % of bare ground was exposed). Various other erosion types were associated with sheet erosion in the North Island. This mainly coincided with scree and wind erosion and only on those areas which were more severely affected by sheet erosion.

In the South Island, widespread distribution of sheet erosion occurs on much of the seasonally dry hill country and mountain areas, particularly inland Marlborough, inland Canterbury and Central Otago (Eyles, 1985). The dominant rock types associated with sheet erosion are schist and greywacke. From the NZLRI, sheet erosion in the South Island was found to be the dominant erosion type for 8318400 ha. Of this, only 12 % (631400 ha) had a severity ranking greater than moderate (that is, greater than 21 % of bare ground was exposed), and less than 0.2 % (10400 ha) was ranked severe. Other erosion types associated with sheet erosion in the South Island include soil slip and scree erosion for when sheet erosion was ranked moderate or less. Scree, gully and debris avalanche types of erosion were associated with sheet erosion when the severity ranking was greater than moderate (Eyles,1985). The mapped distribution pattern of sheet erosion for both Islands, from Eyles (1985), is shown in Figure 1.

Sheet Erosion is not usually a problem in forested steeplands because the impact of rainfall is absorbed by the trees and the litter. However, logging and road building, fires and mass movement can expose the soil to this process. Heavy machinery compacts the soil which increases runoff and thus sheet erosion. Contour ploughing, grass-seeding and aerial top-dressing help to reduce sheet erosion by forming a surface cover and root network which holds the soil particles in place.

Rill erosion in the North Island is most susceptible on loess and tephra parent material, with the Taupo Pumice Formation tephras being particularly susceptible. Rill erosion in the North Island was the dominant erosion type in only 13700 ha from the NZLRI (Eyles, 1985). Of this, 94 % was ranked only slight. This ranking is a subjective assessment and is based on seriousness. Other types of erosion associated with rill erosion in the North Island include sheet and gully erosion.

In the South Island, Rill erosion occurs most extensively on cultivated downlands with loess-derived yellow-grey earth soils. Rills also occur on bare slopes in the steep high country areas. Rill erosion in the South Island was the dominant erosion type in only 9230 ha of NZLRI map units and of which 96 % was only


Figure 1. The mapped distribution pattern of sheet erosion in New Zealand (from Eyles, 1985).

ranked slight. Other erosion types associated with rill erosion in the South Island include sheet and wind erosion.

## Objectives

The main objective of this study was to assess quantitatively the erodibility of several soils under the same conditions. The experiments also determined whether soil particles or aggregates were being selectively eroded over the erosion period.

## Soil Types

This study investigated three soils from the Manawatu region that are suitable for arable farming or market gardening. The soils were the Kiwitea silt loam (Drystrochrept), the Levin silt loam (Dystrochrept) and the Tokomaru silt loam (Fragiaqualf).

### *The Kiwitea silt loam*

The Kiwitea soil is classed as a weakly leached yellow-brown earth and occupies an area approximately 11000 ha. These soils are formed from a thick blanket of quartzo-feldspathic loess derived from mainly greywacke and some volcanic ash, overlying greywacke gravels. They are mapped on the undulating and dissected high terraces between an elevation of 120 and 425 m. These soils occur on level to strongly sloping sites (0 to 15°), however gentle slopes (0 to 7°) are more common. The drainage status is considered well drained.

The Kiwitea soil's profile consists of 0.18 m dark brown friable loam merging into 0.13 m yellowish-brown friable sandy loam to loam which overlies yellowish-brown firm loam with faint mottling. The soil structure is moderately developed in the upper 0.30 m but weakens with depth. Greywacke gravels often occur at 1.80 to 2.00 m depth and overly loose sands. The sands are unstable and down cutting streams cause severe gully erosion. The gullies are formed by a

combination of water and wind erosion and can be extreme.

The present land uses of these soils include sheep farming, fattening, dairying and annual cropping. With the current economic returns from livestock farming, a greater proportion of the Kiwitea soil is being cropped annually. Crops include potatoes, carrots, wheat and barley. Brassica fodder crops are also common.

*The Levin silt loam*

The Levin soil is a moderately leached intergrade between the yellow-brown earth and the yellow-brown loam. These soils occupy an area of approximately 7000 ha and are found on the terraces and fans older than the Ohakean terrace south and east of Te Horo, east of Otaki and north of the Waitohu stream to Manakua between the elevation of 10 to 100 m. They are formed from moderately weathered quartzo-feldspathic loess of Ohakean age, with minor volcanic ash over gravels, sands, colluvium or older loess. In some places the loess contains rhyolitic Aokautere ash 0.05 to 0.15 m thick at a depth between 0.80 and 1.50 m. The thickness of Ohakea loess in the Levin soil varies from 0.60 to 2.00 m. These soils occur on level to strongly sloping sites (0 to 15°), however gentle slopes of 0 to 7° are more common. The soil moisture class is udic and the soil temperature regime is classed as mesic.

The Levin soil is a well drained soil having a dark brown, well structured, friable silt loam A horizon overlying a yellowish-brown and brownish-yellow, friable and generally non-mottled silt loam or silty clay loam textured Bw horizons with moderately developed nut and granular structure. Wet consistence is smeary and non-sticky throughout, with the upper Bw horizon having a weak to moderate reaction to the NaF field test. Few (up to 2 %) low chroma colour mottles can occur within the Levin silt loam but usually only at depths exceeding 0.80 m. Few (up to 2 %) ochreous mottles may sometimes occur between 0.60 and 0.80 m.

The present land uses for the Levin soil are pastural farming, market gardening and fruit orchards. Currently the areas of market gardening and orcharding are increasing.

*The Tokomaru silt loam*

The Tokomaru soil is classified as a weakly leached, moderately to strongly gleyed yellow-grey earth. It is formed on loess under a relatively dry climate, and it is thought that the seasonal wetting and drying typical of this climate was the main factor causing the compaction and hardening of the loess as it accumulated. This compact parent material slows downward drainage of rainfall through the soil, leading to gleyed conditions. Under these conditions, most of the iron that is weathered out is in a reduced form and is removed with the drainage waters or concentrated in mottles or concretions. As a result of the low content of iron oxides in these soils (apart from that in mottles and concretions) the clay is in a dispersed state and is readily washed down from the upper horizons to accumulate in the subsoil. Eluviation of clay is also helped by the cracking that occurs in these soils in summer.

Profiles show 0.15 to 0.20 m of dark greyish-brown loam weakly to moderately developed nut structure and some fine brown mottles, overlying 0.18 m of light brownish-grey to greyish-brown heavy silt loam with many fine dusky red iron and manganese concretions. This passes to 0.38 m of pale olive compact clay loam with abundant strong brown mottles, and towards the lower part moderately thick clay coatings occur on aggregate faces. This horizon rests at 0.76 m from the surface on light grey very compact sandy clay loam with many fine brown mottles. Vertical pale grey veins up to 0.025 m wide and about 0.30 m apart are characteristic of this horizon. They are polygonal in plan and may go down to depths of 2.50 m or more. In road cuttings, the sandy loam clay horizon stands out as a well defined ledge. Below this ledge or fragipan the texture changes to fine sandy loam, but it is still very compact and hard. In places, mainly at the sides of heads of gullies, concretions in the subsoil horizon becomes abundant and may form a solid pan.

The Tokomaru soil occurs on the terraces and fans older than the Ohakean terrace and its elevation range is between 30 and 150 m. The slope is level to strongly sloping sites on flat to more undulating land (0 to 15°), however the gentle slopes of 0 to 7° are more common. The soil moisture class is udic and the soil temperature regime is mesic. Drainage is classified as poor.

The current land use for the Tokomaru soil is mainly pastural farming, with areas of arable farming and cereal cropping. The area occupies approximately 8500 ha. The Tokomaru soil also has similar characteristics to another soil, the Marton silt loam. However the fragipan of the Marton silt loam is less developed. The Marton silt loam occupies approximately 21000 ha and is intensively cropped with cereals.

## Apparatus

The above objectives were fulfilled using a portable rainfall simulator, a settling tube and pipette sedimentation procedures. The rainfall simulator was used to obtain sediment and runoff samples from bare and mulch covered soil plots at set time intervals during a simulated storm event. Pipette sedimentation procedures were used to determine the particle-size distribution of the fine material and the settling tube was used determine the fall velocity characteristics of original soil samples and sediment derived from the rainfall simulator.

# Chapter Two

# Surface Erosion Experiments

## Introduction

In New Zealand, sheet erosion is the most extensively mapped erosion type (Eyles, 1985). To gain a better understanding of sheet erosion and the hydrologic processes, Massey University developed a small rainfall simulator. This rainfall simulator was used to evaluate the rates and amounts of sediment, runoff and infiltration from three cropping soils (Kiwitea, Levin and Tokomaru soils). The effect of a barley straw mulch on rates and amounts of sediment and runoff for the Levin soil was also determined.

## Processes which occur in "sheet" erosion

The combined action of raindrops impacting upon a surface and the flow of water over that surface produce sheet erosion (Eyles, 1985). Soil is initially removed from the soil matrix then transported down the slope. Removal of sediment from the original (parent) cohesive soil may occur due to water shear stresses resulting either from the dissipation of the power of raindrop impact (Al-Durrah and Bradford, 1982; Luk, 1979; Wright, 1987), or from overland flow (Luk, 1979). These processes are termed rainfall *detachment* and *entrainment* respectively (Rose, 1985).

Once sediment is lifted into overland flow a sediment concentration exists and providing the sediment has a positive immersed weight, it will return towards the soil bed (Rose,1985). Rose also showed that sediment resting on the bed, termed the *deposited layer*, is then available to be re-lifted into the water flow by the same type of stresses which originally lifted it from the soil bed. As this layer consists of recently deposited material only, it is considered to be non-cohesive and therefore much more susceptible to the action of erosive agents than the original soil. Raindrop impact removes sediment from the deposited layer in a process termed *rainfall re-detachment*, and stresses caused by overland flow may

remove sediment from the deposited layer by a process called *re-entrainment.* Sediment introduced into the flow by rainfall detachment, entrainment, rainfall re-detachment or re-entrainment is all subject to deposition (Rose, 1985).

*Theoretical aspects of sheet erosion*

The rates of rainfall, infiltration and runoff may be simply related in a water balance. Rainfall excess, $R$, is the difference between rainfall rate per unit area, $P$, and the infiltration rate, $I$. This is the amount of water on the soil's surface available for runoff. If this excess is evenly distributed across the slope then the expression for runoff rate per unit width, $q$, (Hairsine and Rose, 1991) is:

$$R = \frac{dq}{dx} + \frac{dD}{dt} \qquad (1)$$

where $D$ is the depth of flow, $x$ is the distance down-slope and t is time. When the depth is steady over time then the rainfall excess per unit area equals the runoff rate per unit area, $Q$. Therefore equation (1) becomes:

$$q = Qx \qquad (2)$$

It is normal for flow down-slope to be non-uniformly distributed across the slope. Flow channels or rills may form, or variations in the surface micro-relief or vegetation may alter an otherwise uniform "sheet" flow. However equation (2) is still appropriate for such situations providing no large scale across-slope flow occurs.

Hairsine and Rose (1991) described the interaction of the processes of rainfall detachment, rainfall re-detachment and deposition in the presence of overland flow. They derived the expression for the sediment concentration, $c$, (mass of sediment per unit volume of water/sediment mix) by the expression:

$$c = \frac{C_e\, a\, P\, (1-H)}{Q\left(1-\frac{b}{m}\right)} \qquad (3)$$

where $C_e$ is the fractional area exposed to raindrops and not intercepted by living or dead vegetation, or other material such as stone, $a$ is the detachability of the

soil matrix, *P* is the rainfall rate, *H* is the fraction of the soil surface covered by the deposited layer, *Q* is the runoff rate per unit area (assume to equal *R*), *b* is a depth related decay constant (assume *b* equals 0.7) and *m* is a constant describing the degree of turbulence (assume *m* equals 1.66). Hairsine and Rose (1991) and Proffitt *et al.* (1989) derived these assumptions.

Also Hairsine and Rose (1991) suggest that the sediment concentration is related to the rainfall re-detachability of the deposited layer, $a_d$, by the expression:

$$c = \frac{H C_e a_d P}{\frac{1}{I(\text{sum}V)}} \qquad (4)$$

where *1/I (sum V)* is the "depositability" of the original surface soil as determined by settling tube tests. They found typical values of the depositability to be 0.02 m $sec^{-1}$ for a clay loam and 0.04 m $sec^{-1}$ for a sandy soil.

Investigations of rainfall detachment of cultivated aggregates by Proffitt *et al.* (1989) found the fraction of the soil surface covered by the deposited layer to be approximately 90 percent. Therefore *H* equals 0.9.

*Factors affecting rainfall detachment of the soil*

As a raindrop impacts upon the soil surface the energy of the drop (typically travelling at 8 m $sec^{-1}$ (Gunn and Kinzer, 1949; Laws, 1941)) is transferred to both the water covering the soil surface and the soil surface beneath (Laws and Parsons, 1943; Walker *et al.*, 1972; Wischmeier and Smith, 1958). The impact of drops on shallow flows result in the development of a crater in the surface water (Savat, 1981). The movement of water out of and (to a lesser extent) back into this crater causes soil to be lifted into the flow (Moss and Green 1983; Savat, 1981). Moss and Green (1983) and Savat (1981) showed that as the depth of the surface water increases then the crater becomes less developed and more of the raindrops energy is absorbed by the water itself. For deep flows, when the flow depth is greater than three raindrop diameters, the water layer absorbs almost all the raindrop impact and the values of rainfall detachment and re-detachment are insignificant. Factors influencing the depth of water on the

surface are infiltration and rainfall, surface roughness, vegetation in contact with the soil surface and the presence of any rills (Moss and Green, 1983).

Moss and Green (1983) showed that the shearing of water over the surface which occurs in cratering will result in varying amounts of soil detached from either the original soil or the deposited layer. They found a well compacted clay soil will exhibit strong resistance to detachment, whereas a silt loam which has been finely cultivated will have little resistance.

**Rainfall simulators**

Rainfall simulators are research tools designed to apply water in a form similar to natural rainstorms. They are useful for many types of soil erosion and hydrologic experiments. However, rainstorm characteristics must be simulated closely.

The major advantages of rainfall simulators are that:

(1) soil conservation or hydrologic characteristics of newly developed cropping and management practices can be measured in a very short time,

(2) simulated storms can be applied for selected durations on selected treatment conditions and measurements from a few such storms often can show conclusively at least relative information about those treatments,

(3) plot preparation before applications of such storms usually takes much less time than plot maintenance for studies depending on natural rainstorms,

(4) inspection of plots and equipment immediately before and during data collection,

(5) researchers can make measurements and observations during simulated storms that are difficult or impossible during natural rainstorms, and

(6) they are readily adaptable for highly controlled laboratory research on basic infiltration, runoff and erosion processes.

Rainfall simulators can have major limitations and disadvantages. These include the difficulty of simulating natural rainfall characteristics and the proper

interpretation of data obtained from rainfall simulators that fail to fully achieve such characteristics. Other problems are the relatively small area to which rain can be applied by most rainfall simulators and the compromise in rainfall characteristics that is necessary for large area rainfall simulators.

## Characteristics of rainfall simulators

The ideal rainfall simulator would be easy to operate, simulate rainfall perfectly, be simple to move, and could be used whenever and wherever needed. Most researchers realise that such an ideal rainfall simulator is impossible to acquire. Thus, different rainfall simulators have different characteristics to meet their research goals. The most important characteristics of natural rainfall that need to be closely simulated for soil and water management research include:

*1. Raindrop size distribution*

Observations of natural rainfall from a wide range of geographic locations suggests that the distribution of raindrop sizes range from near zero to about 7 mm in diameter (Laws and Parsons, 1943; Mueller and Sims, 1967). Raindrops greater than 7 mm may occur briefly as a result of collisions. However large raindrops so produced will tend to be unstable, given atmospheric turbulence (Blanchard, 1950), and will disintegrate into many smaller raindrops. The medium raindrop diameter, by volume, is between 1 and 3 mm for erosive rainstorms (Walker *et al.*, 1972). Raindrop diameter generally increases with rainfall intensity (Laws and Parsons, 1943; Mueller and Sims, 1967).

*2. Raindrop impact velocities*

Raindrop fall velocities vary from near zero for mist-size drops to more than 9 m $sec^{-1}$ for the largest sizes (Laws, 1941; Gunn and Kinzer, 1949). A common-size raindrop of 2 mm falls at a velocity between 6 and 7 m $sec^{-1}$ (Gunn and Kinzer, 1949).

*3. Raindrop intensities*

Intensities of natural rainfall vary from near zero to several millimetres per minute (Laws and Parsons, 1943). Generally, very low intensities are not of interest for erosion and hydrologic studies, and very high intensities are so rare that they be of limited interest. Those of major interest are between 12 and 120 mm $hour^{-1}$.

Raindrop size distribution, impact velocity and intensity are key features in soil detachment, soil surface sealing and resulting runoff. Other desirable characteristics for rainfall simulators include research area size, raindrop uniformity, angle of impact, rainstorm repeatability and the portability of the rainfall simulator.

**Types of rainfall simulators**

During the past 50 years, researchers have used a broad range of techniques and equipment for simulating rainfall. These techniques and equipment have varied from walking up and down the slope with common sprinkling cans to electronic and hydraulic machines (Hall, 1970; Mutchler and Hermsmeier, 1965). The raindrop former is the key component of rainfall simulators. Their techniques can be grouped into pressurized and non-pressurized systems (Bubenzer, 1980; Mutchler and Hermsmeier, 1965).

*a. Pressurized systems*

The pressurized system utilises nozzles from which water is forced at a significant velocity by pressure. Nozzles can produce a wide range of drop sizes, as do rainstorms. However the large nozzle orifices that are necessary to obtain large drops require that the nozzles spray only intermittently to reduce application rates to typical rainstorm intensities. The non-pressurized system produces raindrops which form and fall from a tip starting at zero velocity. Tips produce only one drop size or a very limited range of sizes, so they are used mostly for fundamental studies when a carefully controlled drop size is important.

Early rainfall simulators were much less sophisticated than today's models. This was because little information was available at the time on rainfall characteristics. The importance of raindrop impact on soil detachment also had not been recognized. Thus, the primary concern was to apply water uniformly over the research area in some manner. Later research (Blanchard, 1950; Gunn, 1949; Gunn and Kinzer, 1949; Laws, 1941; Laws and Parson, 1943; Hudson, 1971; Walker *et al.*, 1972; Wischmeier and Smith, 1958) evaluating the characteristics of rainstorms provided an understanding of appropriate goals for the design of rainfall simulators. Most of the equipment developed in recent decades has considered raindrop size and velocity data as a basis for a more realistic simulation of rainstorms.

The proceedings of the 1979 Tucson, Arizona rainfall simulator workshop (United States Department of Agriculture, 1979) describes several rainfall simulators currently being used for soil conservation research. These rainfall simulators vary from applying rainstorms to runoff-plot-sized areas to being suitable only for very small field plots or laboratory studies.

Several rainfall simulators have been designed for use on field plots that are similar in size to those used in natural rainfall studies of runoff and erosion. The rainulator of Meyer and McCune (1958) was the first simulator designed to apply rainstorms with drop characteristics near those of natural rainfall on several runoff plots simultaneously. Simulated rainfall was applied by downward-spraying nozzles that were moved laterally across the plots and border areas. Spray application was intermittent and only a few intensities could be simulated.

The rotating boom rainfall simulator (Swanson, 1965) used the same nozzles as the rainulator, but the nozzles were located along arms extended from a central vertical shaft which rotated slowly. Only two intensities were possible, and the application was intermittent. The entire rainfall simulator was portable as it was trailer mounted.

The programmable rainfall simulator designed by Foster *et al.* (1982) and the Kentucky rainfall simulator of Moore *et al.* (1983) used rapidly oscillating nozzles that reduced intermittency to short periods. They could produce a wide range of

intensities. Both were electronically and mechanically complex. The Kentucky machine was on wheels for more rapid movement to adjacent plots.

Sprinkler irrigation equipment and the Colorado State University RRER rainfall simulator (Holland, 1969) are suitable for larger runoff plots and small watersheds. These types of rainfall simulators tend to be less successful in achieving natural rainfall characteristics, especially drop size distribution (United States Department of Agriculture, 1979).

Other rainfall simulators have been designed primarily for small field plots of about 1 $m^2$ and for laboratory studies. The Purdue sprinkling infiltrometer (Bertrand and Parr, 1961) and the rotating-disc rainfall simulator (Morin *et al.*, 1967) used static nozzles, but the latter tended to give a much better simulation of raindrop-impact energy. The interrill rainfall simulator (Meyer and Harmon, 1979) used rapidly oscillating nozzles to produce a wide range of intensities at energies very near natural rainfall. This design has also been adapted for use with long plots by using additional nozzles (Meyer and Harmon, 1985).

*b. Non-pressurized systems*

Non-pressurized designs use yarn or capillary tubing of various materials to form drops. These have been mainly used for laboratory studies. Their raindrop sizes are moderate to large, and all are about the same diameter for any specific design. Impact velocity is considerably lower than terminal velocity for drop heights less than 5 to 10 m. Designs that are being used for soil erosion research include those by Blackburn, Bubenzer, Gifford, and Romkens (United States Department of Agriculture, 1979).

**Massey's portable rainfall simulator**

Massey University has developed a small rainfall simulator suitable for the investigation of soil erosion and hydrologic research. It was based on the design of the USDA-ARS demonstration rainfall simulator by Laflen from Ohio State

University (Keen, 1986). It consists of fan spray nozzles which oscillate across the soil bed. The rainfall simulator produces rainfall rates, drop sizes and drop velocities not dissimilar to natural rainfall. Varying the time between sweeps alters the rainfall intensity.

The unit as shown in Plate 1 consists of three horizontal plateaus united by four vertical aluminum pipes. The first plateau consists of a rectangular water tank at ground level. This is used for the collection of runoff water from the second plateau, which is approximately 50 cm above that tank. The second plateau is an adjustable tilting platform holding the soil trays being studied. In front of the tilted platform, a trough is mounted for the collection of runoff water and sediment. On the third plateau, approximately 1.8 m above the tilting platform, the nozzles are mounted on a two-piece shaft that can be adjusted horizontally, allowing the distance between the two nozzles to vary within a range of about 1 m. The shaft makes a partial rotation back and forth on its axis, causing the water to fall in a sweeping arc. The angle of the shaft's back and forth rotation can be adjusted, causing a corresponding change in the size of the arc of falling water.

A 0.012 kw motor, two micro switches and a electronic timer keep the nozzles rotating back and forth. At both extremes of the angle of rotation, the motor shuts off and the nozzles pause. Adjusting the length of the pause varies the rainfall intensity. During the pauses the nozzles continue to spray water which falls into collecting troughs located at the extremes of each angle of rotation. The trough unit resembles a rectangle within a rectangle, the inner rectangle being an open air space and the troughs forming the outer rectangle as shown in Plate 2. As the nozzles sweep over the open air space, water falls onto the soil trays. When the nozzles reach the pause positions on either end of the arc, the water falls into the troughs and is recycled back to the simulators water source. The water source comprises of a 50 *l* container equipped with a 0.375 kw submersible pump. The mains water system supplies the water container. A floating valve attached to the container maintains a constant pressure head at the outlet spray nozzles.

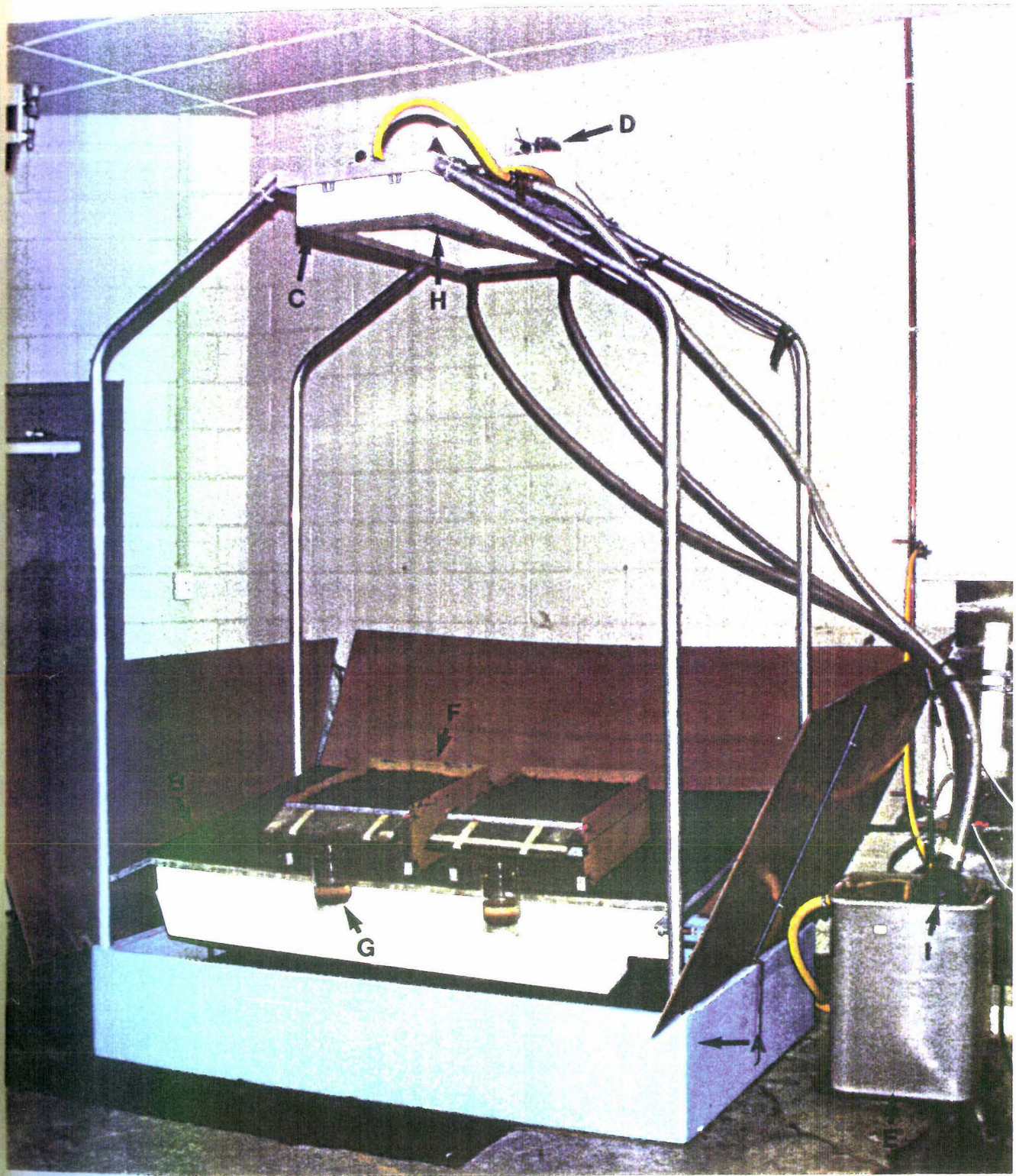


Plate 1. The Massey Rainfall Simulator. (A) the rectangular water tank, (B) the tilting platform supporting the soil trays, (C) the trough unit, (D) motor and micro switches, (E) the water source, (F) the soil containers, (G) runoff collection container, (H) the two spray nozzles, and (I) the floating water valve.

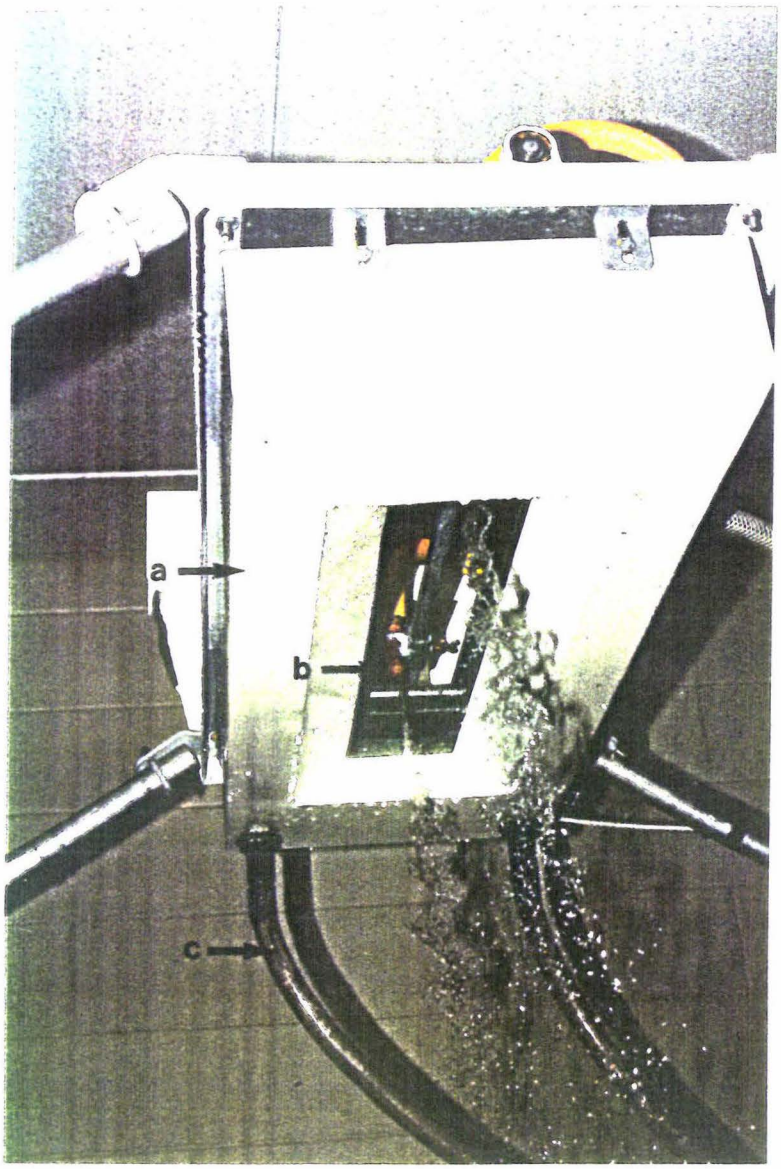


Plate 2. The third plateau consisting of (a) the non-spray time collecting trough, (b) the spray nozzles and (c) the water recycling drain pipes from the collecting trough to the water source.

The tilting platform has sufficient space to contain three soil trays, with dimensions 0.5 m by 0.4 m as shown in Plate 1. Each soil tray represents $2 \times 10^{-5}$ ha (0.2 $m^2$). Grating encloses the front and helps lateral drainage from the container. A runoff flume rests on the top of this grating and is covered by a splash guard to ensure that only runoff originating from the soil surface is collected (Plate 3).

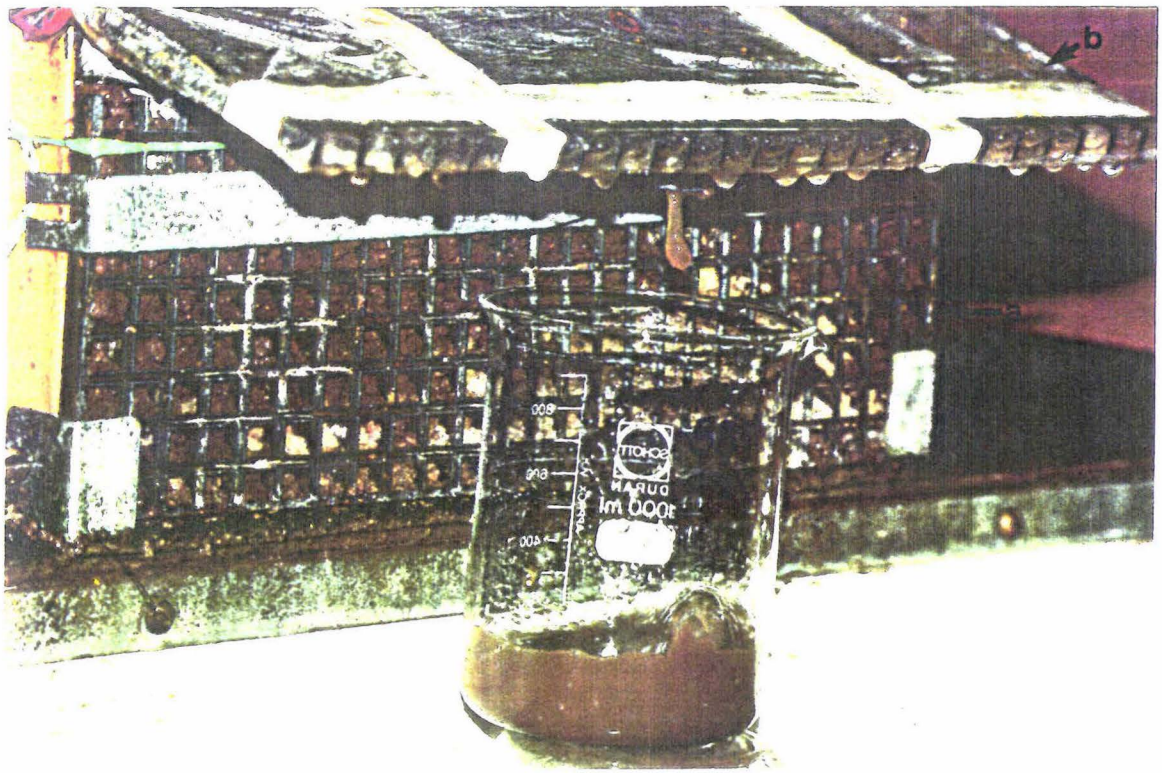


Plate 3. The soil container showing (a) the grating, (b) the runoff flume, (c) the splash guard and (d) the runoff-sediment collection beaker.

## Difficulties with intermittent rainfall

Intermittent rainfall is a common design feature of modern pressurized spray nozzle type rainfall simulators (United States Department of Agriculture, 1979). These simulators generally use spray nozzles of larger diameter sizes. To produce raindrops with the characteristics of natural rain, in terms of raindrop size and velocity, the nozzles must produce very high rainfall rates. In order to produce more realistic time-averaged rainfall rates, the spray pattern must be regularly interrupted or oscillated across the soil surface. This results in intermittent rainfall which may potentially affect both the water balance and sediment transport processes which occur at the soil surface.

Hairsine (1989) showed that rainfall pulsating on a soil will result in time-variability of both the rate of infiltration and runoff. He showed that the degree of such variability compared with the rates of infiltration and runoff when the rainfall rate is steady was important in assessing whether the rainfall simulations were

appropriate. For example, a sandy soil has a steady infiltration rate of 100 mm $hour^{-1}$. Applying a steady rainfall rate of 100 mm $hour^{-1}$ would result in no runoff. However, if this rainfall rate is simulated by applying 500 mm $hour^{-1}$ for two seconds in every ten, then there would be some runoff which would be an artifact of the simulation. Such runoff may subsequently infiltrate or exit the plot being considered so that runoff (and the associated erosion processes) apparently commences at a lower rainfall rate than would be found in a steady rainfall situation. The error of this effect is proportional to the length of the spray cycle. Long cycles allow surface water to flow a significant distance down-slope before completing infiltration. Reducing the cycle to a fraction of a second reduces this effect but does not eliminate it.

Intermittent rainfall may also produce artifacts in erosion processes (Hairsine, 1989). The time-variability of the runoff rate and the depth of water on the soil surface have important ramifications for both raindrop impact and overland flow driven processes. Hairsine and Rose (1991) suggested that the detachabilities of a soil can be related to the flow depth by an inverse power expression. They found intermittent rainfall will produce surface water depths which are greater than the mean for much of the time, producing very low detachabilities. They showed for the period when the flow depth is lower than the mean depth, the detachabilities will be very much higher than the mean case. These researchers showed that the total effect over one cycle is likely to be soil and frequency specific.

It has been suggested that overland flow produced using intermittent rainfall simulators may have an artifactual component through the time-variability described above. If the entrainment or re-entrainment of sediment does occur in the soil under consideration, then it is also affected by the time-variability of runoff. This is particularly so for the threshold of entrainment which is exhibited by soils of significant cohesive strength. Pulses of the high intensity rainfall may temporarily boost overland flow so that it exceeds the threshold streampower (streampower being the energy per unit area which the flow applies to the soil surface), therefore producing entrainment. For the steady state rainfall case, overland flow may not exceed this threshold level and clearly the pulsing of the simulated rainfall is introducing new processes (Hairsine and Rose, 1991).

A further difficulty is the relationship of the rate of rainfall detachment, *a*, to the rainfall rate, *P*. The rates of rainfall detachment and re-detachment are generally proportional to $P^p$, where *p* is an exponent which has been found to vary from 0.8 to 2.0. The recent investigations of Proffitt *et al.* (1989) using the process definitions of Hairsine and Rose (1991), found *p* to be close to unity for two contrasting soils with a range of flow depths and rainfall rates. However, if *p* was not unity, then the time averaged rates of rainfall detachment and re-detachment would not be equal to those expected with continuous rainfall.

In summary, the intermittent nature of some rainfall simulators has important implications for the use and interpretation of simulated erosion or infiltration experiments. The effects on erosion and deposition processes vary with the frequency and "no rain time". These effects may be minimized by increasing the speed of the sweep so that the processes are as near as possible to continuous. This has been achieved in existing rainfall simulators by using high speed spray choppers in spinning disc simulators and by using sweeping frequencies of the order of four cycles per second in oscillating nozzle simulators (Hairsine, 1989).

## Experimental Objectives

Using the rainfall simulator at Massey University, the objectives of this study were:

(1) to determine the rainfall uniformity of the rainfall simulator using "catchcans",

(2) to evaluate the rates and amounts of infiltration, runoff and sediment loss from bare soil subjected to simulated rainfall over similar time periods for the three soils studied, and

(3) to determine the effects of barley mulch on rates and amounts of sediment and runoff generated.

## Experimental methods

### *i. Rainfall uniformity*

Rainfall uniformity of the rainfall simulator was determined using a series of catch-cans laid out across the tilting tray platform in a grid fashion. This is shown in Plate 4. Rain was applied continuously (ie. no delay timer setting) for a period of time. The rain volume in each catch-can was then determined using a calibrated ruler.

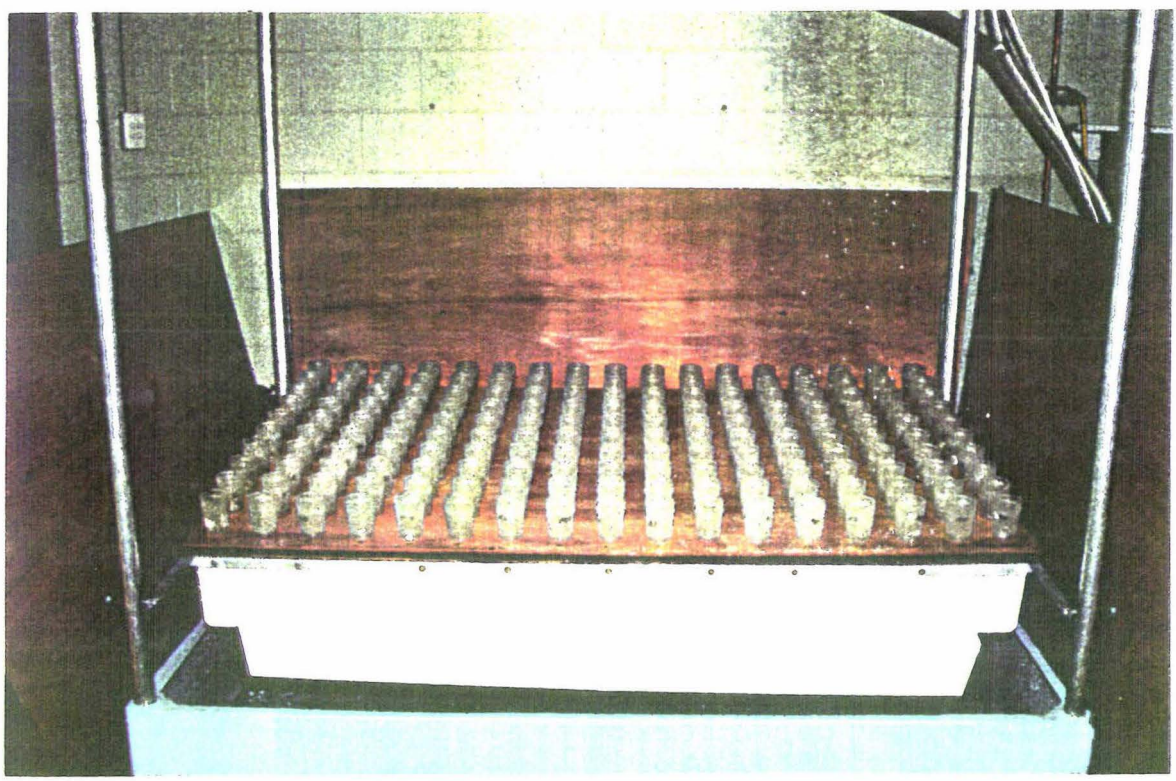

Plate 4. Catch-cans laid out across the tilting tray platform for determining rainfall uniformity.

### *ii. Rainfall simulation experiments*

Three cropping soils of the Manawatu: Kiwitea, Levin and the Tokomaru soils, were subjected to simulated rainfall to evaluate the rates and amounts of sediment and runoff produced. The procedures of soil collection, exposing the samples to rainfall, and the processing of the sediment and runoff are described in the following sections.

*a. Collection of soil material*

All soil collected for rainfall simulation experiments was from the A horizon of pastural land. To simulate tillage under a cropping situation the organic root mass was excluded. Storing soil in air tight plastic bags prevented moisture loss.

*b. Packing of soil containers*

Soil collected was passed through an 8 mm square hole sieve into the soil containers. It was evenly packed to a dry bulk density between 800 and 900 kg $m^{-3}$. This density was selected to simulate soil conditions in the field following cultivation. Re-packing at densities greater than this can destroy the soil structure. A coarse sand layer approximately 10 mm deep was placed at the base of the container to reduce the effect of a perched water table and improve the general drainage. To improve rainfall uniformity, only two soil containers were subjected to simulated rainfall at one time.

*c. Rainfall intensity, duration and slope*

In this study all soil samples were subjected to a rainfall intensity of 65 mm $hour^{-1}$ for 1 hour. This rainfall intensity and duration represents a return period for a storm far in excess of 100 years (Tomlinson, 1980). The reason for choosing a storm of this intensity was primarily to reduce the effect of rainfall intermittency from the rainfall simulator. Although a rainfall intensity of this calibre for 60 minutes is very infrequent, they can occur, but usually for a much shorter duration. It is normally the short duration, high intensity storms that cause most surface erosion damage.

The soil containers were raised to simulate a slope angle of 7°. This is typical of cultivated slopes in the region for the three soils studied.

Rainfall simulation experiments on each soil type were repeated. The Kiwitea soil was repeated 8 times, the Levin soil 6 times, and the Tokomaru soil 10 times. From these results, mean values for each soil type were determined.

*d. Collection of runoff and sediment*

The runoff and sediment displaced from the flume was collected at 5 minute intervals over the storm event. Sediment trapped on the flume was scraped into the collecting beaker. Disruption of aggregates in this procedure was minimal.

*e. Processing of sediment and runoff*

The volume of the water-sediment mix for each interval was obtained by measuring the water depth in the beakers with a calibrated ruler. The dry mass of sediment was determined after evaporating the water off in an oven at 105°C for 24 hours.

Further examination of the sediment generated from the rainfall simulator was carried out. This included particle size distribution analysis and settling tube experiments. These procedures are described in chapters three and four respectively.

*f. Preparation of mulch covered plots*

The effect of a barley mulch on runoff and sediment generation was studied for the Levin soil. On the surface of bare soil packed identically to the procedure described above, barley straw was placed to resemble the situation when cereal trash remains after harvesting (see Plate 5). Rainfall intensity, slope, intervals and procedures for collecting sediment and runoff samples were similar to previously described techniques. However the duration of the storm event was reduced to 45 minutes. This, as will be shown latter, was due to the reduced sediment and runoff generation. Mulch covered experiments were repeated 4 times to obtain mean values.

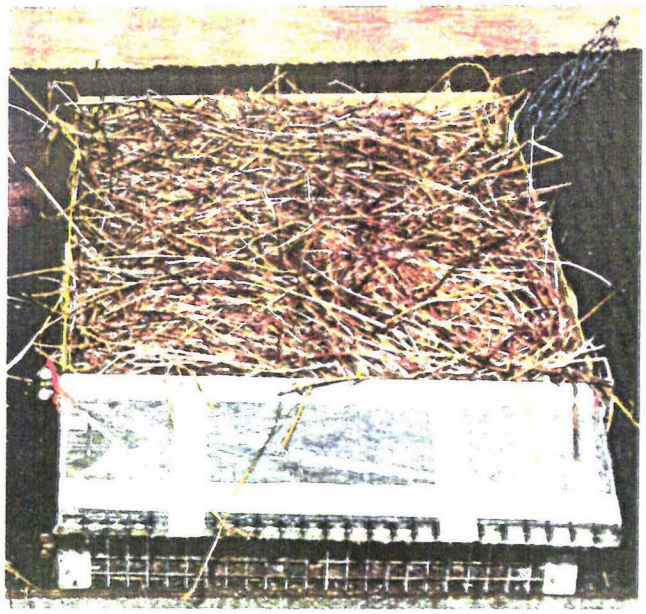

Plate 5. Straw mulch covered runoff plot.

*g. Sediment-runoff concentration*

The sediment-runoff concentration was determined by dividing the mean mass of sediment by the mean volume of runoff from each five minute interval.

*h. Infiltration rate*

The infiltration rate is the volume flux of water flowing into the profile per unit of soil area. In this study it was calculated from a simple water balance equation, the difference between rainfall and runoff.

## Data analysis methods

*a. Rainfall uniformity*

Catch-can data was used to derive Christenson's Coefficient. This is defined as a coefficient of variation for a specified area and was determined by a computer programme written by Hairsine (unpublished).

*b. Runoff volume and rate of runoff*

A Mitscherlich Function (Bowden and Bennett, 1974) was fitted to the mean results of runoff volume over 5 minute intervals for each soil type. The following conditions were applied:

1. $V = 0$ at $T = 0$, and
2. $V \rightarrow V_{max}$ as $T \rightarrow \infty$

where:

V is the runoff volume yield ($V \geq 0$) ($cm^3$)

T is the time from the commencement of rain ($T \geq 0$) (minutes)

$V_{max}$ equals 1100 $cm^3$.

$V_{max}$ is obtained when runoff output equals rainfall input, therefore infiltration is zero. The amount of water falling onto the soil tray in any five minute interval was calculated by multiplying the rainfall intensity with the surface area of the soil tray.

The Mitscherlich functions applied to the runoff volume over time were:

$$V = V_{max} (1-\exp^{(a + bT)T}) \quad (5)$$

$$V = V_{max}(1-\exp^{(aT)}) \quad (6)$$

where V is the runoff volume yield, $V_{max}$ is a maximum yield (1100 $cm^3$), a and b are curvature coefficients, and T is the time.

The consequential requirements on the fitted functions (5) and (6) are:

for equation (5), $(a + bT) < 0$, for all $T > 0$.

Therefore a and $b < 0$.

for equation (6), $a < 0$.

If the requirements from equation (5) failed due to b being calculated greater than zero, equation (6) was preferred. This occurred for the Tokomaru soil.

For the three soil types the following statistics were determined:

(1) The regression coefficient.

(2) The sample standard deviation.

(3) The standard error.

Since the fitted curves for the three soils approach the asymptote $V_{max}$ = 1100 $cm^3$ as time approaches infinity, the time T* at which $0.99V_{max}$ (when V = 1089 $cm^3$) is achieved was calculated.

*c. Mass of Sediment eroded over time*

The Mitscherlich function (Bowden and Bennett, 1974) similar to that used to fit runoff volume over time was fitted to the mean results from the mass of sediment eroded over 5 minute intervals for each soil. The following conditions were applied:

1. $S = 0$ at $T = 0$, and
2. $S \rightarrow S_{max}$ as $T \rightarrow \infty$

where:

S is the sediment yield ($S \geq 0$) (grams),

T is the time from commencement of rainfall (minutes), and

$S_{max}$ is the asymptotic sediment yield.

The function equations fitted for the mass of sediment eroded over time were:

$$S = S_{max}(1-\exp^{(a + bT)T}) \qquad (7)$$

$$S = S_{max}(1-\exp^{(aT)}) \qquad (8)$$

where S is the mass of sediment yield, $S_{max}$ is an asymptotic yield, a and b are curvature coefficients and T is the time from commencement of rainfall.

The consequential requirements on the fitted functions (7) and (8) are the same as for equations (5) and (6).

The statistics determined from the mass of sediment over time for each soil are the same as those calculated for the runoff volume over time (ie. the regression coefficient, standard deviation and the standard error).

The time T* at which $0.99S_{max}$ is achieved for each soil type was also calculated.

## Results and Discussion

### *a. Rainfall uniformity*

Figure 2 represents a three-dimensional graph of the rainfall distribution over the tilting tray platform. The position of the two soil trays during a rainfall event is shown. The Christenson's coefficient from the soil tray area was calculated 87%.

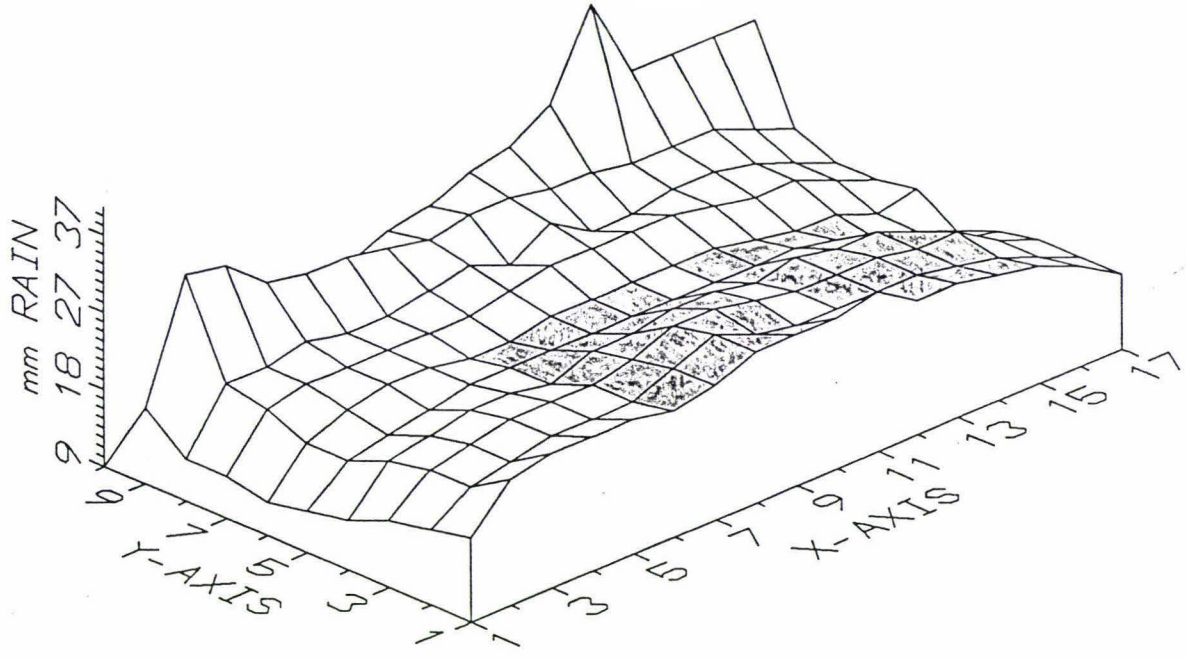


Figure 2. The rainfall distribution over the tilting tray platform and the positions of the soil trays.

### *b. Volume of rain applied*

A rainfall intensity of 65 mm hour$^{-1}$ deposits 1100 cm$^3$ of water on the soil's surface area of 0.2 m$^2$ in a 5 minute interval. This water is then available for either infiltration or runoff.

*c. Runoff volume over time*

Figures 3a, 3b and 3c represent the runoff volume displaced in each five minute interval and the mean runoff rate over time for the Kiwitea, Levin and Tokomaru soils respectively. The solid curves are the fitted function values, while the crosses represent the mean values from all runs for that soil type. The line, $V_{max}$ = 1100 $cm^3$ corresponds to the amount of rain applied in each five minute interval. The mean runoff rate is the volume of runoff per unit surface area available for runoff per unit time ($m^3$ $m^{-2}$ $sec^{-1}$). For each soil type, the volume of runoff increased until a constant rate was attained. Laflen *et al.* (1978), Loch and Donnollan (1982a) and Young and Wiersma (1973) found similar patterns with runoff volume over time. Achieving a constant runoff rate can be attributed to soil saturation and or surface sealing (or crusting). Both these phenomena inhibit the infiltration rate.

Surface crusting was observed on all three soils. However the severity was greatest for the Levin soil, while the Kiwitea soil suffered the least. The observed variations between the actual runoff values and the fitted curves shown in Figures 3a, 3b and 3c can be attributed to changes in storage depression and surface detention, a direct consequence of surface crusting. The processes occurring at the surface have been explained by many researchers (Bradford *et al.*, 1986). Initially, rapid wetting of the surface soil breaks down aggregates by raindrop impact (splashing) and sometimes by slaking. If dispersion takes place, the detached fine material is then washed into the surface pores and their volume is reduced. After aggregate breakdown, raindrop impact causes surface compaction, producing a thin skin or crust. Typically, the crust's bulk density is increased and its permeability is reduced relative to the underlying soil. Because the surface soil's permeability is reduced, excess water accumulates. This cushions raindrop impact and thereby reduces the rate of splash detachment. With time, part of the crust may be removed by the turbulence of the water above it. This effectively increases the soils permeability and enables the percolation of sufficient water to cause the dissipation of raindrop energy on the soil once more. Hence, again there is an increase in splash detachment. The process is then repeated. The greatest variations between actual runoff values and the fitted curves shown in Figures 3a, 3b and 3c occurred for the Levin soil after the

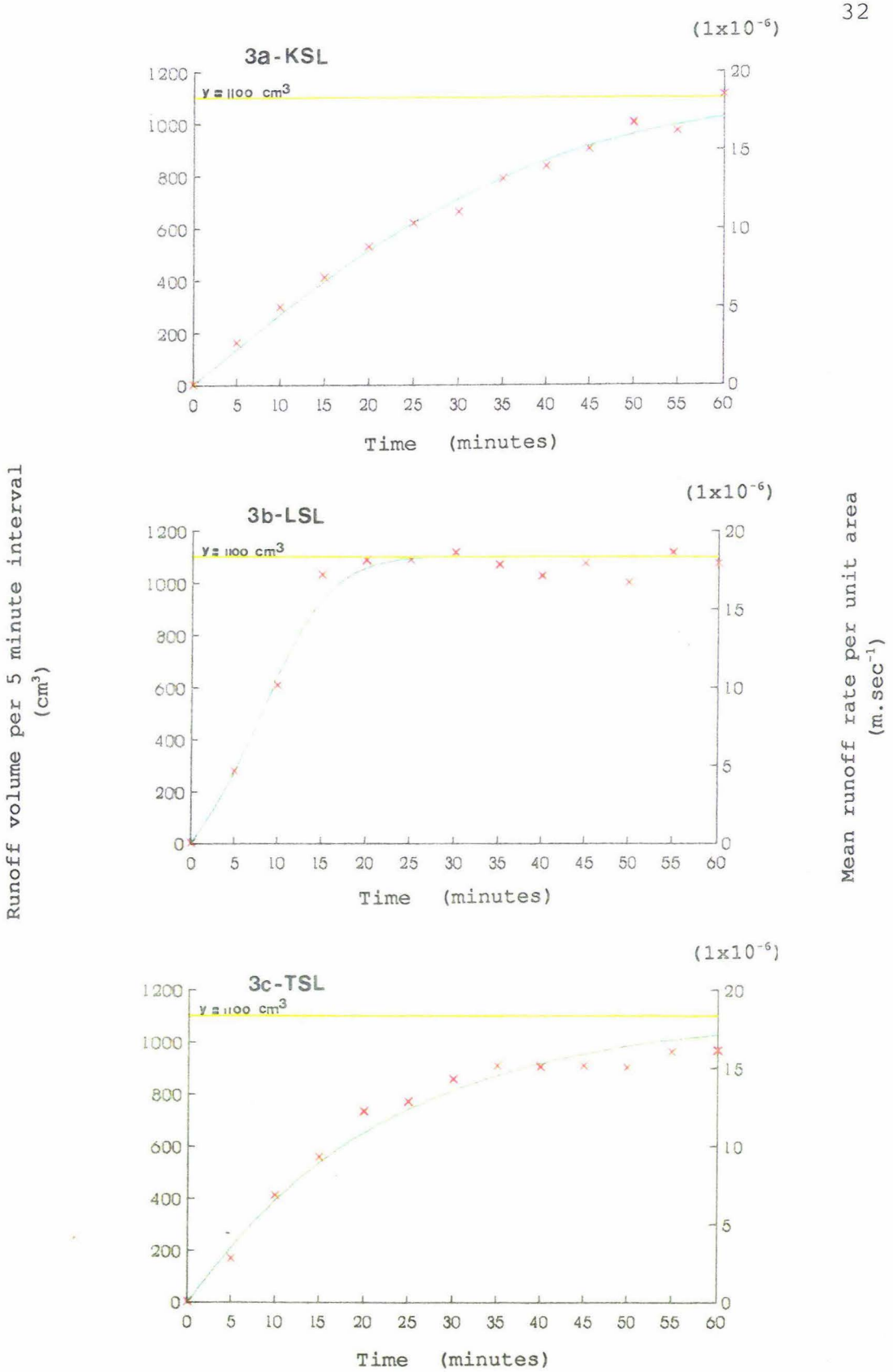


Figure 3a, 3b, and 3c. The runoff volume over time for the three soils. The solid line represents the fitted function values and the crosses represent the mean runoff values from all runs.

mean runoff rate had become constant. The commencement of this constant rate corresponds to when surface crusting was fully developed. Hereafter, the actual variations of values from the fitted function curve occurred through the processes described above. The actual runoff values from Kiwitea soil showed very little variation from the fitted function curve (Figure 3a). This was because a negligible amount of surface crusting was observed. The actual runoff rate for the Tokomaru soil (Figure 3c) seemed to reach a constant rate slightly lower than the fitted function curve and somewhat lower than $V_{max}$ of 1100 $cm^3$. This indicates that the erosive nature of the rainstorm did not fully restrict the Tokomaru soils permeability over the 60 minute period.

The runoff volume fitted function curvature coefficients for each soil type are shown in Table 2, along with the $R^2$ values calculated for n-1 degrees of freedom. The $R^2$ values in brackets were obtained from the function equation (6) when equation (5) was preferred (due to the curvature coefficient b being negative). As shown in Table 2, $R^2$ is improved using equation (5) when equation (6) was possible.

Table 2. The runoff volume curvature coefficients for fitted functions

| Soil Type | Curvature coefficients | | $R^2$ |
|---|---|---|---|
| | a | b | |
| Kiwitea | -0.02520 | -0.00032 | 98.8 % (97.3 %)[1] |
| Levin | -0.00504 | -0.00897 | 98.0 % (93.5 %)[1] |
| Tokomaru | -0.04520 | 0 | 97.6 % |

$R^2$ was adjusted for n-1 degrees of freedom.
(note 1: the $R^2$ values in brackets and the Tokomaru soil value were calculated using equation (6)).

Table 3 shows the statistics calculated for the fitted function and the mean values from all runs for each soil type. The standard errors for the Kiwitea and the Tokomaru soils were lower than the Levin soil because of their larger sampling size (n).

Table 3. Runoff volume statistics

| Soil Type | n | $r^2$ | s | SE |
|---|---|---|---|---|
| Kiwitea | 8 | 98.9 | 37.5 | 13.3 |
| Levin | 6 | 98.2 | 50.9 | 20.8 |
| Tokomaru | 10 | 97.6 | 48.9 | 15.5 |

Figure 4 shows the three soils fitted function curves for runoff volume over time. The volume of rainfall for each 5 minute interval is also included. T* from the Levin soil represents the time in which 0.99 $V_{max}$ was obtained. Table 4 shows the calculated T* for the three soils when T = 0.99$V_{max}$ ($V_{max}$ = 1100 $cm^3$). The times in which T* were reached are dependent on the soil's textural composition, organic matter content and aggregate stability. These are discussed in later chapters.

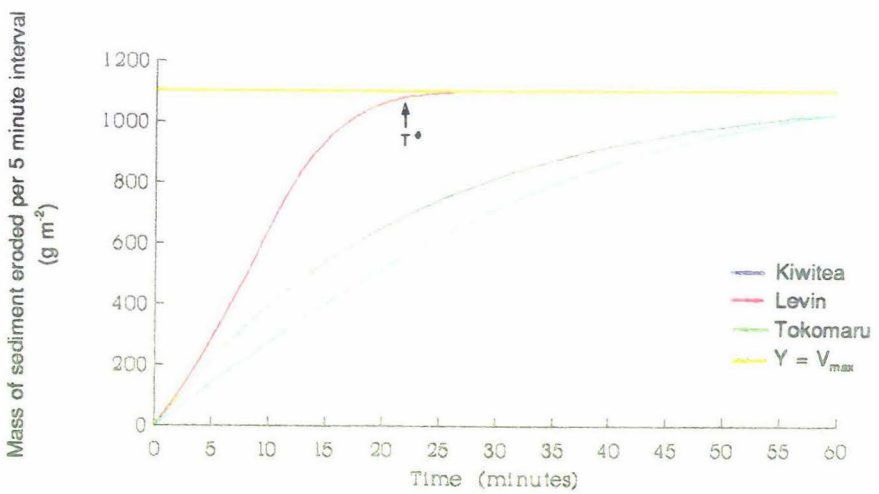


Figure 4. The fitted function curves for runoff volume over time from the three soils. The calculated T* value for the Levin soil is also shown.

Table 4. The calculated T* values for runoff volume when T = 0.99$V_{max}$ ($V_{max}$ = 1100 $cm^3$)

| Soil Type | T* (minutes) |
|---|---|
| Kiwitea | 101.9 |
| Levin | 22.9 |
| Tokomaru | 164.6 |

*d. Mass of sediment eroded over time*

The mass of sediment eroded in each 5 minute interval for the three soils is shown in Figures 5a, 5b and 5c. The solid line represents the fitted function values while the crosses are the mean values from all runs for that individual time period. Also shown on these figures is the equivalent depth of soil eroded during each 5 minute interval.

Table 5 shows the curvature coefficients and the $R^2$ values for the fitted functions from the three soils. The $R^2$ values were calculated for n-1 degrees of freedom. The values in brackets were determined using the function equation (8) when equation (7) was possible.

Table 5. Mass of sediment curvature coefficients for the fitted functions

| Soil Type | $S_{max}$ | Curvature Coefficients | | $R^2$ |
|---|---|---|---|---|
| | | a | b | |
| Kiwitea | 22.1 | -0.02243 | 0 | 97.4 % |
| Levin | 31.9 | -0.22164 | -0.01217 | 98.0 % (96.1 %)[1] |
| Tokomaru | 19.1 | -0.04632 | -0.00583 | 98.9 % (96.5 %)[1] |

$R^2$ was adjusted for n-1 degrees of freedom.
(note 1: the $R^2$ values in brackets calculated from equation (8)).

Statistics calculated from the fitted function and the mean values for all runs are reported in Table 6. The sample standard deviation calculated for the Levin soil was much greater than those of the Kiwitea and the Tokomaru soils. This can be attributed to the large variation in values when the mass of sediment eroded plateaued out, and the smaller sampling size for the Levin soil.

Table 6. Mass of sediment statistics

| Soil Type | n | $r^2$ | s | SE |
|---|---|---|---|---|
| Kiwitea | 8 | 97.4 | 0.87 | 0.31 |
| Levin | 6 | 98.4 | 1.43 | 0.58 |
| Tokomaru | 10 | 99.1 | 0.64 | 0.20 |

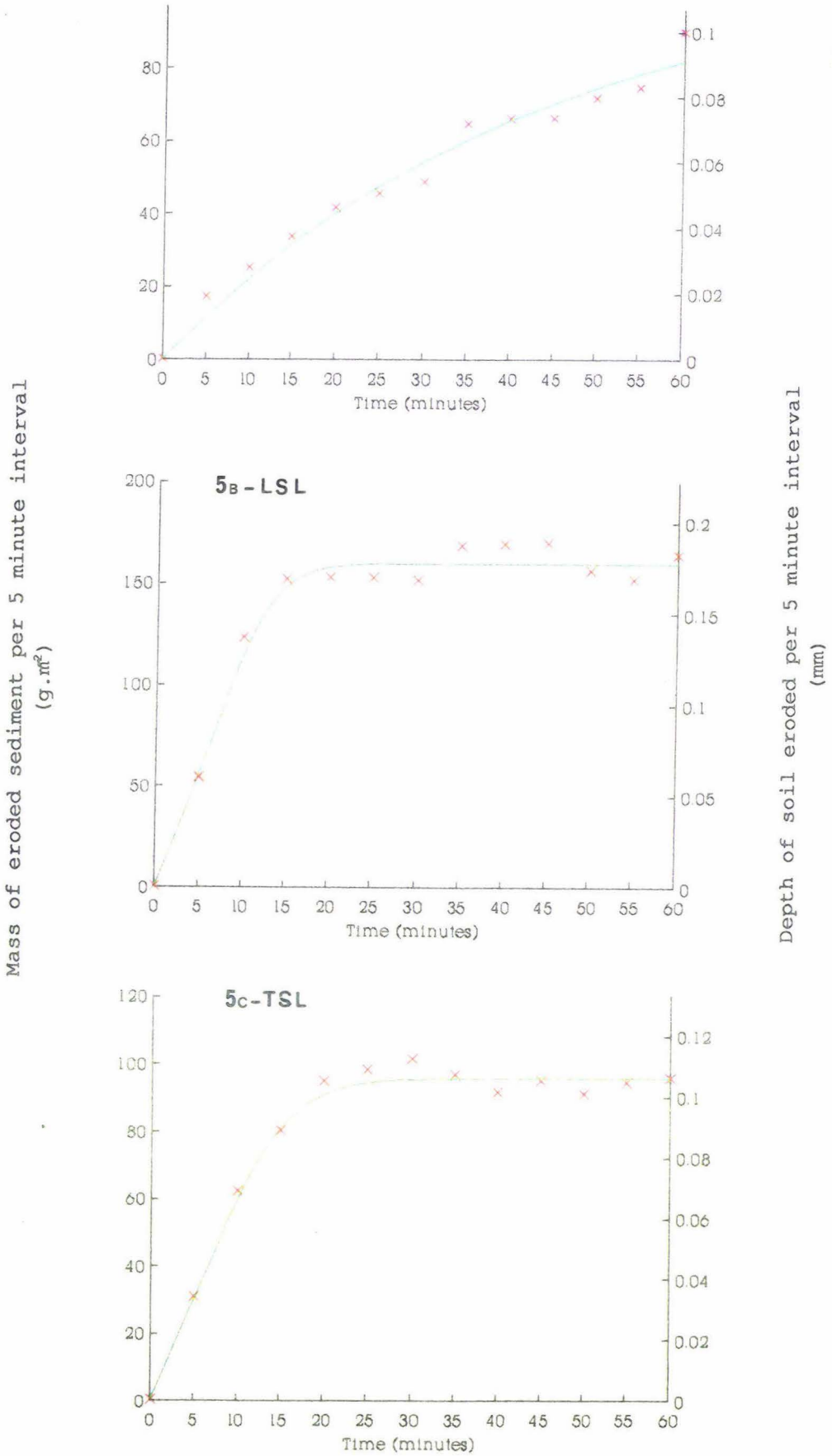


Figure 5a, 5b, and 5c. The mass of sediment eroded over time for the three soil types and the equivalent depth of soil eroded during each five minute rainfall period. The solid line represents the fitted function values and the crosses represent the mean values from all runs.

The fitted functions showed that the mass of sediment eroded over time increased and then plateaued out to some constant value characteristic of that soil type. This constant value was dependent on the textural composition, organic matter and the aggregate stability for each soil. The reduction in the rate of soil loss to a constant value was attributable to the build up of water present on the soil surface. The increase in surface water present resulted from the reduction in permeability due to soil saturation and surface crusting. As mentioned earlier, surface water cushions raindrop impact and reduces splash detachment. The variations between the actual mass of sediment eroded and the fitted curves shown in Figures 5a, 5b and 5c can again be attributed to the processes occurring at the soil surface, particularly the interactions between soil crusting and excess surface water.

Fluctuations in sediment eroded and runoff volume occurred at similar times for the Kiwitea and the Tokomaru soils. However, for the Levin soil, it was common for variations of eroded sediment to be associated with runoff volume variations, but in the opposite direction. Possible explanations for these phenomena are discussed in a later section on sediment-runoff concentration.

The fitted function curves for the three soils are shown in Figure 6. $T^*$ represents the time at which $0.99S_{max}$ was obtained. The values for $0.99S_{max}$ and times of $T^*$ for the three soils are reported in Table 7. Table 8 shows the total equivalent depth (mm) of topsoil eroded in 60 minutes for the three soils. The eroded depth for the Levin soil was considerably greater than those obtained for the other two soils. This can be attributed $T^*$ being achieved earlier and to a greater extent for the Levin soil compared to the Kiwitea and Tokomaru soils. This was due to textural composition, aggregate stability and the organic matter content. Rating the three soils on the depth of topsoil eroded in 60 minutes, $T^*$ times, and the values of $0.99S_{max}$ indicates that the Levin soil was more erodible than the Tokomaru soil, while the Kiwitea soil was the least erodible soil.

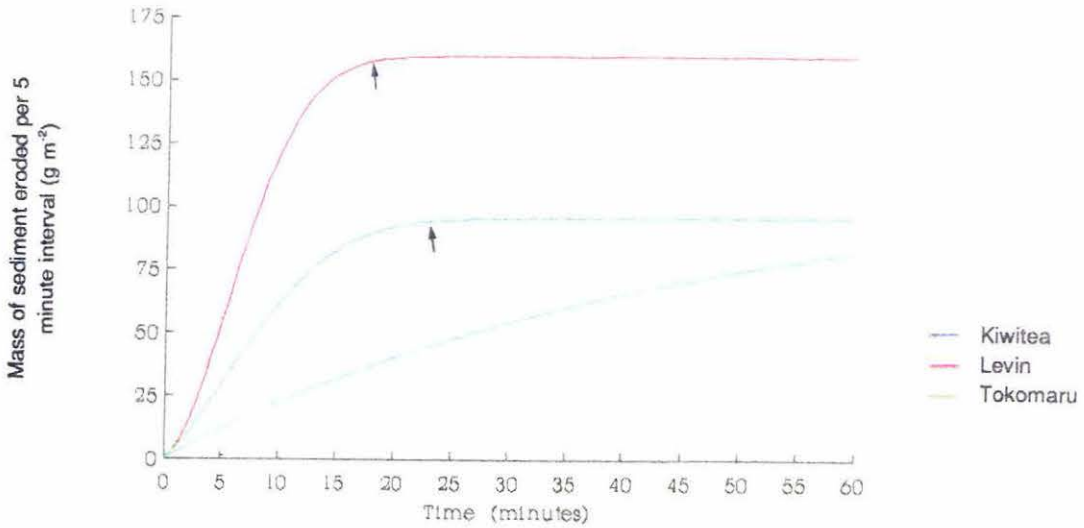


Figure 6. The fitted function curves for the mass of sediment eroded over time from the three soils. The arrows represent the calculated T* values.

Table 7. The calculated T* values for mass of sediment when $T = 0.99S_{max}$

| Soil type | $S_{max}$ ($g.m^{-2}$) | $0.99S_{max}$ ($g.m^{-2}$) | T* (minutes) |
|---|---|---|---|
| Kiwitea | 110.5 | 109.4 | 205.3 |
| Levin | 159.5 | 157.9 | 18.6 |
| Tokomaru | 95.4 | 94.5 | 22.7 |

Table 8. The equivalent depth of topsoil eroded in 60 minutes.

| Soil type | Depth of topsoil eroded (mm) |
|---|---|
| Kiwitea | 0.715 |
| Levin | 1.951 |
| Tokomaru | 1.144 |

*e. Infiltration rate*

Infiltration rate is defined as the volume flux of water flowing into the profile per unit area. It is affected by textural composition, organic matter content, soil structure and the aggregate stability.

Hillel (1982) showed infiltration rate to be relatively high initially, then decrease and eventually reach a constant rate that is characteristic of the soil profile. In this study, as shown by Figure 7, similar patterns to these were observed. At the start of the rainfall period the soil surface was highly porus and of open structure which resulted in the soil absorbing the majority of the applied rain. However as time proceeded, the soils infiltration rate decreased. This can be attributed to the soil profile becoming saturated, the beating action of raindrops causing surface crusting or sealing, or as the result of spontaneous slaking and soil aggregate breakdown during wetting. When the infiltration rate curve flattens out to a constant rate, the soil has reached its saturated hydraulic conductivity. Figure 7 shows that the Levin soil achieved zero infiltration at the surface after 25 minutes. This was the result of surface crusting. Both Kiwitea and the Tokomaru soils had similar infiltration rates after 60 minutes of rainfall. These rates may approximate the soils saturated hydraulic conductivities since the rates of change of infiltrability at this time was not large.

Over the 60 minute rainfall period, Figure 7 shows that the infiltration rate was consistently higher for the Kiwitea soil than the Tokomaru and the Levin soils. The Tokomaru soil was considerably greater than the Levin soil. This indicates that the Kiwitea soil was more permeable than the Tokomaru soil, of which was considerably more permeable than the Levin soil.

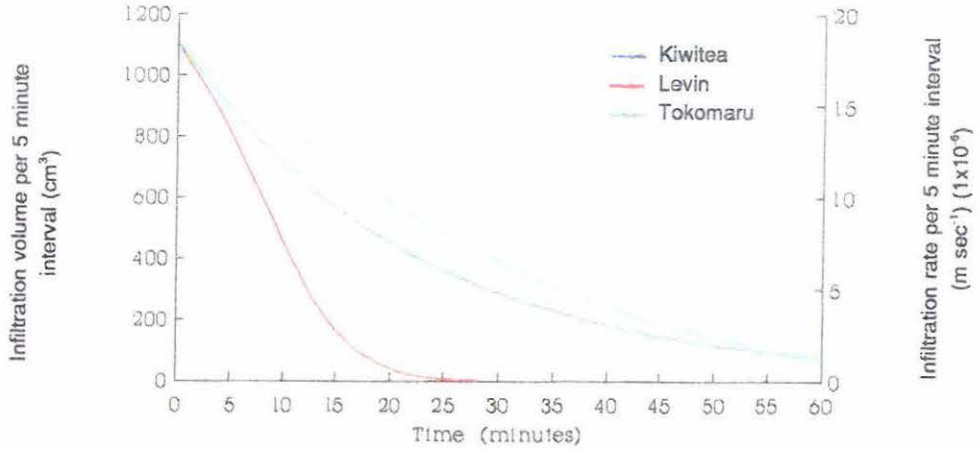


Figure 7. The infiltration volume per each 5 minute interval over the 60 minute rainfall period from the three soils.

### *f. Sediment-runoff concentration*

Figure 8 displays the sediment-runoff concentrations from each 5 minute interval for the three soils.

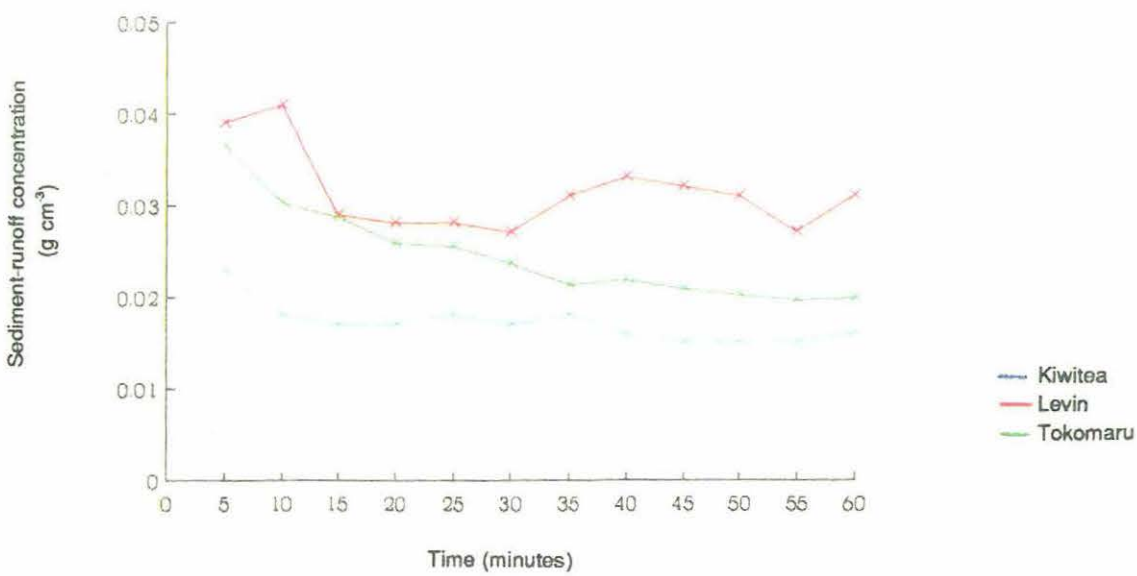


Figure 8. The sediment runoff concentration over the rainfall period from the three soils.

The observed sediment-runoff concentration values at the start of the rainfall event for each of the three soils were greater than those at the end of the rainfall period. Similar patterns were reported by Laflen *et al.* (1978), Loch and Donnollan (1982a) and Young and Wiersma (1973). Initially, soil particles are more easily detached by rainsplash because the soil is yet to become fully saturated, nor has soil crusting developed to an extent to which it inhibits infiltration and enables the build up of a protecting surface layer of water. Without this surface layer of water cushioning splash detachment, the runoff volume is enriched with fine particles.

Over the 60 minute period, Figure 8 shows there was a gradual reduction in sediment-runoff concentration for the Kiwitea and Tokomaru soils. This can be attributed to a decline in infiltration resulting in surface water cushioning splash detachment. However for the Levin soil, Figure 8 showed that the sediment-runoff concentration fluctuated. This can be explained by the early attainment and the greater extent of surface crusting observed for the Levin soil compared to the other two soils. Hence the effect of the cyclic processes occurring at the Levin soil's surface, as described earlier, would be magnified.

Figure 8 shows the Levin soil to have the highest sediment-runoff concentration over the 60 minute period while the Kiwitea soil has the lowest. Similar patterns were found for infiltration, mass of sediment eroded, and the time at which T* was obtained for both eroded sediment and runoff. Again, this can be explained by aggregate stability, soil texture and the organic matter content of the soil.

### *g. Mulch cover and bare soil comparisons*

The variations in the runoff volume and the mass of sediment eroded in each 5 minute interval for bare soil and the barley straw mulch from the Levin soil are shown in Figure 9. Because the mass of sediment varies between the two treatments by a factor in excess of 100, a log scale has been used in Figure 9 to enhance the comparison between the two surface conditions. The runoff volume and mass of sediment graphs for the bare soil are from the fitted function results. The barley straw mulch data are means from 4 simulated rainfall runs.

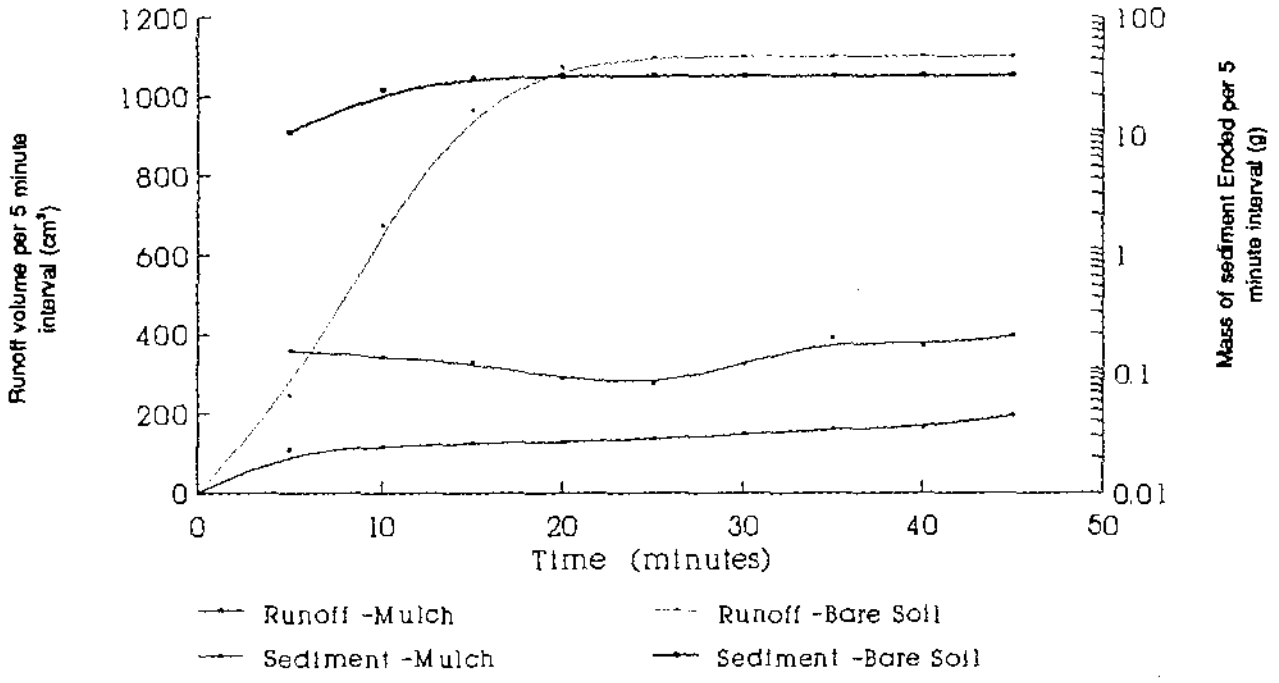


Figure 9. A comparison of the runoff volume and mass of sediment eroded between a mulch cover and a bare soil surface from the Levin soil.

Comparing barley mulch cover with bare soil shows that runoff rate and sediment eroded over time were reduced by orders of magnitude for the mulch covered soil. This resulted from the straw mulch directly intercepting the raindrops and reducing the effect of raindrop impact. Consequently soil detachment was reduced. Splashed soil particles were also intercepted as they leave the eroding surface. There was also an decrease in the flow path lengths of runoff. Localized damming of runoff caused a reduction in flow velocities and the entrainment of surface soil. Consequently, the deposition of transported material was reduced. Infiltration was also increased because the effect of surface crusting was diminished.

**Summary**

1. Over the 60 minute rainfall period, both the mass of sediment eroded and the runoff volume generated increased and then plateaued to some constant rate characteristic of the soil type. These constant values were determined by fitting Mitscherlich function curves to the mean results.

2. A constant runoff rate was achieved when the amount of rain applied and the runoff volume generated are equal. This occurrence can be attributed to soil saturation and or surface crusting (or surface sealing).

3. Surface crusting was observed on all three soils, however the severity was greatest from the Levin soil while the Kiwitea soil suffered the least.

4. The observed variations between actual runoff volume and the fitted function curves can be attributed to the changes in surface depression and surface detention, a direct consequence to the cyclic processes of surface crusting.

5. The 0.99 $V_{max}$ value was reached earlier for the Levin soil. The other two soils failed to reach this value within the 60 minute rainfall period. These results are consistent with the observed degree of surface crusting for each soil.

6. The reduction in the rate of soil loss to a constant value can be attributed to the build up of water present on the soil surface. This resulted from the reduction in the soil's permeability due to soil saturation and surface crusting. Surface water effectively cushions raindrop impact and therefore reduces splash detachment.

7. The variations between the actual mass of sediment eroded and the fitted function curve can be attributed to the interactions between surface crusting and excess surface water.

8. The Levin soil reached 0.99 $S_{max}$ earlier than the other two soils. The

Kiwitea soil was the slowest. Similar trends occurred for the depth of topsoil eroded over the 60 minute period.

9. Infiltration rate decreased with time due to soil saturation and surface crusting.

10. Infiltration rate was consistently higher for the Kiwitea soil, while the Levin soil was the least permeable soil.

11. The sediment-runoff concentration at the start of the rainfall period for the three soils was greater than that after 60 minutes. The higher sediment load initially resulted from soil particles being more easily detached by rainsplash. After 60 minutes, the build-up of surface water inhibits splash detachment.

12. A fluctuation in sediment-runoff concentration can be explained by the cyclic processes of surface crusting. Also, the greater the effect of surface crusting, the larger the fluctuations.

13. A mulch cover severely reduces the amount of runoff volume and sediment yield by intercepting and cushioning raindrop impact. This effectively inhibits surface crusting and promotes infiltration. Runoff flow velocities were reduced and therefore so was the stream power available to entrain sediment.

# Chapter Three

# Surface Erosion and Particle Selectivity

## Introduction

Most agricultural soils are cohesive and have agents that bond primary particles of sand, silt and clay into aggregates (Young, 1980). Eroded sediment is composed of a mixture of aggregates and primary particles. Erosion selectively removes fine soil particles and leaves coarse ones through the processes of detachment, transport and deposition of particles (Foster *et al.*, 1985).

Soil type, textural composition, slope, soil surface conditions and the erosion processes occurring affect the aggregate size distribution and composition of the sediment eroded from the soil matrix.

Particle selectivity occurs because interrill flow does not have sufficient energy to transport many of the sand-size and larger aggregates. Hence, interrill flow is "transport limiting" (Alberts *et al.*, 1980, 1983). Transport limiting flow implies that sediment characteristics which are not directly associated to soil strength, but dependant on the slope and flow characteristics, determine the sediment concentration. Rill flow is seldom transport limiting, thus very large aggregates can be transported.

Textural composition refers to the proportion of individual mineral grains in a soil, i.e. the proportion of sand, silt and clay particles (Hillel, 1982). In soils, sand, silt and clay particles are defined by the size of the grains and not by their composition, colour, or their consistence. Hillel (1982) defined sand particles ranging from 2.0 mm to 0.06 mm in diameter and the grains are visible to the naked eye. Silt particles range from 0.06 mm to 0.002 mm in diameter, while clay particles are less than 0.002 mm in diameter. Soil contains particles of all sizes and the proportion of each size in a sample is determined by sieving and measuring the density of a suspension dispersed in water.

## Experimental Objectives

The objective of this study was to determine if soil particles were selectively eroded from the three soils (Kiwitea, Levin and the Tokomaru soils) subjected to simulated rainfall. This was ascertained by determining:

(1) if the textural composition of eroded sediment varied greatly from that of the original soil,

(2) if textural composition of eroded sediment changed between the start and end of the rainfall period, and

(3) if the size distribution of eroded particles and aggregates varied over time.

The organic matter contents of the three soils were also determined.

## Experimental methods

The three soils used in the experiments (Kiwitea, Levin and the Tokomaru soils) were subjected to simulated rainfall and eroded sediment was collected. The methods and procedures for operating the rainfall simulator were similar to those described in Chapter 2.

Sieving and sedimentation methods were used to determine textural composition. Aggregates were broken down and separated into primary particles. The proportions of these determined the textural composition. In determining the size distribution of eroded particles and aggregates over time, the eroded sediment material was not broken down and dispersed, but simply separated into the size fractions in which they were eroded.

### *a. Determining textural composition*

The textural composition of the soil, the sediment eroded over the entire rainfall period, and the sediment eroded in the first 20 minutes and last 10 minutes of the rainfall period were determined using sieving and sedimentation procedures for the three soils.

For determining the textural composition of the sediment eroded over the entire rainfall period, a sub-sample was taken from the bulk sediment eroded.

The initial 20 minute period and the final 10 minute period were chosen to represent the start and completion of an erosion event respectively. These times were chosen because they enabled the generation of sufficient sediment from the rainfall simulator for textural composition to be determined.

A combination of wet and dry sieving separated the primary particles coarser than 63 *u*m. A sedimentation procedure determined the fractions of clay and silt-size material. This involved taking a 20 ml sample from a dispersed column of sediment at set times and depth with a pipette. The process is based on particles of different sizes settling out through the liquid column at differing rates. This phenomenon is explained by Stokes law (Hillel, 1982). According to Stoke's law, the terminal velocity of a spherical particle settling under the influence of gravity in a fluid of a given density and viscosity is proportional to the square of the particle's radius.

These sieving and sedimentation procedures for particle size analysis have been adopted from Day (1965) and are the standard methods used by the Department of Soil Science, Massey University. Appendix 1 describes the full procedure.

The pre-treatment of samples

Organic matter within soil aggregates has the tendency to bind primary particles together and prevent dispersion. Therefore samples are pre-treated to enhance separation or dispersion of aggregates into primary particles. Removal of organic matter is often the first step in the chemical pre-treatment of soil samples. The most common chemical reagent for organic matter oxidation is hydrogen peroxide ($H_2O_2$). Increasing concentrations of this gradually destroys the organic matter content.

Dispersion of soils is accomplished by a combination of methods. These methods can be either chemical or physical. Chemical dispersion is based primarily on the phenomenon of particle repulsion, as a result of elevation of the

particle zeta potential. This process is usually accomplished by saturating the exchange complex with sodium ions. Physical or mechanical methods of dispersion involve separation of the individual particles by some mechanical or physical process, such as rubbing, rolling, shaking, or vibrating.

This study used a combination of physical and chemical methods for dispersion of aggregates into their primary particles. The physical method used was a laboratory blender. The chemical dispersant used was calgon, a mixture of sodium hexametaphosphate and sodium carbonate (described in Appendix 1).

*b. Determining Size Distribution of Eroded Particles and Aggregates*

The proportion of sand, silt and clay size particles or aggregates in a sample determines its the particle size distribution.

Runoff and eroded sediment samples were collected at five minute intervals from repacked soil trays exposed to simulated rain in the same manner as described in Chapter 2. These samples were then passed through a 63 um sieve to separate the coarse material from the fines. The coarse material was then oven dried at 65°C for 48 hours to determine its mass. The fines were transferred into a 500 ml cylinder and the volume was made up to 500 ml with distilled water.

At set times and depth, 20 ml aliquots were taken using a pipette. The sub-sample was oven dried at 65°C for 48 hours. This procedure is the same as the sedimentation method using a pipette for day five as described in Appendix 1.

*c. Determining the organic matter contents*

The percentage of organic carbon was determined by pyrolitic burning. The standard procedure for this is described by Nelson and Sommers (1982).

## Statistical analysis

In this study, the textural composition of two sub-samples for sediment eroded from the start, completion and the total rainfall period, and four samples from the original soil were determined. A two tailed t-statistic test at a 5% significance level, as described by Snedecor and Cockran (1980), was used to make comparisons between the original soil and eroded sediment.

The results of the two tailed t-statistic test comparing the textural composition of eroded sediment and the original soil from each soil type are reported in Tables 10a to 10c. Table 12 compares the textural composition of the eroded sediment between the start and end of the rainfall period for the three soil types. The symbols used for levels of significant differences in this study were: NS = $P \geq 0.05$ and * = $0.05 \geq P$. Other symbols used include: $T_{0\text{-}20\ min.}$ is the rainfall period from 0 to 20 minutes (the start of the rainfall period), $T_{50\text{-}60\ min.}$ is the rainfall period from 50 to 60 minutes (the end of the rainfall period, and $T_{0\text{-}60\ min.}$ is the rainfall period from 0 to 60 minutes (the total rainfall period).

## Results and Discussion

### *a. Organic matter content of the original soil*

Using the pyrolitic burning technique, the percentages of organic carbon present in each of the original soils is shown in Table 10. Particle aggregation is enhanced by organic carbon (Hillel, 1982).

Table 9. The organic carbon contents from the original soils

| Soil Type | Percent Organic Carbon |
|---|---|
| Kiwitea | 3.47 |
| Levin | 4.32 |
| Tokomaru | 2.34 |

*b. Textural composition of the original soil*

Figure 10 shows the proportions of primary particles for the three soils. The Levin soil has much lower percentages of clay and silt, and a higher percentage of sand compared with the Kiwitea and the Tokomaru soils. The lower percentage of clay suggests the soil has a reduced particle binding capacity. This may be expected to increase the Levin silt loam's susceptibility to particle detachment and entrainment. Sand particles are non-cohesive. Therefore, the higher percent of sand-size particles present in the Levin soil suggests particle aggregation would be lower compared with the other two soils.

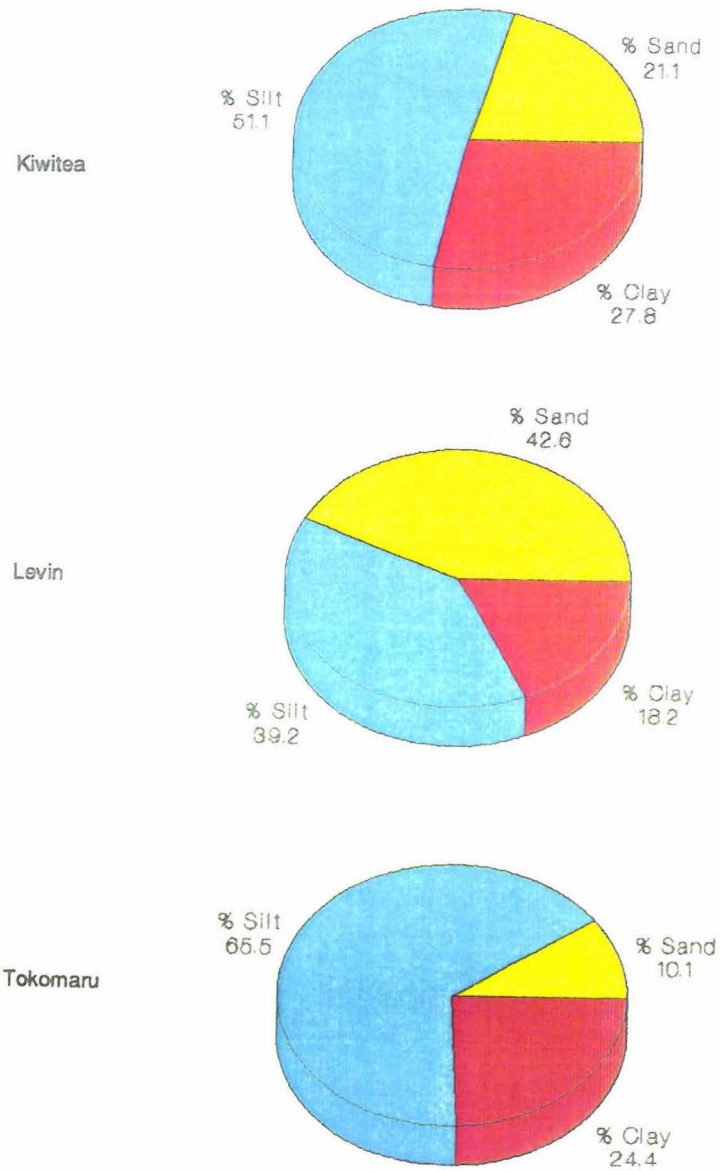


Figure 10. The textural composition of the original soils

*c. Comparing the textural composition of eroded sediment with the original soil*

The deviations in primary particle composition of eroded sediment from the beginning (0 to 20 minutes), end (50 to 60 minutes) and the total rainfall period (0-60 minutes), from the original soil for the three soils are shown in Tables 10a, 10b and 10c. Also shown are the level of significant differences.

Table 10a. Comparing the eroded sediment at the different rainfall periods with the original soil for the Kiwitea soil.

| Rainfall Period | Particle Size | | | | | |
|---|---|---|---|---|---|---|
| | Sand | | Silt | | Clay | |
| $T_{0\text{-}20\ min.}$ | -0.9 % | NS | -9.6 % | * | 18.3 % | * |
| $T_{50\text{-}60\ min.}$ | -2.9 % | NS | -12.7 % | * | 25.5 % | * |
| $T_{0\text{-}60\ min.}$ | -1.9 % | NS | -5.5 % | NS | 11.5 % | * |

Table 10b. Comparing the eroded sediment at the different rainfall periods with the original soil for the Levin soil.

| Rainfall Period | Particle Size | | | | | |
|---|---|---|---|---|---|---|
| | Sand | | Silt | | Clay | |
| $T_{0\text{-}20\ min.}$ | -36.5 % | * | 12.8 % | * | 58.0 % | * |
| $T_{50\text{-}60\ min.}$ | -13.2 % | * | 8.8 % | NS | 11.9 % | NS |
| $T_{0\text{-}60\ min.}$ | -17.0 % | * | 10.1 % | NS | 18.1 % | * |

Table 10c. Comparing the eroded sediment at the different rainfall periods with the original soil for the Tokomaru soil.

| Rainfall Period | Particle Size | | | | | |
|---|---|---|---|---|---|---|
| | Sand | | Silt | | Clay | |
| $T_{0\text{-}20\ min.}$ | -25.0 % | * | -3.2 % | NS | 19.1 % | * |
| $T_{50\text{-}60\ min.}$ | -37.8 % | * | 3.0 % | NS | 7.7 % | NS |
| $T_{0\text{-}60\ min.}$ | -30.2 % | * | 0.4 % | NS | 11.5 % | * |

The proportion of sand from the eroded sediment in each period (Tables 10a, 10b and 10c) was always less than the original soil. However, it was only significantly lower for all periods from the Levin and Tokomaru soils. The reduced sand content of the eroded sediment can be explained by the difficulty in which primary sand particles are entrained into overland flow. This can be attributed to the size and weight of sand particles.

The eroded sediment silt content from the Kiwitea soil for the three periods was always lower than the original soil. Both the 0 to 20 minute and the 50 to 60 minute periods were significantly lower. This can be attributed to its high clay content and clay type, allophane. A feature of allophanic soils is their ability to form stable aggregates and the inability of these aggregates to disperse under physical force (Tuohy, 1980). Therefore, silt particles from the Kiwitea soil less readily detached by rainsplash due to their more stable aggregates.

The silt content found in the eroded sediment from the Levin soil was always greater than the original soil, however only the 0 to 20 minute period was significantly larger. This increase may be attributed to the low clay and high sand contents present in the original soil which results in less stable aggregates. Consequently silt particles are more easily detached by rainsplash and entrained into overland flow.

The eroded sediment silt content from the Tokomaru soil for the 0 to 20 minute period was lower than that of the original soil but greater for the 50 to 60 minute and the total rainfall period. However, none of the three periods differed significantly. This suggests that aggregate strength decreased over the rainfall period, a direct result of raindrop impact, and resulted in aggregate breakdown.

The three sampling periods from each soil type showed an increase in the proportion of clay present in the eroded sediment compared to the original soil (Tables 10a, 10b and 10c). All periods, except the 50-60 minute period from the Levin and Tokomaru soils were significantly greater than the original soil. This indicates that the dispersed clay enrichment ratio (ie. the proportion of dispersed clay present in the eroded sediment compared to the original soil) was always greater than one for each sampling period. These results are quantified in Table

11. Laflen *et al.* (1978) also found this ratio to be greater than one.

Table 11. The dispersed clay enrichment ratios for the three sampling periods from each soil type.

| The Dispersed Clay Enrichment Ratio Period | Soil type | | |
|---|---|---|---|
| | Kiwitea | Levin | Tokomaru |
| 0-20 minutes | 1.183 | 1.580 | 1.190 |
| 50-60 minutes | 1.255 | 1.119 | 1.080 |
| 0-60 minutes | 1.115 | 1.181 | 1.114 |

Table 11 shows that between the 0 to 20 minute period and the 50 to 60 minute period, the dispersed clay enrichment ratio for the Levin and Tokomaru soils decreased while the Kiwitea soil increased. The increase from the Kiwitea soil can be attributed to the high allophanic content, resulting in more structurally stable aggregates. These aggregates can only be entrained into overland flow when the transporting force is sufficiently large enough. The reduction in the dispersed clay enrichment ratio between the start and the end of the rainfall period from Levin soil reflects the ease in which soil particles were detached from the aggregates initially by rainsplash. At the start of the rainfall period there was insufficient surface water present to cushion raindrop impact. Consequently, the effect of aggregate slaking into smaller aggregates or particles during this period would be greatest. These smaller aggregates and particles are also more easily entrained into the shallow overland flow present initially. The dispersed clay enrichment ratio between the start and the end of the rainfall period from the Tokomaru soil decreased slightly, however the reduction was not significant.

A comparison of the eroded sediment between the start ($T_{0\text{-}20\ min.}$) and the end ($T_{50\text{-}60\ min.}$) of the rainfall period for the three soils is shown in Table 12. Only the sand content and the clay content from the Levin soil showed any significant change. The increase in the percent of sand eroded between the start and the end of the rainfall period from the Levin soil can be attributed to the attainment of overland flow caused by soil saturation. This would have resulted in the entrainment of sand particles. Although there was an increase in the amount of sand eroded between the two time periods, the amount of sand present in the $T_{50\text{-}60\ min.}$ period was still lower than that found in the original soil. The reduction

in the eroded clay contents between the start and the end of the rainfall period from the Levin soil again reflects the ease in which soil particles were detached from aggregates by rainsplash during the 0 to 20 minute period.

Table 12. A comparison of the eroded sediment between the two rainfall periods, $T_{0\text{-}20\ min.}$ and $T_{50\text{-}60\ min.}$

| Soil Type | Particle Size | | | | | |
|---|---|---|---|---|---|---|
| | Sand | | Silt | | Clay | |
| Kiwitea | -2.4 % | NS | -3.2 % | NS | 6.1 % | NS |
| Levin | 36.8 % | * | -3.5 % | NS | -40.8 % | * |
| Tokomaru | -17.0 % | NS | 6.4 % | NS | -9.5 % | NS |

*d. Distribution of eroded sediment size with time*

The dispersed sediment-size distribution is an indicator of fine-particle enrichment, surface area and chemicals transported with the sediment, but it is not appropriate for determining the transportability of the sediment during runoff (Meyer *et al.*, 1980). In this study, undispersed eroded sediment from each soil was separated into sand, silt and clay size fractions over five minute intervals. The results are shown in Figures 11a, 11b and 11c for the Kiwitea, Levin and Tokomaru soils respectively.

The proportion of eroded silt-size material (primary particles and aggregates) decreased rapidly during the early stages of the storm and reached an equilibrium constant value characteristic of the soil type. This equilibrium value for the three soils was 20-25% lower than the proportion of primary silt particles present in the original soil. The proportion of eroded silt-size material for the initial reading (T = 5 minutes) was similar to or slightly lower than the silt content of the original soil. The proportion of silt-size material was greatest at the start of the rainfall event. This could be attributed to the ease in which silt particles are detached by raindrop impact because of the low cohesive forces binding them together. Also, at the start of the rainfall period, the capacity of thin flows to transport sediment may be limited by the volume and velocity of the runoff. This would result in the selective removal of finer particles such as silt.

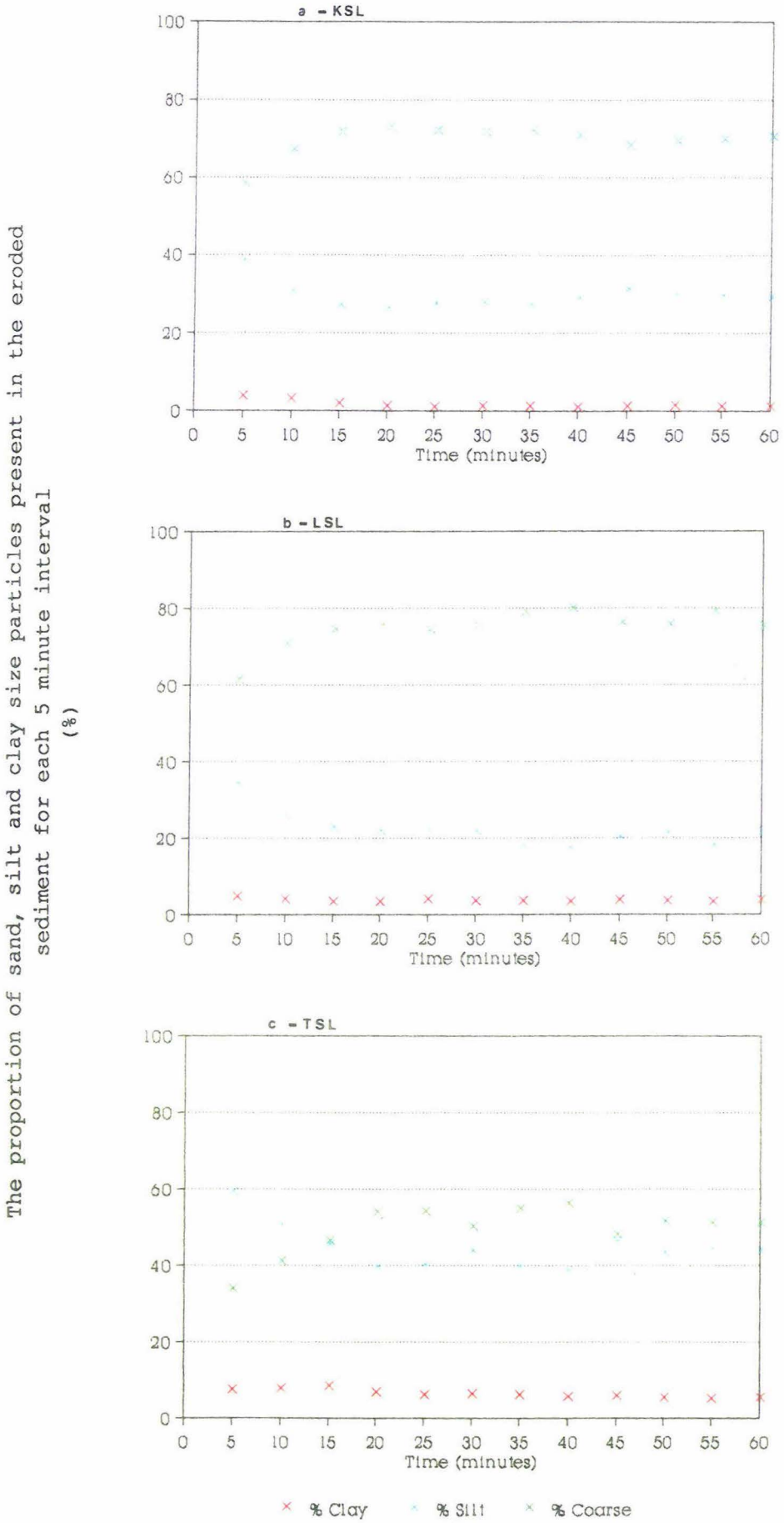


Figure 11a, 11b and 11c. The undispersed eroded sediment size fractions over the 60 minute rainfall period for the Kiwitea, Levin and Tokomaru soils respectively.

Figures 11a, 11b and 11c show that clay-size material was eroded at a constant rate. Gabriels and Moldenhauer (1978) reported similar trends. The proportion of undispersed clay-size material from the eroded sediment for the three soils were significantly lower than the dispersed clay content from the original soil. These results are displayed in Table 13, along with the dispersed clay enrichment ratios between the eroded sediment and the original soil.

Table 13. Comparing the dispersed and undispersed clay-size fractions from the eroded sediment with the dispersed clay fraction from the original soil.

| | Soil Type | | |
|---|---|---|---|
| | Kiwitea | Levin | Tokomaru |
| Clay enrichment ratio of dispersed particles (0-60 minutes) | 1.115 | 1.181 | 1.114 |
| The ratio of undispersed eroded sediment clay-size particles to the proportion of dispersed clay particles in the original soil (0-60 minutes) | 0.051 | 0.187 | 0.255 |

These results suggest that most of the clay is eroded in the form of aggregates and very little is transported as primary clay particles. This can be attributed to the bonding capacity of clay particles. Young and Onstad (1978), Alberts *et al.* (1980), Young (1980), Loch and Donnollan (1982b), and Miller and Baharuddin (1987) found similar results. Table 13, along with Figures 11a, 11b and 11c also show that there was a much smaller proportion of clay-size material eroded from the Kiwitea soil compared to the Levin and Tokomaru soils. This may be explained by the high allophanic clay content present in the Kiwitea soil. The Tokomaru soil had a higher clay enrichment ratio of undispersed particles over the total rainfall period compared to the Levin soil although its proportion of clay particles was larger. This may be accounted for by the higher percentage of organic carbon present in the Levin soil.

The proportion of eroded sand-size material (also referred to as coarse material) increased over time until an equilibrium value was reached. The Kiwitea and Levin soils had similar equilibrium proportions of eroded sand-size material (approximately 70 and 75 % respectively) while the Tokomaru soil was somewhat lower (50 %). The reason for the reduced equilibrium value obtained from the

Tokomaru soil may be attributed to its lower organic carbon content. The higher value obtained for the Levin soil may be explained by both the high proportion of primary sand particles (42 %) and the high organic carbon content (4.32 %). The amount of clay, and the dominant clay type for the Kiwitea soil are responsible for its high equilibrium value of sand-size material eroded. The times at which the equilibrium value for both sand and silt-size material within each soil type was achieved were similar. Since it was shown that most of the clay was eroded and transported in the form of aggregates, coarse material was composed of both aggregates and primary sand particles. These aggregates may also contain silt-size material that were not eroded and transported individually. The degree of aggregation of eroded sediment varied according to the rate of soil loss. At low rates of soil loss, the runoff energy was insufficient to transport large aggregates. This explains why the percentage of coarse material eroded was lowest at the first sampling time, T = 5 minutes.

Deviations in the amount of sand, silt and clay size material eroded over time can be attributed to changes in runoff storage depression and surface detention.

## Summary

1. Primary sand particles are less easily entrained into overland flow because of their size and weight. Consequently, the proportion present in the eroded sediment was always lower than that from the original soil.

2. The eroded sediment always showed a positive clay enrichment ratio.

3. There was an increase in the clay enrichment ratio for the Kiwitea soil between the start and the end of the rainfall period. The opposite effect occurred for the Levin and Tokomaru soils. The increase for the Kiwitea soil can be attributed to its high allophanic clay content which produces more stable soil aggregates that are less affected by slaking compared to the other two soils. These aggregates, rich in clay, can only be entrained into overland flow when the runoff energy is sufficient to transport them.

4. The Levin and Tokomaru soils clay enrichment ratios declined between the

start and the end of the rainfall period. The dominant clay types present in these two soils are susceptible to slaking. This process can only occur at the early stages of the rainfall period before surface water builds up and cushions the raindrop impact. Initially, slaked material containing both primary particles and small aggregates, can easily be entrained into the thin sheets of overland flow.

5. The eroded sediment from the Kiwitea soil contained less silt compared to the original soil. This could be attributed to the high proportion of clay present and its dominant clay type, allophane, surrounding silt particles in the form of aggregates.

6. More silt was contained in the eroded sediment from the Levin soil compared to the original soil. Soil aggregates from the Levin soil are more easily slaked due to the low clay content and its dominant type of clay present.

7. The proportion of eroded silt-size material (both primary silt particles and silt-sized aggregates) decreased over time until an equilibrium value was reached. This equilibrium value was 20 to 25 percentage points lower than the proportion of primary silt particles present in the original soil.

8. The majority of the primary clay particles were eroded and transported in the form of aggregates. Only a very small fraction was transported as primary particles.

9. The size of course material eroded varied according to the rate of soil loss. At low rates, the runoff energy was insufficient to transport large aggregates.

# Chapter Four

## Settling Velocity Distribution and Characteristics

### Introduction

Settling velocity distribution of soil aggregates in a fluid is fundamental to the study of erosion and deposition. Recent process-based erosion models, (Knisel, 1980; Rose *et al.*, 1983) describe the interactions of entrainment, transport and deposition processes for a runoff event. Aggregate settling velocities are primary inputs to such models. For example, the model of Rose *et al.* (1983) describes the rate of deposition from flowing (or stationary) sediment as:

$$d_i = v_i \cdot c_i \qquad (9)$$

where:

d = the deposition rate of sediment per unit area per unit time (kg $m^{-2}$ $sec^{-1}$), for sediment with a settling velocity of v (m $sec^{-1}$).

c = concentration (kg $m^{-3}$).

i = an integer labelling the particular settling velocity class.

By considering a given soil sample as composed of various fractions or classes, each with identifiable characteristics, the total deposition rate of the soil can be obtained by summation.

Settling tubes provide the most direct method of measuring the settling velocity characteristics of soils in a fluid. Eroded sediment commonly exists in the form of aggregates which settle at a rate dependent upon the aggregate size, shape, roughness and density relative to the fluid.

Settling tubes have been used in a number of fields to analyze two-phase systems for most of this century. Developments have led to very accurate discrimination between particle sizes using the associated variation in settling velocity (Emery, 1938; Schlee, 1966; Felix, 1969). However, measurements of the size distributions of soil aggregates for use in soil erosion-deposition models pose particular problems. Childs (1969), in reviewing the assumptions behind Stoke's Law, suggests that significant surface and form drag effects limit its use

to particles smaller than 60 *u*m in diameter. For these particles the standard pipette or hydrometer methods (Black, 1965) are convenient to use. However, for sediment greater than 60 *u*m the relationship between size and settling rate is complex and depends on the particular variations found in aggregate shape and density (Watson, 1969; Gibbs *et al.*, 1971). Therefore measurements of settling velocity cannot be accurately converted into aggregate size or visa versa without the complex task of obtaining the relationship between these two measurements for each particular soil type.

The most common method used to measure aggregate size is wet sieving devised by Yoder (1936). Under wet sieving, the results will vary with the degree of abrasion, and this depends upon the sieving technique. Settling tubes in general, involve minimal abrasion and thus reduce this source of variation.

The settling tube used in this study (referred to as the Massey tube hereafter) is a modified version of the Griffith settling tube developed by Hairsine and McTanish (1986). The Massey tube, as shown in Plate 6, consists of three basic components: a perspex tube, a sample introduction device, and a submerged collection turntable on which settled sediment samples are collected. Plates 7, 8 and 9 show the sample introduction device, perspex settling tube, and the submerged collection table respectively. The sample introduction device and activation lever differ from the Griffith tube. However, the operational principles are the same. A full description of the Massey tube is outlined in Appendix 2.

The Massey tube is designed to provide information on the fall velocity distribution of sediment outside the size range covered by Stoke's Law. It provides this information for aggregates settling in clear water without the interaction which would occur in a natural polydispersed system. This interaction is due to the fall velocity of faster sediment being inhibited by falling through slower (smaller) sediment.

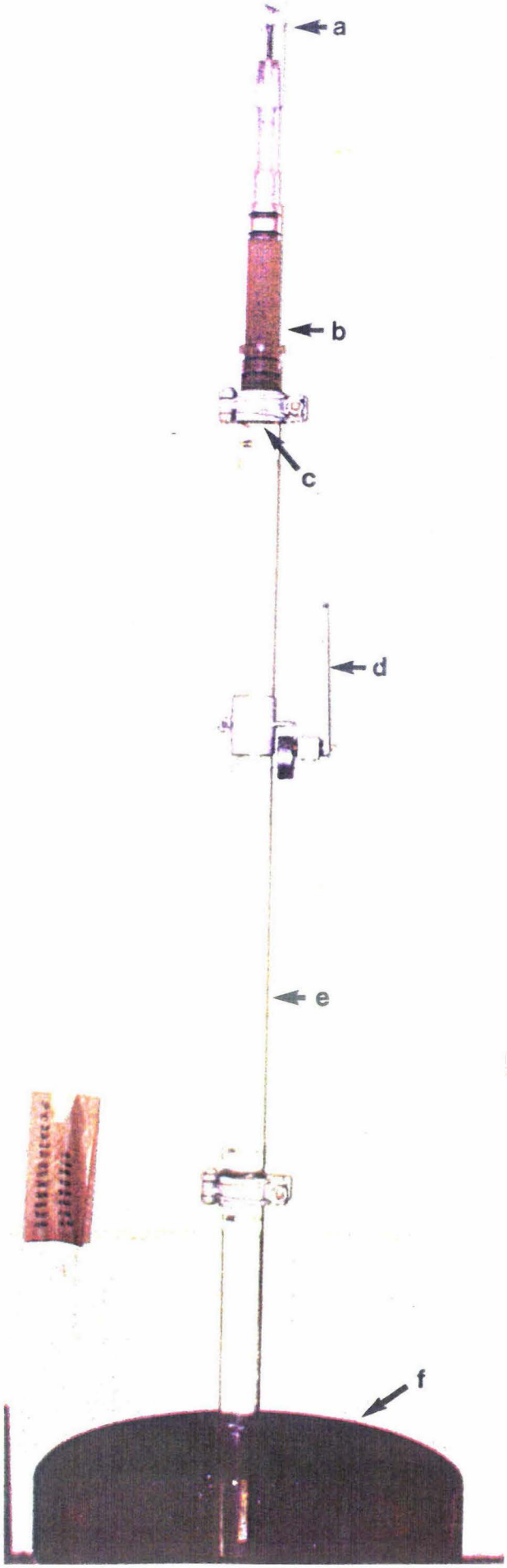


Plate 6. The Massey Settling Tube showing (a) the end stopper for the sample introduction device, (b) the sample introduction device, (c) the sample introduction device seal, (d) the activation lever, (e) the perspex settling tube, and (f) the collection turntable.

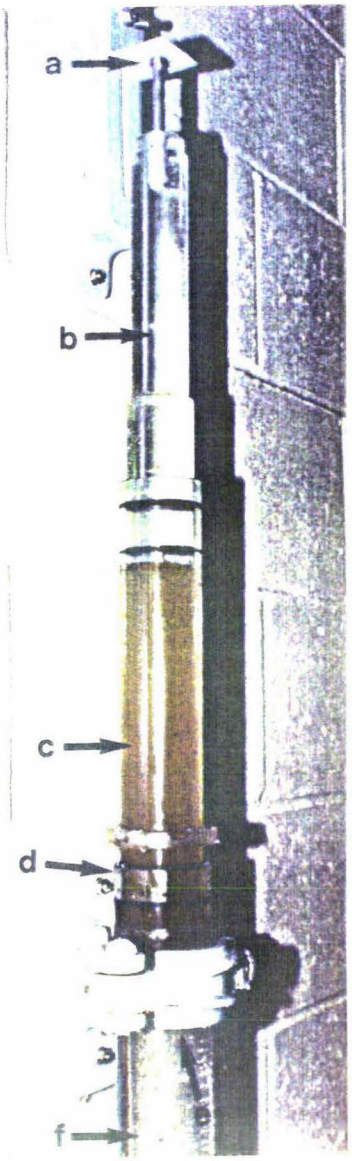


Plate 7. The sample introduction device showing (a) the stopper which prevents (b) the solid perspex from rising when the activation lever raises the settling tube. When the lever is activated, it results in a pressure change in (c) the sample introduction device and causes (e) the seal to break, thus releasing the sample into (f) the perspex settling tube. O-rings (d) seal the sample introduction device and the perspex settling tube together.

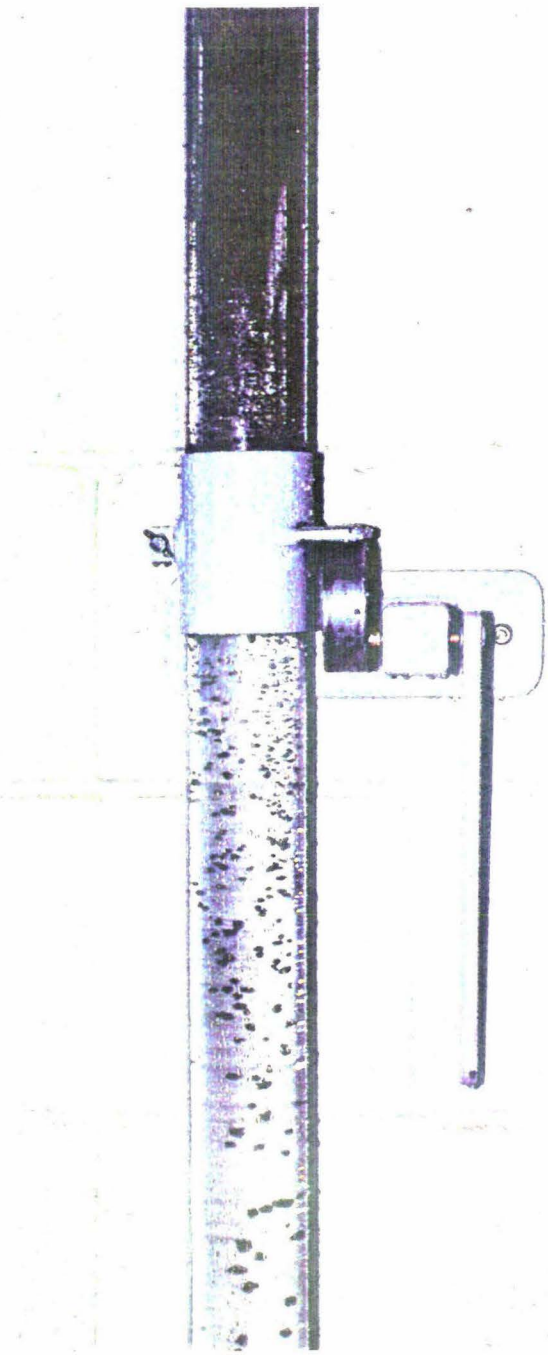

Plate 8. The perspex settling tube after the lever has been activated.

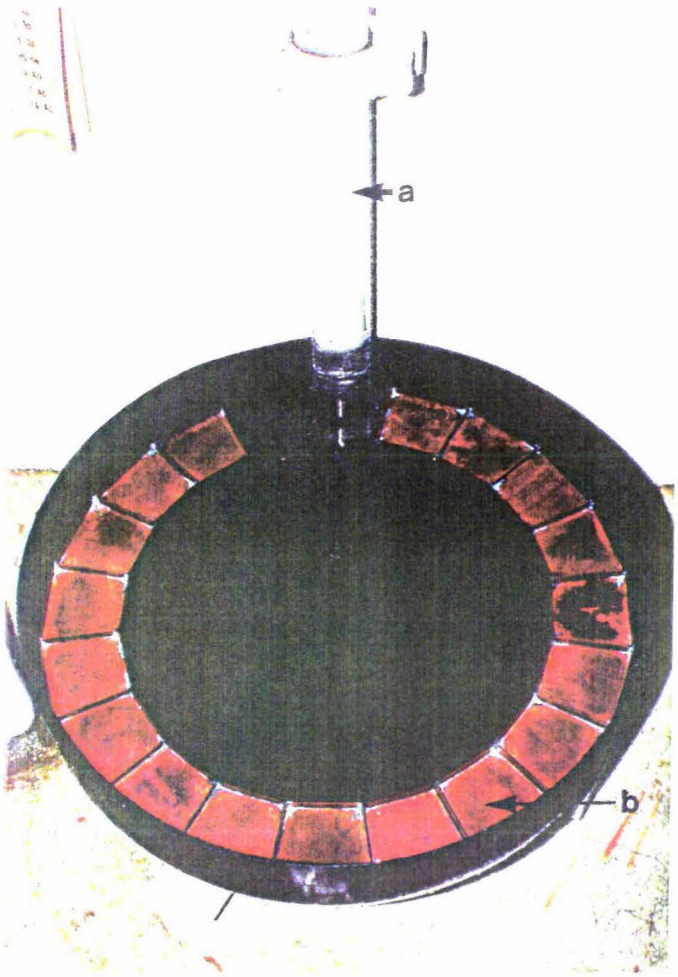


Plate 9. The submerged collection table showing (a) the perspex settling tube and (b) the sample collection trays. The collection trays and the end of the perspex settling tube are immersed in water so as to maintain a perfect seal. The submerged collection table is rotated at pre-determined times.

## Objectives

The objective of this study was to determine the settling velocity distribution and characteristics of the original soil and the eroded sediment over time for the Kiwitea, Levin and the Tokomaru silt loams.

## Materials and Methods

For each soil type, samples from the original soil and those from the eroded sediment collected at five minute intervals for one hour from the rainfall simulator experiments (by the procedure described in chapter two), were passed through the Massey tube to determine the proportion of material in each settling velocity class.

### *Trial Procedure*

The trial procedure for the Massey tube is similar to that for the Griffith tube described by Hairsine and McTanish (1986). The full procedure adopted for the Massey tube is summarized in Appendix 2.

### *Sample Pre-treatment*

Eroded sediment samples were initially saturated with runoff water. For such samples to be tested in the Massey tube, the sediment had to be gently separated from the suspension. This was achieved by passing the sample through a 63 *u*m sieve. The material finer than 63 *u*m is beyond the normal range of the Massey tube because of the long periods required for these aggregates to settle 2 m. The mass of solid material finer than 63 *u*m present in suspension was determined by evaporating the supernatant at 105°C for 48 hours. According to Stoke's law, material finer than 63 *u*m has a maximum settling velocity of $2.0 \times 10^{-3}$ m $sec^{-1}$. Therefore, all the material finer than 63 *u*m is included in the final calculations as material slower than $2.0 \times 10^{-3}$ m $sec^{-1}$. The material retained on the sieve (that is, the material greater than 63 *u*m) was placed into the Massey tube's sample-introduction device and its settling velocity

distribution was determined.

In order to provide a reference settling velocity distribution for each soil type after possible aggregate breakdown by rainfall, a separate soil sample was placed in a shallow container and gently wetted before being exposed to 60 minutes of rainfall at a rate of 65 mm $hour^{-1}$. All sediment produced was collected and combined with the soil remaining in the container. The larger aggregates were then separated from suspension by passing the sample through a 63 *um* sieve. This sample hereafter is referred to as the *treated soil*. The maximum settling velocity of the material finer than 63 *um* was taken as $2.0 \times 10^{-3}$ m $sec^{-1}$.

The settling velocity distribution of the *original soil* was also determined for each soil type. This was material which had not been exposed to simulated rainfall for 60 minutes but was immersed in water for 30 minutes before being added to the sample introduction device.

*Sample Collection from the settling tube*

For the treated soil and sediment derived from runoff, 14 sub-samples were collected at 8, 10, 15, 20, 30, 40, 70, 100, 150, 200, 300, 400, 700, and 1000 seconds from the time the sample-introduction device was activated. These sub-samples were then oven dried for 24 hours at 105°C to determine the mass of material in each settling velocity class. Plate 10 shows the particle-size variations for each settling velocity class.

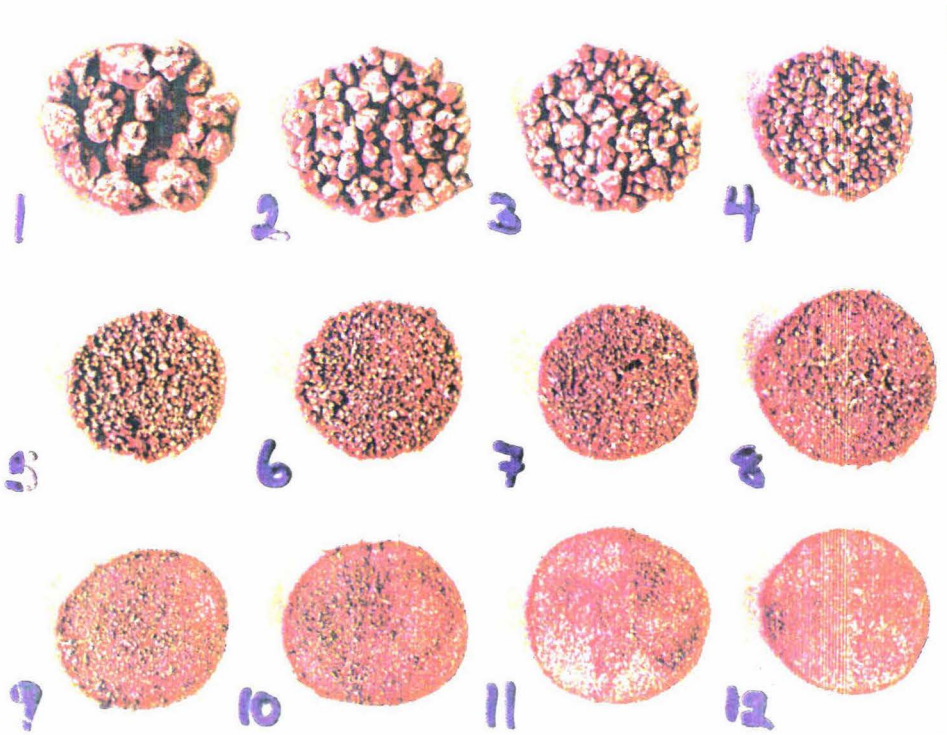


Plate 10. The particle-size variations from the different settling velocity classes. The period for each sample are also shown.

## Data Analysis Methods

Settling velocity was determined from the settling tube length and the time required for material to settle that distance. From the cumulative mass of material settling out at each sampling time, the percentage of material still remaining in suspension was calculated. This value is referred to as the "percentage-slower-than". Appendix 2 shows an example of the calculation procedure. The percentage slower-than is then plotted against settling velocity. The 95% confidence levels for the various settling velocity classes are shown.

The total mass of material (when percentage slower-than is 100%) includes all the material placed into the sample introduction device (the material retained on the 63 *u*m sieve after separation from suspension) and that present in suspension after sieving.

**Results and Discussion**

Figures 12, 13 and 14 show the measured settling velocity distribution curves of the original soil, treated soil and the eroded soil samples at selected times for the Kiwitea, Levin and the Tokomaru soils respectively. The data in Figures 12 to 14 are for samples subjected to simulated rainfall at a rate of 65 mm $hour^{-1}$. The distribution curves for times when there was very little change in settling velocity distribution from the previous sampling time have been omitted for clarity. In the interpretation of these results, the slope of the distribution curves over a particular range of settling velocities may be used as an indicator of the percentage of the total sediment in that settling velocity range. A greater slope indicates a larger percentage of sediment in that range, and vice versa.

For the three soil types, the settling velocity distribution of eroded sediment at the first sampling time (after 5 minutes) showed that the eroded sediment contained a greater proportion of fine particles (indicated by slow settling velocities) than that measured after 40 minutes of rainfall. Changes in settling velocity distribution showed that eroded sediment became progressively coarser with time until its settling velocity characteristics were similar to those of the treated soil which had been subjected to a simulated rainfall as described above. This indicates that there was insufficient runoff energy initially available to transport the larger particles or aggregates.

For the Kiwitea soil (Figure 12), there was no significant difference (5% level) between the treated soil and eroded sediment after 40 minutes for all settling velocity classes. However, eroded sediment sampled after only 5 minutes was significantly different from all other samples. When comparing the 10 and 40 minute sampling times, only the settling velocity classes slower than $6.67 \times 10^{-3}$ m $sec^{-1}$ were significantly different.

For the Levin soil (Figure 13), there was no significant difference between any eroded sediment sampling times for settling velocity classes faster than $2.0 \times 10^{-2}$ m $sec^{-1}$. At settling velocity classes slower than this, eroded sediment from the 5 minute sampling time was significantly different from the other sampling times.

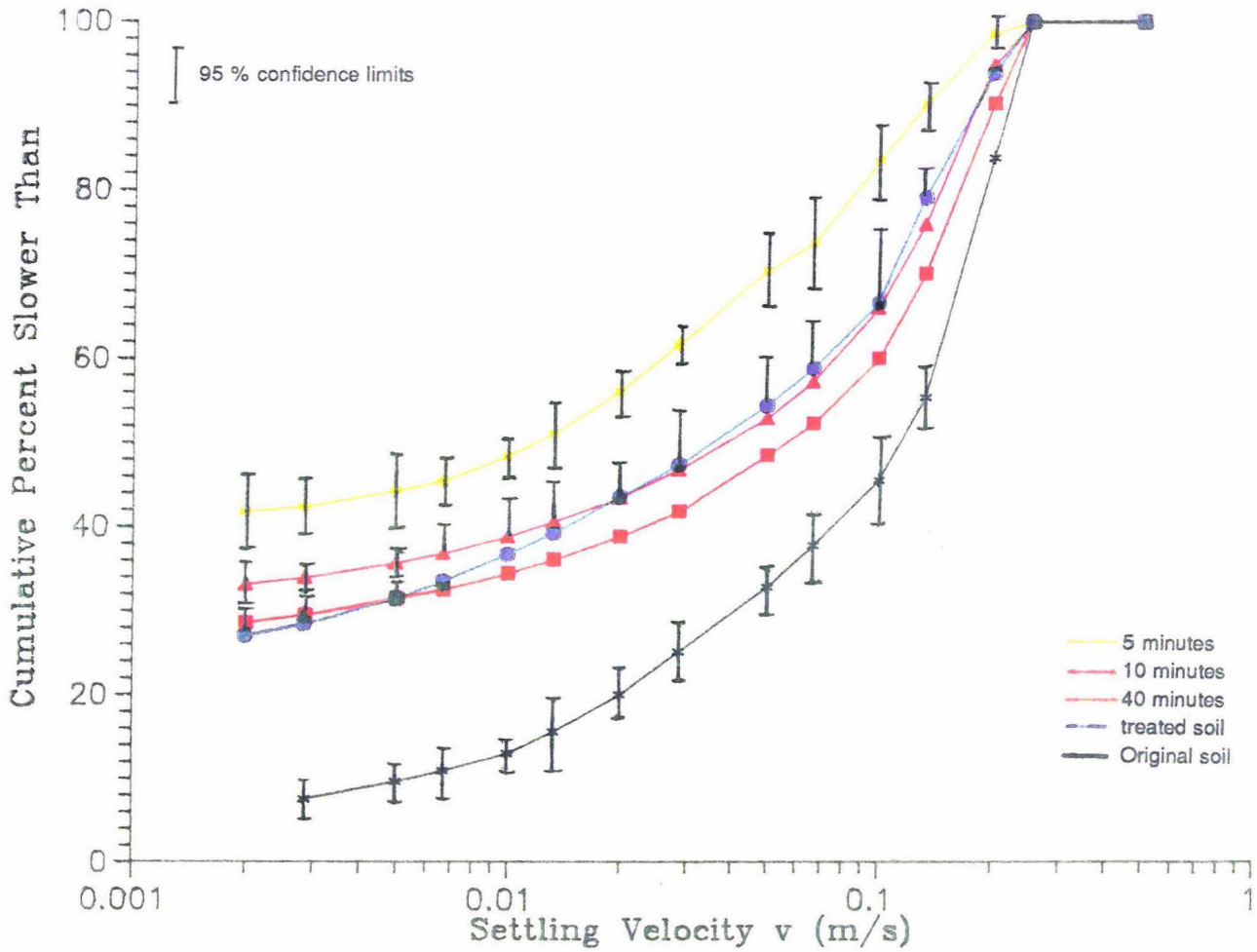


Figure 12. The original soil and the eroded sediment settling velocity distribution patterns from selected times for the Kiwitea soil.

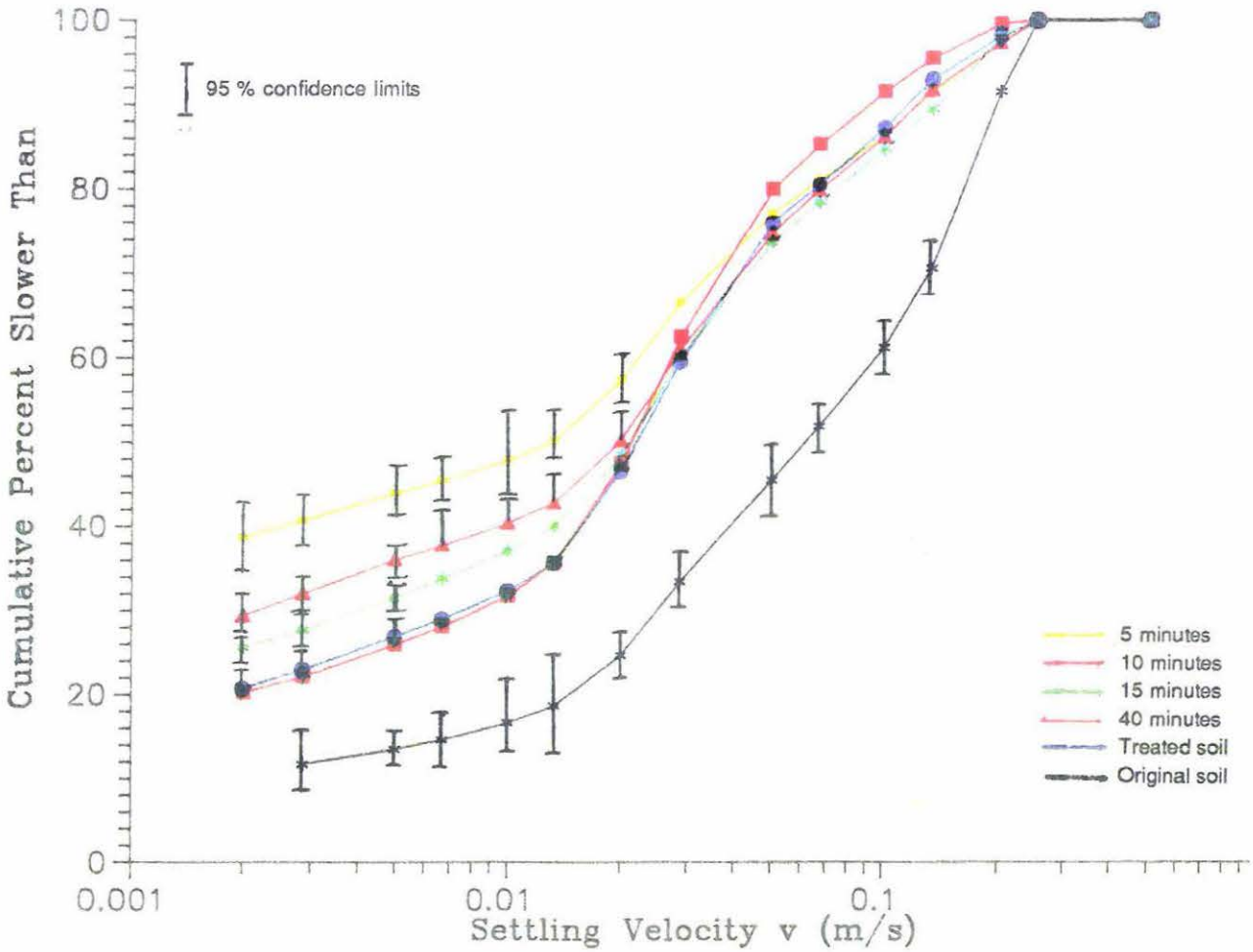


Figure 13. The original soil and the eroded sediment settling velocity distribution patterns from selected times for the Levin soil.

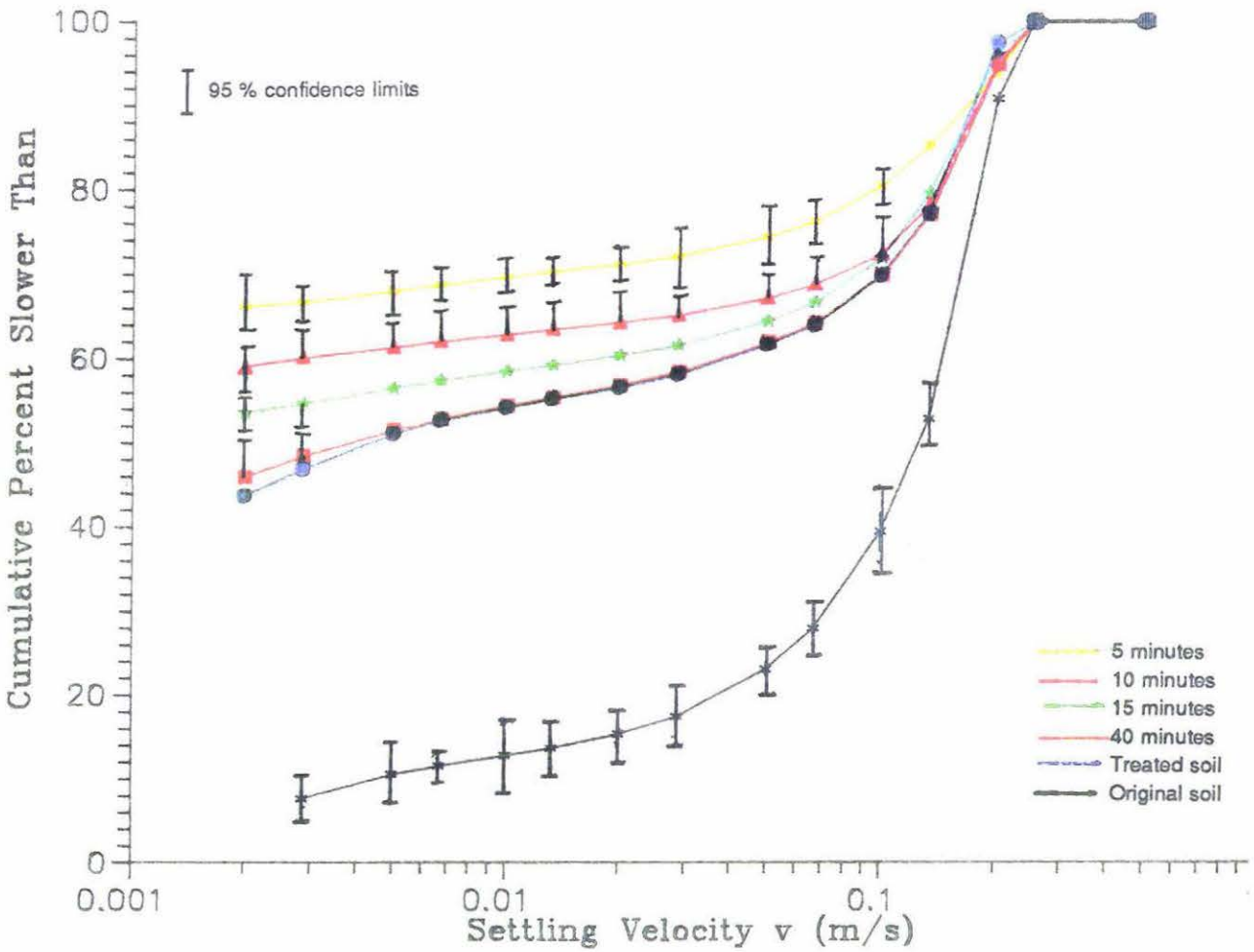


Figure 14. The original soil and the eroded sediment settling velocity distribution patterns from selected times for the Tokomaru soil.

All the sampling times shown in Figure 13 are significantly different for settling velocity classes slower than $5.0 \times 10^{-3}$ m $sec^{-1}$.

For the Tokomaru soil (Figure 14), eroded sediment from the 5 minute sampling time was again significantly different from all other sampling times at settling velocity classes slower than $1.0 \times 10^{-1}$ m $sec^{-1}$. There was no significant change in the settling velocity distributions of the eroded sediment from time 40 minutes and the treated soil.

Also shown on Figures 12 to 14 are the settling velocity distributions of the original soil. These figures demonstrate that the original soil contained a larger proportion of course aggregates or particles compared to the treated material. Also the proportion of slower settling material contained in the original soil was considerably lower. This indicates that the forces exerted by raindrop, and possibly osmotic swelling and ion hydration, caused aggregate breakdown of the treated soil.

A comparison of the settling velocity distribution curves of the treated soils is shown in Figure 15. This shows a higher proportion of fine sediment with low settling velocity for the Tokomaru soil than for the Kiwitea soil. The Levin soil had the lowest proportion of fine sediment of the three soils. For the Tokomaru soil, 44% of the sediment had a settling velocity less than $2.0 \times 10^{-3}$ m $sec^{-1}$ compared to 27% and 21% for the Kiwitea and the Levin soils respectively. According to Stoke's law, the settling velocity of $2.0 \times 10^{-3}$ m $sec^{-1}$ correlates to approximately 63 *u*m, the diameter of silt-size particles. However, 76% of sediment from the Levin soil has a settling velocity less than $5.0 \times 10^{-2}$ m $sec^{-1}$ compared to 62% and 54% for the Tokomaru and Kiwitea soils respectively. This suggests that the Levin soil has a lower proportion of large aggregates (aggregates with a faster settling velocity) than both the Kiwitea and the Tokomaru soils.

Particle selectivity of eroded sediment shown in Figures 12 to 14 was thought by previous investigators to occur because "rainflow transportation" (Moss *et al.*, 1979) or "interrill flow" (Alberts *et al.*,1980) has insufficient energy to transport many of the coarser, faster settling aggregates (Alberts *et al.*, 1983). Many

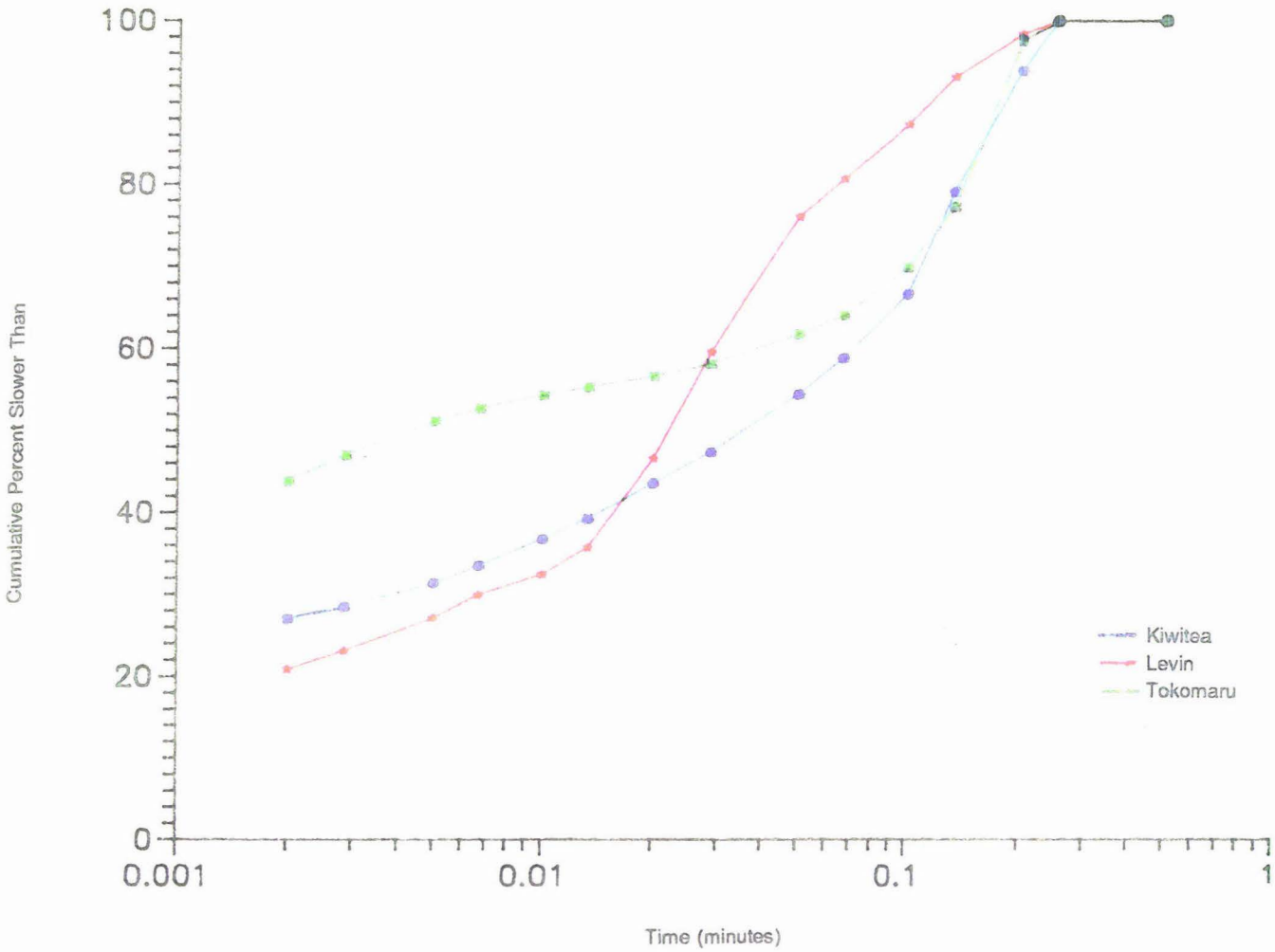


Figure 15. A comparison of the treated soils settling velocity distribution curves.

researchers have reported that when rainfall detachment is the main erosion process, (interrill as opposed to rill erosion), the eroded soil is finer in composition than the parent soil (Ellison, 1944; Meyer *et al.*,1975; Monke *et al.*, 1977; Moss *et al.*, 1979; Alberts *et al.*, 1980, 1983; Loch *et al.*, 1988). There is also evidence in the literature supporting the data which show that the proportion of fine fractions contained in the eroded sediment declines with time (Walker *et al.*, 1977; Moss *et al.*, 1979; Young and Onstad, 1978; Bryan and Luk, 1981), and the particle-size distribution of the eroded sediment tends to approach that of the treated soil with time (Walker *et al.*, 1978; Moss *et al.*, 1979). These phenomena have also been observed in this study.

Since the settling velocity characteristics of eroded sediment at equilibrium were similar (although not identical) to those of the treated soil (soil exposed to 60 minutes of rainfall but without loss of sediment), it appears that under these experimental conditions there was little additional breakdown by the transport process. This agrees with Meyer (1985) who showed that aggregated sediment did not suffer additional breakdown during transport by cropland runoff. Furthermore, this suggests that for these soil types, the settling velocity characteristics determined by subjecting soil in small containers to rainfall (but returning any detached sediment as described in the materials and methods section) are reasonably accurate estimates of settling velocity characteristics of eroded sediment at equilibrium from a flume where rainfall detachment is the principal erosion process.

The general trends with time in settling velocity distribution of eroded sediment measured in these experiments for one rainfall rate might be expected to be similar for other rainfall rates. Meyer *et al.* (1980) found that higher rainfall rates eroded a higher percentage of fine sediment, but the differences were not large compared with the differences in sediment sizes from differing soil types affected by raindrop impact.

**Summary**

1. Eroded sediment is generally much finer than the original soil.

2. The sediment derived from the start of an erosion event contained a greater proportion of fine particles and smaller proportion of coarse material than that obtained from the end of the erosion event. This was because initially there was insufficient runoff energy available to transport the larger particles.

3. The change in settling velocity distributions of eroded sediment showed that eroded material became progressively coarser with time until their settling velocity characteristics became similar to the treated soil.

# Chapter Five

# Aggregate Stability

## Introduction

Soil structure is a property of fundamental importance in determining the physical behaviour of soils. It has been defined as "the physical constitution of soil material as expressed by the size, shape and arrangement of the solid particles and voids, including both the primary particles to form compound particles or aggregates, and the aggregates themselves" (Brewer, 1964).

The disintegration of the soil mass into aggregates requires the imposition of a disrupting force. The stability of aggregates is a function of whether the cohesive forces between particles can withstand the applied disruptive force. If the measurements of aggregate stability are to have any practical significance, the forces causing disintegration should be similar to the forces expected in the field. The information provided by an aggregate stability test refers primarily to the erodibility of surface soils by rainsplash and wash (Bryan, 1976; Chorley, 1959). Therefore, the forces involved in these processes should be standardized. For the three soils used in this study, the aggregate stability was determined using a sedimentation procedure.

## Forces involved in aggregation

Two of the primary forces holding particles together in aggregates for moist soils are the surface tension of the air-water interface, and the cohesive tension (negative pressure) in the liquid phase. As the soil dries, the water phase recedes into capillary wedges surrounding particle-to-particle contacts and films between closely adjacent platelets. The interfacial tension and internal cohesive tension pulls adjacent particles together with great force as soil dries. This induces an increase in the concentration in the liquid phase of soluble compounds such as silica, carbonates, and organic molecules. As the capillary

wedges of the supersaturated soil solution retreat toward the particle-to-particle contact points, the potential adsorption spots which offer the lowest free energy for the solute molecules or ions are at the junctions of the adjacent particles. Many of these solute molecules and ions thus precipitate as inorganic semi-crystalline compounds or amorphous organic compounds around the particle-to-particle contacts and cement them together.

As the highly adhesive liquid phase pulls adjacent mineral particles into closer proximity, there are also more opportunities for hydrogen bonding between adjacent oxygen and hydroxyl groups and for other intermolecular, interionic, and crystalline bonds to develop. When the relative humidity in the soil falls below 75 %, the last molecular layer of water on the mineral surface begins to leave. If the relative humidity decreases below 30 %, the water molecules hydrated to absorbed $Ca^{2+}$ ions are drawn off into the gaseous phase (Kemper and Rosenau, 1986). With a reduction in soil moisture, most soils generally have greater strength because of cementation. However, cementation is generally crystalline and brittle, and once broken by mechanical forces (eg. Wheel traffic on a dry earth road), it does not reform unless the wetting and drying process is repeated.

**Weakening and disintegration of aggregates by wetting**

The wetting process can be highly disruptive. The forces involved are major causes of aggregate weakening and disintegration that occur on the surface soil in the field.

Ion hydration and osmotic swelling forces pull water between clay platelets, pushing them apart and causing swelling of the aggregate in which they are incorporated (Emerson, 1967). If an aggregate is wetted quickly, the wetted portion can swell appreciably compared with the dry portion, causing a shear plane to accompany the wetting front which can break many of the bonds.

Some of the bonding materials are soluble and dissolve as water enters the soil. Others are hydratable and may become weaker, but more flexible when hydrated. If the soil aggregates are wetted slowly at atmospheric pressure or quickly under

a vacuum, the bonding is still significantly strong enough to hold most of the primary particles together as aggregates.

The stresses produced by wetting increase as the sample dryness increases (Collis-George and Lal, 1971) and the rate of aggregate breakdown into finer fractions increases as the rate of wetting increases (Emerson and Grundy, 1954; Panabokke and Quirke, 1957). Immersion of air-dry aggregates induces an extreme rate of wetting. When this is compared with the wetting of moister soil, incipient failure in the former is more intensive and the number of smaller aggregates formed is greater. This results from increased formation of planes of weakness (Quirke and Panabokke, 1962).

Air contained within quick-wetted aggregates plays a role in their disintegration. Kemper *et al.* (1985) found that when a soil sample is stored at relative humidities of less than 50 %, substantial amounts of oxygen and nitrogen are absorbed on the mineral surfaces. When the sample is wetted by immersion, these oxygen and nitrogen molecules are displaced by the more tightly absorbed water molecules. The oxygen and nitrogen molecules from the adsorbed phase join the entrapped air inside the pores and the pressure increases as capillarity pulls water into the aggregate. Finally the aggregate ruptures and the air bubble emerges.

## Previous tests for aggregate stability determination

Two types of methods have been used previously to determine aggregate stability. Firstly, there are tests which subject aggregates to forces designed to simulate those occurring in the field (physical tests) while the second are those aimed at measuring intra-aggregate bond strength by specific chemical procedures (chemical tests).

### *i. Physical Tests*

The most popular method of this type has been wet-sieving. This procedure sieves aggregates under water and the resulting size distribution is used as an

index of stability. The fewer aggregates in the large size classes, the greater the breakdown, and the lower the aggregate stability.

The usefulness of physical tests is related to the accuracy with which the forces occurring in the field are simulated. In wet-sieving the breakdown force is twofold. First there is the force of water entry when air-dry soil aggregates are wetted before sieving. This may be varied by altering the method of pre-wetting the aggregates. Most studies reported in the literature have used rapid wetting by direct immersion of dry aggregates in water. Rapid wetting causes considerable aggregate breakdown. This results from the wetting front advancing into the aggregate from all sides, causing compression and eventual explosion of trapped air.

Grieves (1979) suggests that the aims of the study must be considered when selecting the type of sample pre-treatment. Where the soils are bare surface liable to rapid wetting, then a rapid wetting test should be employed. He showed that wetting by capillary action at zero suction significantly reduces the technique variability. When the study involves subsurface or vegetated soils, Grieves suggests tension wetting procedures are the logical choice.

Some workers (Baver *et al.*, 1972; Kemper, 1965) have sought to reduce the rate of wetting by pre-wetting aggregates slowly against an applied suction force. Here the wetting front passes through the aggregates more slowly, allowing air to escape from the pores in the aggregates (Baver *et al.*, 1972) and thereby reducing the breakdown force. Alternatively, air may be eliminated from the aggregates before wetting by flood wetting in a vacuum desiccator after evacuation (Kemper, 1965).

The second force imposed on aggregates during wet-sieving is a mechanical abrasion caused by the impact of aggregates with one another and with sieves under water during the sieving process. It may be varied by altering the length of time of sieving or increased by shaking the aggregates in a cylinder of water before sieving (Low, 1954).

Tests of aggregate stability which are similar in principle to wet-sieving have been

suggested by McCulla (1945), Childs (1942) and Williams (1963). McCulla's method involved studying the breakdown of surface soils under raindrop impact. Aggregates were placed on a sieve and subjected to the impact of water drops falling from a burette placed at a standard height above the sieve. The number of drops needed to wash the aggregates through the sieve was used as the index of stability. This method was refined by Low (1954) by slowly moistening the aggregates under tension before testing and standardizing drop size and impact energy to simulate conditions imposed by a natural rainstorm.

The tests proposed by Childs (1942) subjected a bed of aggregates to wetting and drying cycles on a tension plate device. Stability was determined as the loss in inter-aggregate pore space. Grieves (1979) considered this method unsuitable because no mechanical forces were imposed on the aggregate in the test.

Williams method (Williams, 1963) was similar to that of Childs, but subjected aggregates to a mechanical force after the initial wetting. The volume of inter-aggregate pore space was expressed as a percentage of the volume remaining in a duplicate sample of artificially stabilized aggregates, thereby controlling for the effect of aggregate size and shape on pore volume.

*11. Chemical tests*

Some workers (Emerson, 1954; Russell, 1973) were not satisfied that the aggregate stability tests developed to simulate the forces occurring in the field measured the intra-aggregate bond strength satisfactorily. This led to the development of tests designed to measure this strength using chemical dispersion procedures.

Emerson (1954) published details of such a technique. In this test the exchangeable cations in a bed of soil crumbs were replaced with sodium ions. When the bed of crumbs was leached with a 1 N NaCl solution, the swelling pressure of the ions was reduced. This pressure was then slowly increased by lowering the concentration of NaCl in the leaching solution. Emerson monitored changes in structure by measuring the permeability of the soil bed and the critical concentration of $Na^+$ ions at which the structure collapsed. The sharp fall in

permeability was used as the index of stability. He found the lower this concentration was, the higher the aggregate stability.

This method was subsequently modified by Dettman and Emerson (1959) and by Williams *et al.* (1966), but these refinements only affected the expression of stability, and the principles of the test were unchanged.

## Settling Velocity as a measure of Aggregate Stability

The aggregate settling velocity of a soil sample is slowed when the structural stability of aggregates is reduced. A reduction in aggregate stability can be caused by the immersion of an unsaturated or air-dried soil sample in water, a direct consequence of aggregate slaking and dispersion. Aggregate structural stability could also be decreased as a result of a particular agricultural practice.

Cole and Edlefson (1935), Clement and Williams (1958) and Grieve (1979) each recognized that mechanical dispersion of sediment is caused by wet-sieving, and they advocated the use of a method which employs wetting forces only. Aggregate settling velocity measured by a sedimentation method satisfies this criterion. Furthermore, sedimentation methods are faster than wet-sieving (Emery 1938) and yield results of equal or improved reproducibility (Felix, 1969; Sandford and Swift, 1971). Another advantage is that certain settling tubes yield the entire settling velocity distribution, preferable to the individual points on a size distribution given by wet-sieving. For these reasons, aggregate settling velocity measured by a sedimentation method is suggested as a useful method for comparative studies of structural stability, with more advantages than the wet-sieve method widely used at present.

## Experimental Objectives

The objective of this study was to determine the stability of aggregates from the Kiwitea, Levin and the Tokomaru soils by comparing the settling velocity distributions of moist soil samples to air-dried samples.

## Experimental Methods

From the three soils, moist and air-dried samples were passed through the settling tube to determine the proportion of material in each settling velocity class. The settling tube trial procedures were the same as those described in Chapter 4.

Moist samples from the three soils were immersed in water for 30 minutes before being added to the sample introduction device. These samples are referred to as the *moist samples* hereafter. Once the settling tube was activated, samples were collected at 4, 8, 10, 15, 20, 30, 40, 70, 100, 150, 200, 300, 400, 700 and 1000 seconds.

Quantities of each soil were allowed to air-dry for 72 hours before being immersed in water for 30 minutes. These samples are known as the *air-dried samples* from hereafter. These were then passed through the settling tube and samples collected at the same times as those for the moist soils. The collected samples were then oven dried at 105°C for 48 hours to determine the percentage-smaller-than for each settling velocity class.

The gravimetric moisture contents for both the moist and air-dried samples for each soil type were also determined.

## Data Analysis Methods

The cumulative percentage-slower-than for each settling velocity class from the moist and air-dry samples as determined by the same procedure described in Chapter 4. The 95% confidence limits for each settling velocity class from the mean of three replicates were calculated using a paired "*t*" statistic test (Snedecor and Cockran, 1980).

Using equation 10 below, an indicator for aggregate stability was determined by calculating the percentage increase (or decrease) in the total area beneath the

settling velocity distribution curve for air-dried aggregates re-immersed in water ($A_{air\text{-}dry}$) from the moist aggregates ($A_{moist}$) settling velocity distribution curve. This value is referred to the aggregate stability index (*ASI*).

$$ASI = \frac{A_{air\text{-}dry} - A_{moist}}{A_{moist}} * \frac{100}{1} \qquad (10)$$

The lower the *ASI* obtained from the above equation, the greater is the aggregate stability. In this study, the area calculated was between the settling velocities $5.00 \times 10^{-1}$ and $2.00 \times 10^{-3}$ m $sec^{-1}$. The slower settling velocity represents aggregates or particles approximately 63 $\mu$m in diameter, as determined by Stokes law. Hence, all material greater than silt-sized particles was examined.

**Results and Discussion**

Figures 16, 17 and 18 illustrate the effect of slaking and dispersion on the setting velocity distribution of aggregated soil from the Kiwitea, Levin and Tokomaru soils respectively. For each figure, distribution A (squares) represents the moist sample while distribution B (circles) shows the air-dried sample.

Distributions A and B in Figures 16 to 18 are each the mean of three replicates. The 95 % confidence limits were calculated using a paired "t" statistic test (Snedecor and Cockran, 1980). Although distributions A and B are not totally significantly different, immersion wetting of air-dry soil is shown to cause a general decrease in aggregate settling velocities relative to velocities measured with the moist soil. This reduction in velocity is due to the breakdown of coarser aggregates, predominantly by slaking, when the air-dry sample is immersed in water.

The aggregate stability index was calculated for each soil type using equation 10 and the results are shown in Table 14. These indices may be estimated in Figures 16 to 18 by the gap between the two distribution curves. The larger the gap, the greater the aggregate stability index and the less stable the aggregates.

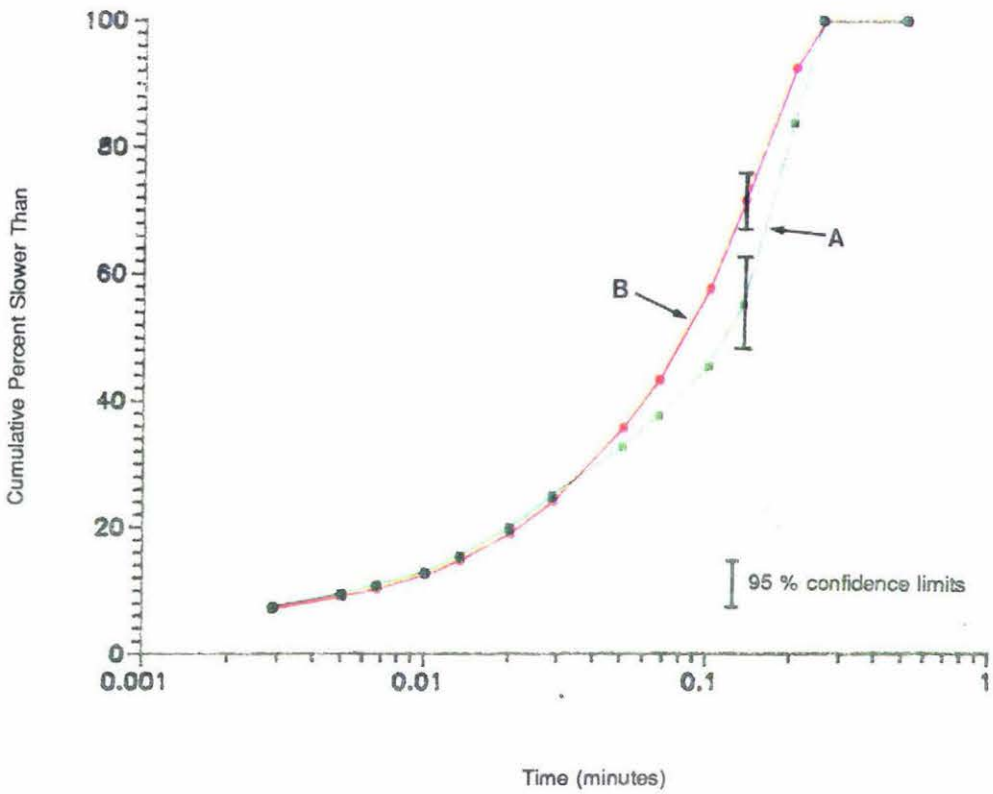


Figure 16. The settling velocity distributions of moist (distribution A) and air-dried (distribution B) samples from the Kiwitea soil for aggregate stability determination.

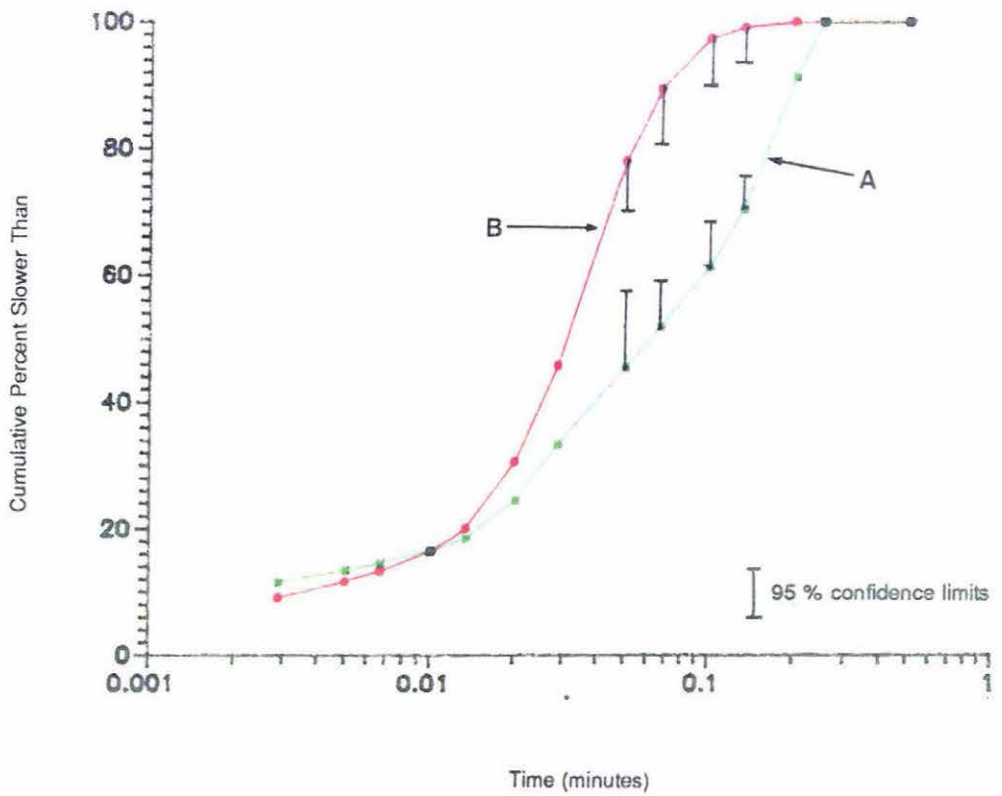


Figure 17. The settling velocity distributions of moist (distribution A) and air-dried (distribution B) samples from the Levin soil for aggregate stability determination.

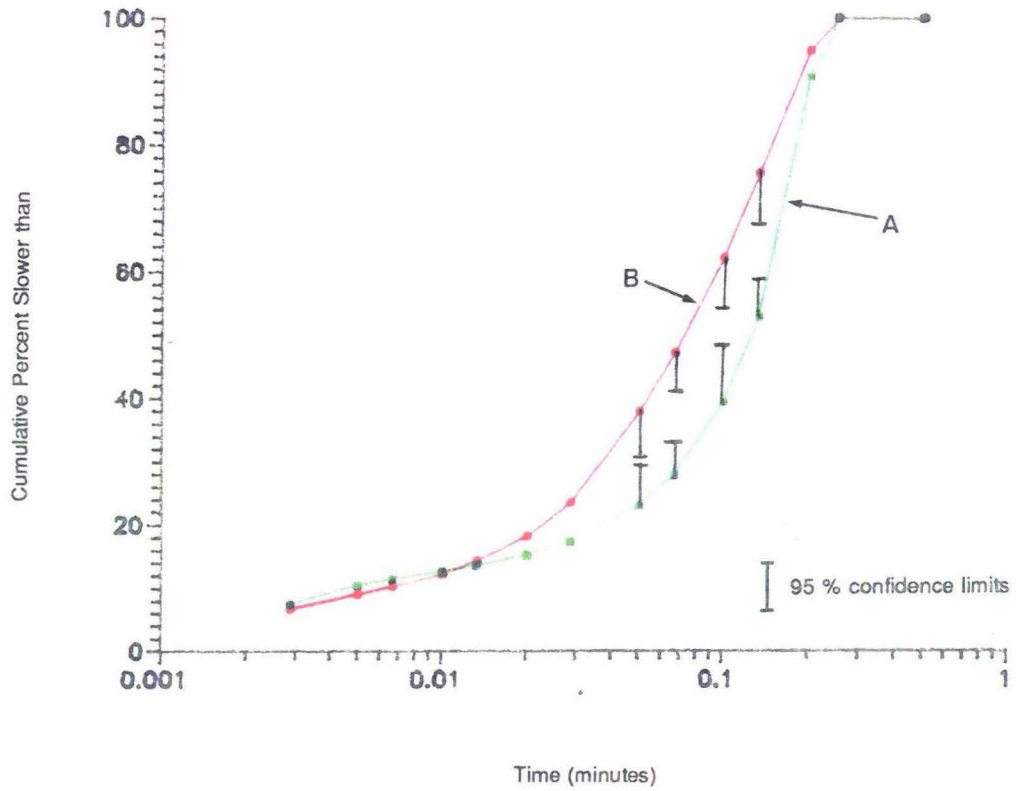


Figure 18. The settling velocity distributions of moist (distribution A) and air-dried (distribution B) samples from the Tokomaru soil for aggregate stability determination.

From the soils in this study, aggregates from the Kiwitea soil were the most stable, while the Levin soil aggregates were the least stable.

Table 14. The aggregate stability index for each soil type.

| Soil Type | Aggregate Stability Index |
|---|---|
| Kiwitea | 7.1 % |
| Levin | 24.1 % |
| Tokomaru | 16.9 % |

For each soil type, the larger aggregates from the air-dried soil were affected most by slaking following re-immersion in water. This is illustrated in Figures 16 to 18 by the reduction of material which settled out at the faster settling velocities from the air-dried samples. An example of this for each soil type is portrayed in Table 15.

Table 15. Comparing the percent of moist and air-dried material which has settled out when the stated settling velocity was obtained.

| Soil Type | Settling velocity greater than ($m.sec^{-1}$) | Percent of material settled out (%) | |
|---|---|---|---|
| | | Moist sample | Air-dried sample |
| Kiwitea | $1.33 \times 10^{-1}$ | 44.7 | 22.2 |
| Levin | $6.66 \times 10^{-2}$ | 48.1 | 10.5 |
| Tokomaru | $1.33 \times 10^{-1}$ | 47.1 | 24.4 |

The Levin soil contained a smaller proportion of large aggregates compared with the Tokomaru and the Kiwitea soils. Evidence for this was the lack of material from the Levin soil which settled out at the faster settling velocities.

The number of the small-sized particles or aggregates (indicated by the slower settling velocity classes) from the air-dried samples increased slightly, although not significantly. This can be attributed to slaking of larger aggregates following immersion.

The slope of the settling velocity distribution curve indicates the rate of deposition for each settling velocity class. The greater the slope, the higher the rate of

deposition. For the three soils, the moist sample always achieved its maximum rate of deposition at a faster settling velocity than the air-dried sample (Figures 16 to 18). This indicates that the modal settling velocity class was faster for the moist sample compared with the air-dried sample.

Not all moisture is removed from within the aggregates when soils are air-dried at room temperature. Moisture that remains is held tightly in the very small pores or micropores and its removal requires large suction forces. For the soils in this study, the gravimetric moisture contents from the moist and air-dried samples were calculated. There was not much variation between the air-dried samples, however for the moist samples, the Tokomaru soil was much wetter than the Levin and Kiwitea soils. These results are presented in Table 16.

Table 16. The gravimetric moisture contents of both the moist and air-dried samples for each soil type.

| Soil Type | Gravimetric Moisture Content | |
|---|---|---|
| | moist sample | Air-dried sample |
| Kiwitea | 0.256 | 0.102 |
| Levin | 0.274 | 0.088 |
| Tokomaru | 0.384 | 0.093 |

The effect of the Tokomaru soil having a high initial moisture content may reduce the effect of the moist sample slaking when immersed into the sample introduction device. This would increase the area between the moist and air-dried settling velocity distribution curves and therefore raise the aggregate stability index (which indicates lower aggregate stability).

## Summary

1. Comparing the settling velocity distribution of moist and air-dried soil samples may be taken as an indicator of aggregate stability. Aggregate settling velocity distributions change if samples are allowed to dry prior to analysis which involves immersion. The number of course aggregates are reduced while fine aggregates and particles are more abundant. This can be attributed to the slaking of larger aggregates following immersion.

2. A comparison of the settling velocity distributions of moist and air dried samples produced an indicator of aggregate stability. This index showed aggregates from the Kiwitea soil were the most stable while the Levin soil were the least stable.

# Chapter Six

## Summary and Conclusions

Sheet erosion is the most extensively mapped erosion type in New Zealand. The conditions most conducive to sheet erosion are found on sloping soils which lack a vegetative cover and have been cultivated. With the current economic returns from pastoral farming, a greater percentage of those soils which were previously unaffected by sheet erosion are being cultivated and therefore becoming more susceptible to sheet erosion.

The main objective of this study was to assess quantitatively the erodibility of three cropping soils under the same conditions of slope, cover and rainfall. Whether soil particles or aggregates were selectively eroded was also determined.

Three soils from the Manawatu region which are suitable for arable farming or market gardening were investigated. They included the Kiwitea silt loam, the Levin silt loam and the Tokomaru silt loam. A portable rainfall simulator was used to generate eroded sediment and runoff samples. Particle selectivity was determined by pipette analysis and a settling tube.

A summary of all results from the three soil types is shown in Table 17.

Previous investigators have noted that the higher the percentage of clay present, the greater the binding capacity of the soil and therefore the soil aggregates tend to be more stable. This suggests, on clay content alone, soil aggregates from the Kiwitea soil would be the most stable, while those from the Levin soil would be the least stable.

Allophane is the dominant clay type present in the Kiwitea soil. The cohesiveness of allophane enables it to form strong aggregates which are difficult to disperse under physical force. Both the Levin and Tokomaru soils have illite as their dominant clay type. Illite is much less cohesive than allophane.

Table 17. Summary of mean results from all rainfall simulation storms for each soil type.

| | | Kiwitea soil | Levin soil | Tokomaru soil |
|---|---|---|---|---|
| Primary particle composition | % sand particles | 21.1 | 42.6 | 10.0 |
| | % silt particles | 51.1 | 39.2 | 65.5 |
| | % clay particles | 27.8 | 18.2 | 24.5 |
| Dominant clay type | | Allophane | Illite | Illite |
| Organic carbon content (%) | | 3.47 | 4.32 | 2.34 |
| Aggregate stability index | | 7.1 | 24.1 | 16.9 |
| Total volume of rain applied in 60 minutes ($cm^3$) | | 13200 | 13200 | 13200 |
| Total runoff volume from 60 minutes ($cm^3$) | | 8281 | 11554 | 9031 |
| Time at which 0.99 $V_{max}$ was achieved (minutes) | | 102 | 23 | 165 |
| Total mass of sediment eroded after 60 minutes (g) | | 129 | 352 | 206 |
| Time at which 0.99 $S_{max}$ was achieved (minutes) | | 205 | 19 | 23 |
| Value of 0.99 $S_{max}$ (g) | | 109 | 158 | 94 |
| Equivalent depth of soil eroded (mm) | | 0.715 | 1.951 | 1.144 |
| Clay enrichment ratios | Dispersed, 0 to 20 minutes | 1.183 | 1.580 | 1.190 |
| | Dispersed, 50 to 60 minutes | 1.255 | 1.119 | 1.080 |
| | Dispersed, 0 to 60 minutes | 1.115 | 1.181 | 1.114 |
| | Undispersed, 0 to 60 minutes | 0.051 | 0.187 | 0.255 |

The percentage of organic carbon present in each soil type was determined by the pyrolitic burning technique. Organic matter generally improves the structure of the soil by producing more stable aggregates, although this depends on soil texture.

The aggregate stability for each soil type was determined using a Settling Tube. This technique compared the settling velocity distribution of moist soil aggregates with those from air-dried soil aggregates which were shock wetted before being placed into the settling tube. It works on the principle that the aggregate settling velocity distribution of a soil sample changes as the structural stability of aggregates is reduced. Determining the aggregate stability of a soil sample using a settling tube has advantages over other techniques in that only wetting forces are employed for sediment dispersion. Wet sieving, for example, imposes two forces on aggregates. The first is the force of water entry into the aggregates before sieving and the second is the mechanical abrasion caused by the impact of aggregates with one another and with the sieves under water during the sieving process.

Results of the aggregate stability analysis showed that the Kiwitea soil contained the most stable aggregates of the three soils. This may be attributed to the high proportion of clay (27.8 %) and the dominant clay type allophane in the Kiwitea soil. The organic carbon content was also reasonably high (3.47 %). The Levin soil's aggregates were the least stable because of its low clay content (18.2 %) and especially high sand content (42.6%). The high silt content present in the Tokomaru soil (65.5 %) may have contributed to its lower aggregate stability. Silt-sized particles are more easily slaked from aggregates due to their weaker binding properties compared with clay particles.

An examination of the settling velocity distributions of both the moist and air-dried samples from the three soils suggested that the proportion of coarse aggregates was reduced, while the proportion of fine aggregates was increased slightly for the air-dried sample. The decrease in the number of large aggregates may be attributed to slaking which also results in increasing numbers of fine particles or aggregates.

Surface crusting was observed on all three soils. However the severity was greatest for the Levin soil while the Kiwitea soil suffered the least. Surface crusting is thought to be a cyclic process. The extent of surface crusting from each soil type showed similar trends to that found in the aggregate stability results. Again these results can be explained in terms of proportions of primary particles, especially the clay and silt contents, and the dominant clay types present. A higher percentage of clay enhances aggregate stability. Silt particles are most easily detached by raindrop impact compared to clay particles.

Over the 60 minute period, 65 mm of rainfall was applied to all soil types. This either infiltrated into the soil or became runoff. During each rainstorm simulation, 13200 $cm^3$ of rain was applied over the 60 minute period and the amount which was collected varied from 8281 $cm^3$ from the Kiwitea soil to 11554 $cm^3$ from the Levin soil. Runoff amounted to 63 %, 88 % and 68 % of the total rain applied for the Kiwitea, Levin and Tokomaru soils respectively. These values also indicated the extent of surface crusting which occurred on the three soil types.

The runoff volume generated increased over time during the initial stage of the "storm" and then plateaued to a constant value. The maximum runoff rate possible equates to the amount of rain applied when the infiltration rate becomes zero. In this study the maximum volume of rain applied in any 5 minute period was 1100 $cm^3$ (this is referred to $V_{max}$). Based on this assumption, fitted function curves were plotted from the runoff volume results to determine the time in which 0.99 $V_{max}$ was achieved. Only the Levin soil reached 0.99 $V_{max}$ within the 60 minute rainfall period. This was achieved after nearly 23 minutes and was a reflection of the Levin soil's poor aggregate stability and the degree to which it was affected by surface crusting. After extrapolating the fitted function curves, it was estimated that the Kiwitea and Tokomaru soils would have reached 0.99 $V_{max}$ after nearly 102 and 165 minutes respectively. This indicates that surface crusting did not totally restrict infiltration for both the Kiwitea and Tokomaru soils over the 60 minute rainfall period.

The observed variations between the actual runoff volume and the fitted function curves can be attributed to the changes in surface depression and surface detention, a direct consequence of the cyclic processes of surface crusting.

There seemed to be greater variation once the runoff volume plateaued out. This was more obvious for the Levin soil due to the earlier time at which 0.99 $V_{max}$ was achieved.

The total mass of sediment eroded over the 60 minute rainfall period for each soil varied from 129 g to 352 g. The Levin and Tokomaru soils eroded nearly 174 % and 60 % more sediment respectively than the Kiwitea soil. Similar patterns were evident from the aggregate stability results. These amounts of sediment are equivalent to 1 to 2 mm depth of soil eroded. Although 1 to 2 mm may seem insignificant, this is only from one storm event. If the same storm intensity and conditions were to occur on a large scale, it may be predicted that 6.4, 17.6 and 10.3 tonnes of sediment would be eroded per hectare from the Kiwitea, Levin and Tokomaru soils respectively.

Like the runoff volume generated over time, the mass of sediment eroded increased during the initial stages of the "storm" and then plateaued at a constant value. The reduction in the rate of soil loss to a constant value can be attributed to the build up of water present on the soil surface. This resulted from the reduction in the soil's permeability because of soil saturation and surface crusting. A fitted function curve similar to that plotted for the runoff volume results, was plotted for each soil type so that the 0.99 $S_{max}$ and the time in which it was achieved could be determined. The Levin soil had the highest $S_{max}$ value and this was achieved in the quickest time. Although the estimated mass of sediment ceiling value was higher for the Kiwitea soil compared to the Tokomaru soil, the time in which it was achieved was somewhat slower. This explains why more sediment was generated from the Tokomaru soil over the total rainfall period.

Variations in the measured masses of eroded sediment once 0.99 $S_{max}$ had been achieved may be attributed to the cyclic processes of surface crusting and excess surface water.

The sediment-runoff concentration at the start of the rainfall period for the three soils was greater than that after 60 minutes. The higher sediment load initially resulted from soil particles being more easily detached by rainsplash. After 60 minutes, the build up of surface water inhibited splash detachment. The

fluctuations in sediment-runoff concentration can also be explained by the cyclic processes of surface crusting. Evidence from the Levin soil shows that the greater the effect of surface crusting, the larger the fluctuations.

The proportion of sand present in the eroded sediment was always lower than that of the original soil. Primary sand particles are less easily entrained into overland flow due to their size and weight.

The eroded sediment from the Kiwitea soil contained a lower percentage of silt particles compared to the original soil. This may be attributed to the high proportion of clay present and the dominant clay type, allophane in the original soil preventing aggregate disintegration by raindrop impact. A higher percentage of silt was found in the eroded sediment from the Levin soil compared with the original soil. The aggregate stability test for the Levin soil showed its particles were more easily slaked compared to those of the other soil types.

The Tokomaru soil initially showed a lower silt content in the eroded sediment compared to the original soil, and a greater silt content at the end of the erosion period. This may be explained by clay binding the silt particles in aggregates. As the rainfall event proceeded, these aggregates were broken down, as a direct result of raindrop impact, which exposed more silt particles for slaking and eventual overflow entrainment. As shown earlier, the Tokomaru soil had a reasonably high clay content (24.5 %), however its organic carbon content was low (2.34 %). This may explain why the aggregate stability was initially high until the aggregate moisture content increased to such an extent that it caused the bonding forces to rupture.

The three sampling periods for each soil type always showed an increase in the proportion of clay present in the eroded sediment compared with the original soil, ie. the clay enrichment ratio was always greater than one. There was an increase in the clay enrichment ratio between the start and the end of the rainfall period for the Kiwitea soil. This increase may be attributed to the high allophanic clay content which produced more stable soil aggregates which were less affected by slaking compared to the other two soils. These aggregates, rich in

clay, can only be entrained into overland flow when the runoff energy is sufficient to transport them, ie. during the later stages of the storm.

The dispersed sediment-size distribution is an indicator of fine-particle enrichment, and surface area of the sediment, but it is not appropriate for determining the transportability of the sediment during runoff. Therefore undispersed eroded sediment samples from each soil type were separated into sand, silt and clay size fractions over five minute intervals. Results from both the particle size analysis and the settling tube analysis showed that the proportion of eroded silt-size material (primary silt particles and silt-size aggregates) decreased rapidly during the early stages of the storm and then reached an equilibrium constant value 20 to 25 % lower than the proportion of primary silt particles present in the original soil. The proportion of eroded silt-size material from the initial sample (T = 5 minutes) was similar to or slightly less than the silt content of the original soil. The reason silt-size material was greatest at the start of the rainfall event could be attributed to the ease in which silt particles were detached by raindrop impact because of the low cohesive forces binding them together. Also, at the start of the rainfall period, the capacity of thin flows to transport sediment may be limited by the volume and velocity of the runoff.

Clay size material was shown to be eroded at a constant rate. This constant rate for the three soils was significantly lower than the clay content of the original soil. This resulted in clay enrichment ratios less than one for the undispersed sediment. This suggests that most of the clay was eroded in the form of aggregates and very little was transported as primary clay particles.

The proportion of eroded sand-size material increased over time until an equilibrium value was reached. This material was composed of both primary sand particles and soil aggregates. Both The Kiwitea and Levin soils had similar equilibrium proportions of eroded sand-size material (70 and 75 % respectively), while the Tokomaru soil was somewhat lower (50 %). These values indicate that the Levin soil contained a greater proportion of aggregates than the other two soils, although it has been shown that the Levin soil had the lowest aggregate stability index and the lowest clay content. This suggests that it is the larger aggregates from the Levin soil that are the most unstable and that when these

aggregates are disrupted, they are broken down into smaller aggregates that are more structurally stable. Also, nearly 43 % of the Levin soil is composed of primary sand particles. This would enhance the proportion of eroded sand-size material present. The high proportion of eroded sand-size material from the Kiwitea soil can be explained by the percentage clay present in the original soil, the dominant clay type and also the soils high aggregate stability index. The degree of sand-size material eroded varied according to the rate of soil loss. At low rates, the runoff energy was insufficient to transport large aggregates. This explains why the percentage of sand-size material was lowest at the first sampling time (T = 5 minutes).

A mulch cover placed on the Levin soil severely reduced the amount of runoff volume and sediment yield by intercepting and cushioning the raindrop impact. In this study, the runoff volume and the mass of sediment generated over the 60 minute rainfall period under the mulch cover was nearly three times and 1000 times lower respectively than that generated from the bare soil. This confirms the supposition that a mulch cover inhibits surface crusting and promotes infiltration. Runoff flow velocities are reduced and so is the stream power available to entrain sediment.

## Conclusions

1. Quantitatively comparing the erodibility of the three soils, it was found that the Levin soil was the most erodible and the Kiwitea soil was the least erodible. If the same storm intensity and soil conditions used in this study were to occur on a large scale, 6.4, 17.6 and 10.3 tonnes of sediment would be eroded per hectare from the Kiwitea, Levin and Tokomaru soils respectively.

2. Soil particles and aggregates are selectively removed by rainsplash detachment and overland flow. The proportion of sand particles present in the eroded sediment was always lower than that of the original soil due to their inability to be entrained by overland. Silt particles are easily detached and are most commonly eroded as individual particles. Clay

particles are commonly eroded and transported in the form of aggregates, a result of their binding properties.

3. The size distribution of the eroded sediment became progressively coarser over the rainfall period. This was because initially there was insufficient runoff energy available to entrain and transport the larger particles or aggregates.

4. A mulch cover severely reduces the volume of runoff and the amount of sediment. It effectively cushions the raindrop impact. Therefore surface crusting is reduced and infiltration is promoted. Runoff flow velocities are reduced as is the stream power available to entrain sediment.

5. Comparing the settling velocity distributions of moist and air-dried soil samples is a good indicator of soil aggregate stability.

# Appendix One

## Sieving and Sedimentation Procedures

The following procedure has been adapted from Day (1965) and is the standard method for particle size analysis used by the Department of Soil Science, Massey University.

Day 1.

1. Weigh 30-40 grams of soil into a large beaker.

2. Add approximately 50 ml of 6% hydrogen peroxide ($H_2O_2$), swirl around, note the reaction and leave for about 2 hours. The purpose of adding $H_2O_2$ is to oxidise the organic matter which may be binding particles and aggregates together.

3. Add more $H_2O_2$ depending on the initial reaction to 6%
   -if the reaction was nil, or slight, add 100 ml of 30% $H_2O_2$
   -if the sample was bubbly, or mildly frothy, add 50 ml of 30% $H_2O_2$
   -if the sample was very frothy, add 100 ml of 6% $H_2O_2$.

4. After a further hour or two, any sample that has not had 30% $H_2O_2$ added should now have some added. Make the volume up to approximately 200 ml with 30% $H_2O_2$ on all samples.

5. Leave overnight.
   Note: If the sample looks like bubbling over the top of the beaker, add several drops of capryl alcohol. This neutralizes the reaction.

Day 2.

1. Heat the sample gently on a hot plate (65 °C) until the reaction subsides. Once the initial frothing has ceased, add more 30% $H_2O_2$ (50

ml) and wait for the reaction to cease again. Stir the sample frequently. Applying heat to the sample increases the reaction of the $H_2O_2$ to the organic matter.

2. i. If the sample froths a great deal and threatens to overflow, remove the sample from the heat and stir.
   ii. If the sample is still rising, add several drops of capryl alcohol and stir.
   iii. If the sample is still rising, repeat with capryl alcohol. 6% $H_2O_2$ can be added to cool the sample down.

3. Continue adding 30% $H_2O_2$ in small amounts until its addition does not cause any new frothing.

4. Turn the hot plate up to 105 °C, and let the sample boil down to approximately 100 ml.

5. Remove from the heat and rinse the sides of the beaker with a minimum amount of distilled water. Leave the sample to cool.

Day 3.

1. Decant the sample into 2 or 3 centrifuge tubes, rinsing out the beaker as well as possible.

2. Centrifuge at 3000 rpm for 15 minutes. This is to wash $H_2O_2$ from the particles.

3. Discard the liquid and then refill the centrifuge tubes with distilled water. Stir the sediment well and clean the stirring rod.

4. Centrifuge at 3000 rpm again for a further 15 minutes, and discard the liquid.

5. Transfer the soil from tubes into a laboratory blender container with approximately 200 ml of distilled water. Mechanically disperse for 10 minutes using a laboratory blender.

6. Stand for approximately 15 seconds, then pour the sample through a 63 *u*m sieve into a beaker, washing with a minimum of distilled water. This separates the sand size particles from the silt and clay size particles.

7. Wash the remaining sand fraction into an evaporating basin and dry for 8 hours in an oven at approximately 65 °C. This temperature prevents the structural breakdown of clay particles attached to the larger sand grains.

8. Transfer the filtered sample into a 500 ml cylinder and leave to settle (i.e. the silt and clay sized particles). It is this material in which the size distribution is determined by taking a sample using a pipette.

Day 4.

1. Sieve the dried sand fraction into their required size classes and weigh. Re-sieve the dried sand fraction through a 63 *u*m dry sieve to remove silt and clay particles that were attached to the sand grains when previously sieved wet.

2. The silt and clay particles that passed through the dry 63 *u*m sieve are added to the 500 ml cylinder that contained the wet-sieved fines.

3. Check for good dispersion in the cylinders. To test for flocculation, the cylinder containing the suspension is tilted approximately 20° -if settled sediments or stratified layers flow to maintain a horizontal level, flocculation has occurred.
   If the sample has flocculated, the procedure is to:
   (a) add 3-4 drops of ammonium solution. Stir well, and leave to settle for approximately 1 hour.
   (b) If the dispersion has improved slightly, but the cylinder is still not well dispersed, add more ammonium solution.
   (c) If the addition of ammonium solution increases flocculation, add 10 ml of 5% calgon (66 grams of sodium hexametaphosphate and 14 grams of sodium carbonate dissolved in distilled water made to a volume of 1 litre).

(d) For improved dispersion of the cylinder, the sample may require repeated additions of small amounts of calgon. The amount of calgon added must be recorded so its mass can be accounted for in the pipette sample.

4. If the sample in the cylinder is still flocculated after several hours or overnight, decant off the clear liquid and re-suspend in distilled water. This may disperse the sample.

5. Once the sample is well dispersed, make the volume in the cylinder up to 500 ml.

Day 5.

1. Take the temperature of the cylinder and calculate the settling times for the required particle sizes according to Stoke's Law.

2. At set times and depth, pipette out a 20 ml aliquot. Oven dry the sample at 65°C for two days.
   To sample:
   (a) Stir the cylinder well prior to taking the sample with a drawing stirring rod 30 seconds before the set sampling time $T_o$.
   (b) 15 seconds before time, the pipette is carefully inserted into the cylinder to the required depth. The pipette is held steady at the required depth by resting a hand on the rim of the cylinder. The sample is slowly sucked up at the time using a rubber bulb. The pipette is carefully removed.

3. Further 20 ml aliquots at other times and depths are taken as required.

4. The beakers are removed from the oven when fully dried and placed in a desiccator for 30 minutes before weighing to four decimal places.

# Appendix Two

# The Massey settling tube

## Apparatus Description

The perspex tube is semi-fixed, 2.0 m long and 65 mm in diameter. A lever to raise and lower the tube 10 mm, located at the centre of the tube, permits sample trays in the submerged collection turntable at the tubes exit to be interchanged. A static column of water through which the sediment passes is maintained by sealing the top of the tube.

The sample introduction device is comprised of an injection barrel (see plate 7). The barrel is filled with the sample (pre-treated as described later) and is initially supported by an aluminium flap which prevents the sample from pre-maturely falling into the perspex barrel. O-rings maintain the water seal at the top of the tube. Lifting the simple lever automatically draws the plunger into the tube and activates the release of the aluminium flap due to a pressure change within the sample introduction device and consequently the sample is injected into the settling tube. The injection barrel produces localised turbulence during the entry of the sample into the settling column because the soil enters with a small relative velocity. This allows the sample to breakdown into its component aggregates. This turbulence may however result in a loss in sensitivity in the discrimination of settling velocities.

The turntable base supports of a 700 mm diameter by 100 mm deep tray constructed of PVC plastic. This contains twenty 10 mm deep sub-sampling trays submerged in water (see plate 9). Water in the base tray seals the tubes exit to prevent air entering and displacing the hanging column of water. The turntable rotates to enable sub-samples to be taken from the exit of the settling tube.

**Sample Pre-treatment**

In discussing the pre-treatment of samples for wet sieving, Grieve (1979) comments that the initial condition of the sample is more significant than the choice of the test itself. Similarly, the appropriateness and consistency of the pre-treatment is equally important for tests conducted with the modified version of the Griffith Tube. Varying initial moisture contents and rates of wetting have been investigated by a number of workers (eg. Low, 1954; and Russell and Feng, 1947). Emerson and Grundy (1954) clearly demonstrated the effects of varying rates of wetting on aggregate stability. Grieve (1979) presents a review of the appropriateness of such pre-treatment to different applications.

Massey's settling tube permits a range of pre-treatments to be employed. Consideration of the intended use of the data will dictate the particular sample preparation adopted. For instance, flood wetting or immersion is generally appropriate were erodibility and deposition characteristics of an *in-situ* soil under consideration (Kemper, 1965). However, if the sample under test has already been eroded the sample should be more gently wetted (eg. under tension) to prevent further aggregate breakdown.

**Length of trial**

As previously mentioned the settling tube may be used to complement the data for fine fractions provided by pipette or hydrometer analysis.

From Stoke's equation, a particle of size 60 *u*m and a specific density of 2.65 Mg $m^{-3}$ would settle at a rate of 3.3 mm $sec^{-1}$ in water at 22 °C. This corresponds to 605 seconds to settle 2 m. Therefore, when pipette or hydrometer analysis is being employed to measure the less than 60 *u*m fraction of a sample, this time would correspond to the last sample. Massey's settling tube is also capable of measuring settling velocity distributions of aggregates smaller than 60 *u*m. However this is not recommended because of the long periods for these aggregates to settle 2 m.

## Trial Procedures

*Tube Preparation*

i. The sub-sampling trays are arranged in the turntable tray (see plate 9). The closed-cell foam pad is placed in one of the trays and the tube lowered onto the pad to seal the tube during filling.

ii. The tube is filled with water in the temperature range 15 to 25 °C and the water temperature is allowed to stabilise (as discussed earlier).

iii. The trays in the turntable bath should be submerged by at least 10 mm. water to seal on the bottom of the tube during the conduct of the trial.

iv. The sealing o-ring on the sample introduction device should be cleaned and vacuum grease applied.

*Sample Preparation*

As discussed earlier, pre-treatment of aggregates generally falls into one of the following categories: shock wetting, slow wetting and no pre-treatment required. The sample preparation follows the sequence: split sample to the required size, wet (if at all) at the required rate and place in the sample introduction device.

*Sub-sampling*

The field sample is gently split to obtain a representative sample of approximately 10 grams of oven dry mass. For a sample in a dry granular condition, a riffle box is used. Where a sample is in a more cohesive state it may be appropriate to cone and quarter the sample. A suspended sample could be split using a riffle box. All types of sediment require a duplicate sample so that the moisture content of the sediment can be measured.

*Sample Wetting*

1. Shock wetting

   The empty sample introduction device is placed upon the balance and a small quantity of distilled water is poured into the introduction chamber (to a depth of approximately 2 mm). This ensures that the sample does not adhere to the bottom of the chamber and provides even wetting of the sub-sample.

   The balance is tared and the sub-sample introduced. The mass is recorded as the total moist mass. The remainder of the chamber is filled with distilled water and the plunger is set such the barrel is brimming with water. The aluminium flap, attached permanently as a hinge point is then placed over the chamber and temporarily sealed in place with vacuum grease. The injection barrel is them gently placed in the top of the tube.

2. Controlled Wetting

   A range of controlled wetting pre-treatments were reviewed by Grieve (1979). Slow wetting on a tension plate or in a humidifier are two popular methods. Transferring the wetted sample to the introduction device must be made with a minimum of disturbance, therefore the use of a filter paper in the wetting procedure should be avoided.

3. Preparation of a sample in suspension

   Samples collected in the field frequently are saturated (eg. runoff samples). To permit the testing of such samples in the settling tube the sediment must be gently separated from the suspension. This can be performed by pouring the sample through a 63 *u*m sieve, using distilled water to wash the sample vessel. Some material finer than 63 *u*m will pass through the sieve, however this portion of the sample is beyond the normal range of the settling tube. If pipette or hydrometer analysis are planned, retain the less than 63 *u*m fraction.

## Calculation Procedure

Table 18. An example of the calculation procedure for obtaining cumulative percentage slower than settling velocity results.

Soil Type: Gourdie Silt loam. Pre-treatment: Shock wetted within barrel
Sample Date: 21.2.92 Test Date: 29.2.92
Room Temperature: 17.4°C Water Temperature: 16.3°C
Initial Total Moist Mass (TMM): 9.882 g.
Calculated Total Dry Mass = TMM * Duplicate Dry Mass / Duplicate Moist Mass
= 9.882 * 5.060 / 6.433
= 7.773 g.

| Sample Time (secs) | Settling Velocity (m $sec^{-1}$) | Mass of sub-sample (g) | Cumulative Read Down (g) | % Slower Than |
|---|---|---|---|---|
| | | | 7.773 | |
| 0 | | | | |
| | | 0.000 | 7.773 | 100.00 |
| 10 | $2.00*10^{-1}$ | | | |
| | | 1.475 | 6.298 | 81.03 |
| 15 | $1.33*10^{-1}$ | | | |
| | | 0.999 | 5.299 | 68.17 |
| 20 | $1.00*10^{-1}$ | | | |
| | | 1.799 | 3.500 | 45.03 |
| 30 | $6.67*10^{-2}$ | | | |
| | | 0.899 | 2.601 | 33.46 |
| 40 | $5.00*10^{-2}$ | | | |
| | | 1.228 | 1.372 | 17.66 |
| 70 | $2.86*10^{-2}$ | | | |
| | | 0.431 | 0.941 | 12.11 |
| 100 | $2.00*10^{-2}$ | | | |
| | | 0.293 | 0.648 | 8.34 |
| 150 | $1.33*10^{-2}$ | | | |
| | | 0.133 | 0.515 | 6.63 |
| 200 | $1.00*10^{-2}$ | | | |
| | | 0.129 | 0.386 | 4.97 |
| 300 | $6.67*10^{-3}$ | | | |
| | | 0.072 | 0.314 | 4.04 |
| 400 | $5.00*10^{-3}$ | | | |
| | | 0.061 | 0.253 | 3.26 |
| 700 | $2.86*10^{-3}$ | | | |

# Bibliography

**Alberts, E.E., W.C. Moldenhauer, and G.R. Foster. 1980:** Soil aggregates and primary particles transported in rill and interrill flow. *Soil Sci Soc Am J. 44: 590-595.*

**Alberts, E.E., R.C. Wendt, and R.F. Piest. 1983:** Physical and chemical properties of eroded soil aggregates. *Transactions, American society of Agricultural Engineers 26(2): 465-471.*

**Al-Durrah, M.M., and J.M. Bradford. 1982:** The mechanism of raindrop splash on soil surfaces. *Soil Sci Soc Am J. 46: 1086-1090.*

**Bates R.L. and J.A. Jackson. 1980:** Glossary of Geology. *2nd Edition, American Geological Institute, USA.*

**Baver, L.D., W.H. Gardner, and W.R. Gardner. 1972:** Soil Physics. *4th Ed. John Wiley and Sons, New York. 498pp.*

**Bertrand, A.R., and J.F. Parr. 1961:** Design and operation of the Purdue sprinkling infiltrometer. *Research Bulletin No. 723. Purdue University, West Lafayette, Indiana. 16pp.*

**Black, C.A. 1965:** Methods of soil analysis, Volume 1. Physical and Mineralogical. *American Soc of Agronomy, Madison Wis.*

**Blanchard, D.C. 1950:** The behaviour of water drops at terminal velocity in air. *Transactions, American Geophysical Union 31: 836-842.*

**Bowden, J.W., and D. Bennett. 1974:** The Decide Model for predicting superphosphate requirements. Australian Institute of Agricultural Science, Victorian branch, Nov 1974.

**Bradford, J.M., P.A. Remley, J.E. Ferrish, and J.B. Santini. 1986:** Effect of soil surface sealing on splash from a single waterdrop. *Soil Sci Soc Am J. 50: 1547-1552.*

**Brewer, R. 1964:** Fabric and mineral analysis of soils. *Wiley.*

**Bryan, R.B. 1976:** Considerations on soil erodibility indices and sheetwash. *Catena 3: 99-111.*

**Bryan R.B. and S.H. Luk, 1981:** Laboratory experiments on the variation of soil erosion under simulated rainfall. *Geoderma 26: 245-265.*

**Bubenzer, G.D. 1980:** An overview of rainfall simulators. *Paper No. 80-2033. American Society of Agricultural Engineers, St. Joseph, Michigan.*

**Childs, E.C. 1969:** An introduction to the physical basis of soil water phenomena. *Wiley and Sons, London.*

**Childs, E.C. 1942:** Stability of stay soils. *Soil Sci. 53: 79-92.*

**Choley, R.J. 1959:** The geomorphic significance of some Oxford soils. *American Journal of Sci. 257: 503-515.*

**Clement, C.R. and T.E. Williams. 1958:** An examination of the method of aggregate analysis by wet-sieving in relation to the influence of diverse leys on arable soil. *Journal Soil Sci. 9: 252-266.*

**Cole, R.C. and N.E. Edlefson. 1935:** A sedimentation tube for analyzing water-stable soil aggregates. *Soil Sci. 40: 473-479.*

**Collis-George, N. and R. Lal. 1971:** Infiltration and structural changes influenced by initial moisture content. *Australian Journal of Soil Research. 9: 107-116.*

**Day, P.R. 1965:** Particle fractionation and particle-size analysis. In: C.A. Black *et al.* (Ed.) *Methods of soil analysis, part 1. Agronomy 9: 545-567.*

**Dettman, M.G. and W.W. Emerson. 1959:** A modified permeability test for measuring the cohesion of soil crumbs. *Journal of Soil Science. 10: 215-226.*

**Ellison, W.D. 1944:** Studies of raindrop erosion. *Agricultural Engineering Michigan. 25: 131-136 and 181-182.*

**Emerson, W.W. 1954:** The determination of the stability of soil crumbs. *Journal of Soil Science. 5: 233-250.*

**Emerson, W.W. 1967:** A classification of soil aggregates based on their coherence in water. *Australian Journal of Soil Research. 5: 47-57.*

**Emerson, W.W. and G.M.F. Grundy. 1954:** The effect of rate of wetting on water uptake and cohesion of soil crumbs. *Journal of Agricultural Sci. 44: 249-253.*

**Emery, K.O. 1938:** Rapid method of mechanical analysis of sands. *Journal of Sediment. Petrol. 8(3): 105-111.*

**Eyles, G.O. 1985:** New Zealand land resource inventory erosion classification. *Water and Soil miscellaneous publications No. 85.*

**Felix, D.W. 1969:** An inexpensive settling tube for analysis of sands. *Journal of Sediment. Petrol. 36(2): 777-780.*

**Foster, G.R., W.H. Neibling, and R.A. Natterman. 1982:** A programmable rainfall simulator. *American Society Agricultural Engineers. St. Joseph, Michigan. Paper No. 82-2570.*

**Foster, G.R., R.A. Young, and W.H. Neibling. 1985:** Sediment composition for non-point source pollution anaylsis. *Transactions, American Society of Agricultural Engineers 28: 133-139 and pp 146.*

**Gabriels, D., and W.C. Moldenhauer. 1978:** Size distribution of eroded material from simulated rainfall: Effect over a range of texture. *Soil Sci Soc Am J. 42: 954-958.*

**Gibbs, R.J., M.D. Matthews, and D.A. Link. 1971:** The relationship between sphere size and settling velocity. *Journal of Sediment. Petrol. 41(1): 7-18.*

**Grieves, I.C. 1979:** A comparison of aggregate stability test procedures in determining the stability of fine sandy soils in Fife, Scotland. *Catena 6: 123-129.*

**Gunn, R., and G.D. Kinzer. 1949:** Terminal velocity of water droplets in stagnant air. *Journal of Meterology 6: 243-248.*

**Gunn, R. 1949:** Mechanical resonance in freely falling drops. *Journal of Geophysical Research 54: 383-385.*

**Hairsine, P. 1989:** A practical guide to the portable rainfall simulator. *Department of Soil Science, Massey University Publication.*

**Hairsine P. and G. McTanish. 1986:** The Griffith Tube: A simple settling tube for the measurement of settling velocity of aggregates. *AES. Working paper 3/86, Griffith University.*

**Hairsine, P.B., and C.W. Rose. 1991:** Rainfall detachment and deposition: Sediment transport in the absence of flow-driven processes. *Soil Sci Soc Am J. 55(2): 320-325.*

**Hall, M.J. 1970:** A critique of methods of simulating rainfall. *Water Resources Research 6: 1104-1114.*

**Hillel, D. 1982:** Introduction to soil physics. *Academic Press, Inc. 365 pp.*

**Holland, M.E. 1969:** Design and testing of a rainfall system. *CER 69-70, MEH 21. Colorado State University station, Fort Collins.*

**Hudson, N. 1971:** Soil conservation. *Cornell University Press.*

**Keen, R. 1986:** Rainfall's the game, education's the aim. *Journal of Soil and Water Conservation 41(5): 311-313.*

**Kemper, W.D., 1965:** Aggregate stability. *In: Methods of soil analysis. Ed. C.A. Black (1965).*

**Kemper, W.D., and R.C. Rosenau, 1986:** Aggregate stability and size distribution. *In: Methods of soil analysis, Part 1. Physical and Mineralogical Methods -Agronomy Monograph no. 9 (2nd Edition).*

**Kemper, W.D., R.C. Rosenau, and S, Nelson. 1985:** Gas displacement and aggregate stability of soils. *Soil Sci Soc Am J. 49: 25-28.*

**Knisel, W.G. 1980:** Creams: a field scale model for chemicals, runoff and erosion from agricultural management systems. *USDA Conservation Research Report 26. In: Morgan (1986)*

**Laften, J.M., J.L. Baker, R.O. Hartwig, W.F. Buchele, H.P. Johnson. 1978:** Soil and water losses from conservation tillage systems. *Transactions, American Society of Agricultural Engineers 26(5): 881-885.*

**Laws, J.O. 1941:** Measurements of the fall velocity of water drops and raindrops. *Transactions, American geophysical Union 22: 709-721.*

**Laws, J.O., and D.A. Parsons. 1943:** Relation of raindrop size to intensity. *Transactions, American Geophysical Union 24: 452-460.*

**Loch, R.J., J.L. Cleary, E.C. Thomas, and S.F. Glanville. 1988:** An elevation of the use of size distributions of sediment in runoff as a measure of aggregate breakdown in the surface of a cracking clay soil under rain. *Earth Surfaces Processes and Landforms 13: 37-44.*

**Loch, R.J., and T.E. Donnollan. 1982a:** Field rainfall simulator studies on two clay soils of the Darling Downs, Queensland I. -The effects of plot length and tillage orientation on erosion processes and runoff and erosion rates. *Australian Journal of Soil Research 21: 33-36.*

**Loch, R.J., and T.E. Donnollan 1982b:** Field rainfall simulator studies on two clay soils, Queensland; II -Aggregate breakdown, sediment properties and soil erodibility. *Australian Journal of Soil Research 21: 47-58.*

**Low, A.J. 1954:** The study of soil structure in the field and in the laboratory. *Journal of Soil Sci. 5: 57-74.*

**Luk, S.H. 1979:** Effect of soil properties on erosion by wash and splash. *Earth Surface Processes 4: 241-255.*

**McCulla, T.M. 1945:** Water drop method of determining the stability of soil structure. *Soil Sci. 58: 177-183.*

**Meyer, L.D. 1985:** Interrill erosion rates and sediment characteristics. *pp 167-177. In: S.A. El-Swaify, W.C. Moldenhauer, and A. Lo (Eds.). Soil erosion and conservation. Soil Cons Soc Am.*

**Meyer, L.D., G.R. Foster, and L. Nikolov. 1975:** Effect of flow rate and canopy on rill erosion. *Transactions, American Society of Agricultural Engineers 18(5): 905-911.*

**Meyer, L.D., and W.C. Harmon. 1979:** Multiple intensity rainfall simulator for erosion research on row side slopes. *Transactions, American Society of Agricultural Engineers. 22(1): 100-103.*

**Meyer, L.D., and W.C. Harmon. 1985:** Sediment losses from cropland furrows of different gradients. *Transactions, American Society of Agricultural Engineers 28: 448-453.*

**Meyer, L.D., W.C. Harmon, and L.L. McDowell. 1980:** Sediment sizes eroded from crop row sideslopes. *American Society of Agricultural Engineers 23(4): 891-898.*

**Meyer, L.D., and D.L. McCune. 1958:** Rainfall simulator for runoff plots. *Agricultural Engineering 39: 644-648.*

**Miller, W.P., and M.K. Baharuddin. 1987:** Particle size of interrill-eroded sediments from highly weathered soils. *Soil Sci Soc Am J. 51: 1610-1615.*

**Monke, E.J., H.J. Marelli, L.D. Meyer, and J.F. DeLong. 1977:** Physical-chemical composition of eroded soil. *Transactions, American Society of Agricultural Engineers 20(1): 58-61.*

**Moore, I.D., M.C. Hirschi, and B.J. Barfield. 1983:** Kentucky rainfall simulator. *Transactions, American Society of Agricultural Engineers 26: 1085-1089.*

**Morgan, R.P.C. 1986:** Soil erosion and conservation. *Editored by D.A. Davidson. Longman Scientific and Technical Publications.*

**Morin, J., D. Goldberg, and I. Seginer. 1967:** A rainfall simulator with a rotating disk. *Transactions, American Society of Agricultural Engineers 10: 74-77.*

**Moss, A.J., and P. Green. 1983:** Movement of solids in air and water by raindrop impact. Effects of dropsize and water depth variations. *Australian Journal of Soil Research 21: 257-269.*

**Moss, A.J., P.H. Walker, and J. Hulka. 1979:** Raindrop simulated transportation in shallow water flows: an experimental study. *Sediment. Geology. 22: 165-84*

**Mueller, E.D., and A.L. Sims. 1967:** Raindrop distribution at Island Beach, New Jersey. *In: Walker et al. (1972).*

**Mutchler, C.K., and L.F. Hermsmeier. 1965:** A review of rainfall simulators. *Transactions, American Society of Agricultural Engineers 8: 63-65.*

**Nelson D.W., and L.E. Sommers. 1982:** Total carbon, organic carbon, and organic matter. *Methods of soil analysis, Part 2, 2nd Ed. American Society of Agronomy. Chapter 29 pp 539-579.*

**Panabokke, C.R., and J.P. Quirke. 1957:** Effect of initial water content on stability of soil aggregates. *Soil Sci. 83: 185-197.*

**Panabokke, C.R., and J.P. Quirke. 1962:** Incipient failure of soil aggregates. *Journal of Soil Sci. 13: 60-70.*

**Proffitt, A.P.B., C.W. Rose, and C.J. Lovell. 1989:** A comparison between modified splash cup and flume techniques in differentiating between soil

loss and detachability as a result of rainfall and deposition. *Australian Journal of Soil Research. 27: 759-77.*

**Rose, C.W. 1985:** Developments in soil erosion and deposition models. *Advances in Soil Science, Volume II. Springer-Verlog. pp 2-60.*

**Rose, C.W., J.R. Williams, G.C. Sanders, and D.A. Barry. 1983:** A mathematical model of soil erosion and deposition processes: 1. Theory for a plain land element. *Soil Sci Soc Am J. 47(5): 991-995.*

**Russell, E.W. 1973:** Soil conditions and plant growth. *Longmans: London.*

**Russell, M.B., and C.L. Feng. 1947:** Characterisation of the stability of soil aggregates. *Journal paper J-870, Iowa Agricultural Research Station, Ames, Iowa, USA.*

**Sandford, R.B., and D.J.P. Swift. 1971:** Comparison of sieving and settling techniques for size analysis, using a Benthos Rapid Sediment Analyzer. *Sedimentology, 17: 257-264.*

**Savat, J. 1981:** Work done by splash: Laboratory Experiments. *Earth Surface processes and Landforms 6: 275-283.*

**Schlee, J. 1966:** A modified woods hole rapid sediment analyzer. *J Sediment. Petrol. 36(2) 403-413.*

**Snedecor G.W., and W.G. Cockran. 1980:** Statistical methods. *Iowa State University Press, Ames, Iowa, USA.*

**Swanson, N.P. 1965:** Rotating boom rainfall simulator. *Transactions, American Society of Agricultural Engineers 8: 71-72.*

**Tomlinson, A.I. 1980:** The frequency of high intensity rainfalls in New Zealand, Part 1. *Water and Soil Technical Publication No. 19.*

**United States Department of Agriculture. 1979:** Proceedings of the rainfall simulator workshop, Tucson, Arizona. *ARM-W-10. Northern Plains Soil and Water Research Center, Sidney, Montana. 185 pp.*

**Walker, P.H., J. Hutka, A.J. Moss, and P.I.A. Kinnell. 1977:** Use of a versatile system for soil erosion studies. *J Soil Sci Soc Am. 41: 609-612.*

**Walker, P.H., P.I.A. Kinnell, and J. Hutka. 1972:** Some concepts and techniques in rainfall simulation for soil erosion studies. *Unpublished CSIRO. Div. Soils report, Canberra, Australia.*

**Walker, P.H., P.I.A. Kinnell, and P. Green. 1978:** Transport of a non-cohesive sandy mixture in rainfall and runoff experiments. *J Soil Sci Soc Am. 42: 793-801.*

**Watson, R.L. 1969:** Modified Rubey's Law accurately predicts sediment settling velocity. *Water Resources Res. 5: 1147-1150.*

**Williams, R.J.B. 1963:** A new method for measuring soil stability. *Chemistry and Industry, June 22, 1031-1033.*

**Williams, B.G., D.J. Greenland, G.R. Lindstorm, and J.P. Quirke. 1966:** Techniques for the determination of the stability of aggregates. *Soil Sci. 101: 157-163.*

**Wischmeier, W.H. and D.D. Smith. 1958:** Rainfall energy and its relation to soil loss. *Transactions, Geophysical Union 39: 258-291.*

**Wischmeier, W.H., and D.D. Smith. 1978:** Predicting rainfall erosion losses - A guide to conservation planning. *Agricultural Handbook 537. Agricultural Research Service, U.S. Department of Agriculture, Washington, D.C. 58 pp.*

**Wright, A.C. 1987:** A model of the re-distribution of disaggregated soil particles by rainsplash. *Earth Surface Processes and Landforms 12: 583-596.*

**Yoder, R.E. 1936:** A direct method of aggregate analysis of soils, and a study of the physical nature of erosion losses. *J Am Soc of Agron. 28: 337-351.*

**Young, R.A., and C.A. Onstad, 1978:** Characterisation of rill and interrill eroded soil. *American Society of Agricultural Engineers 21(6): 1126-1130.*

**Young, R.A. 1980:** Characteristics of eroded sediment. *Transactions, American Society of Agricultural Engineers 23(5): 1139-1146.*

**Young, R.A., and J.L. Wiersma. 1973:** The role of rainfall impact in soil detachment and transport. *Water Resource Research 9(6): 1629-1636.*